UNIVERSITY OF TRENTO

Doctoral School in Civil, Environmental and Mechanical Engineering

Curriculum 4. Architecture and Planning, Landscape

Elena Bernardini

Digital Models for the Decarbonization of the Built Environment



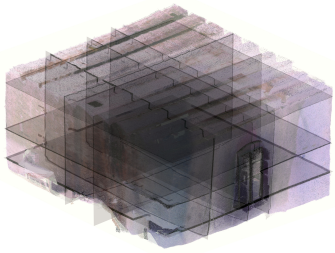



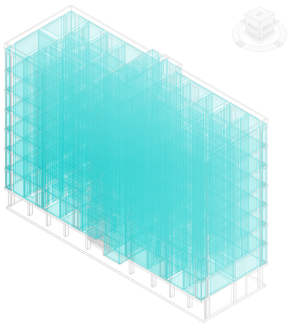



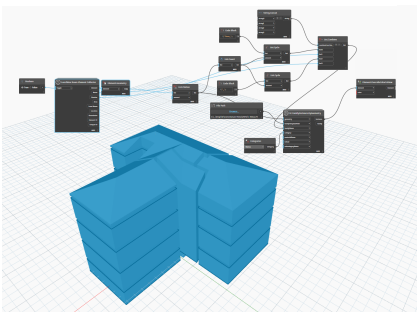

2026 - Doctoral thesis

UNIVERSITY OF TRENTO - Italy
Department of Civil, Environmental and Mechanical Engineering



Doctoral School in Civil, Environmental and Mechanical Engineering
Topic 1. Civil and Environmental Engineering - XXXVIII cycle 2022/2025

Doctoral Thesis - July 2026

Elena Bernardini

Digital models for the decarbonization of the built environment

Supervisors
Prof. Giovanna A. Massari, University of Trento
Prof. Rossano Albatici, University of Trento
Prof. Michela Dalprà, University of Trento

Credits of the cover image. Collage of picture produced by the author.
Pictures on the left from top to bottom:
- Main façade of Casa Demartin in Calliano (TN) by LAMARC;
- A8-3 buildings of the Antonio Rueda neighbourhood in Valencia by the author;
- Residential building in Povo (TN) by Sovecar s.r.l.
Pictures on the right from top to bottom: digital models elaborated by the author.

Contents on this book are licensed under a Creative Common Attribution
Non Commercial - No Derivatives
4.0 International License, except for the parts already published by other publishers.

University of Trento
Doctoral School in Civil, Environmental and Mechanical Engineering
http://web.unitn.it/en/dricam
Via Mesiano 77, I-38123 Trento
Tel. +39 0461 282670 / 2611 - *dicamphd@unitn.it*

Abstract

The building sector is one of the main contributors to global greenhouse gas emissions, making the energy renovation of the existing building stock a priority for achieving decarbonization targets, particularly in Europe where most buildings are already constructed. This stock includes both historical and modern heritage, often characterized by architectural, cultural and regulatory constraints that complicate intervention processes. In this context, digitalization offers significant potential to support more informed and effective renovation strategies, although its application remains fragmented and not fully aligned with the needs of different stakeholders.

This research investigates how digital models can support the decarbonization of existing buildings, focusing on their role within renovation workflows. The study is structured around three research questions: how data acquisition methodologies influence the construction of digital models; which characteristics digital models must possess to support the different phases of energy retrofitting; and how the usability and interoperability of BIM models can be ensured for actors with diverse skills and objectives.

The research adopts a combined theoretical and experimental approach, based on three case studies representative of different building types and intervention goals. The first case study focuses on historical heritage and investigates the development of geometric models to support knowledge and documentation processes, analysing the transition from data acquisition to representation. The second case study, addresses modern heritage and explores the use of informative models to support the comparison of renovation strategies, integrating energy analysis and design communication while considering conservation requirements. The third case study, examines a design-oriented workflow in

which digital models support renovation interventions based on prefabricated components, linking modelling activities with technical development and construction processes.
Across the three case studies, workflows are defined and compared through the phases of data acquisition, data processing and integration, and modelling for different purposes.
The research contributes to the definition of a flexible and integrated methodological framework for the development of digital models supporting renovation processes. By aligning data acquisition strategies, modelling approaches and intended uses, the proposed framework enhances the effectiveness, replicability and scalability of digital workflows.

Table of Contents

1. Introduction and focus of the research.....1

   1.1. Existing buildings: built environment as heritage.....2

   1.2. Decarbonization.....6

   1.3. Digitization.....9

   1.4. Decarbonization through digitization for the built environment.....13

   References chapter 1.....15

2. Research questions.....25

   2.1 Structure of the case studies.....27

3. Geometric models to support historical heritage knowledge. A case study in Calliano (TN).....30

   3.1. Theoretical framework. From data acquisition to knowledge representation.....31

   3.2. Contextualisation. *Casa Demartin*, a historical landmark of the Vallagarina.....38

   3.3. Workflow. Knowledge for the evaluation of appropriate modelling strategies.....42

   3.4. Answer to the RQ. Considerations on the case Calliano study.....71

   References chapter 3.....72

4. Informative models to support modern heritage reuse. A case study in Valencia.....78

   4.1. Theoretical framework. Multi-criteria performance simulation for ecodesign assessment in architectural retrofitting.....79

4.2. Contextualisation. *Antonio Ruedа*'s Housing Complex....86

4.3. Workflow. Informative modelling to support the comparison of renovation strategies....90

4.4. Answer to the RQ. Considerations on the Valencia case study....116

References chapter 4....118

5. Geometric and informative models to support renovation design workflow. A case study in Povo (TN)....124

5.1. Theoretical framework. From data acquisition to construction site....125

5.2. Contextualisation. The *ARV* project and Povo residential building....130

5.3. Workflow. Design modelling to support a renovation intervention through prefabricated components....137

5.4. Answer to the RQ. Considerations on the Povo case study....153

References chapter 5....156

6. Conclusions....159

6.1. Discussion: the case studies in relation to the research questions....159

6.2. Limitations and future developments....162

6.3. Conclusions....163

1. Introduction and focus of the research

Climate change mitigation is increasingly recognized as inseparable from the transformation of the built environment. Buildings mediate nearly every dimension of daily life, such as dwelling, working, producing, gathering, and in doing so they consume energy, materials, and land throughout construction, operation, and eventual demolition.

At European level, this premise is confirmed by convergent data: buildings account for approximately 40% of the European Union's final energy consumption and 36% of its energy-related greenhouse gas emissions (European Commission, 2020; 2024). According to the European Building Stock Observatory, the EU counted approximately 111 million buildings in 2020, of which 101 million residential and 10 million non-residential, generating direct fossil-fuel emissions exceeding 300 and 130 megatonnes of CO_2-equivalent respectively in 2021 (European Commission, 2024). A large share of this stock predates any form of energy regulation: roughly 85% of EU buildings were constructed before 2000, and about 75% are today classified as energy-inefficient (European Commission, 2020).

This condition is corroborated at national scale. In Italy, the sixth annual report on building energy certification (ENEA & CTI, 2025), based on the national registry of Energy Performance Certificates (SIAPE), records that 45.3% of certified residential buildings still fall within the lowest efficiency classes (F–G), against approximately 20% in the highest classes (A4–B), with the gap between the two figures widening sharply for buildings constructed before 1972. This performance gap mirrors the age structure of the national housing stock itself: according to the 2021 Permanent Population and Housing Census, 56.3% of Italian dwellings were built between 1961 and 2000, and a further 32.4% before 1961, of which roughly 18% before 1945 (ISTAT, 2024); only

11.4% postdate 2001, the period in which national energy-performance requirements began to take effect.

Because the environmental footprint accumulates over decades rather than being fixed at the moment of design, the building stock that already exists today will remain the dominant driver of the sector's emissions for a long time to come, regardless of how sustainably future buildings are built. Achieving the EU's 2050 climate-neutrality target therefore depends less on how new buildings are designed than on how the existing stock is understood and transformed. This shifts the focus of the decarbonization problem from design to intervention on the built environment, and to the broader question of how existing buildings can be approached.

Since the existing stock is not a homogeneous object, addressing decarbonization at the scale required by EU targets cannot rely on a single renovation paradigm, but must be capable of adapting to this heterogeneity. In this context, digitization has increasingly been proposed as the connective infrastructure capable of supporting this adaptation, by providing the information base on which renovation decisions of very different kinds can be grounded (European Commission, 2020).

This picture justifies treating the existing stock as the central object of this research, which is developed in the sections that follow through three interlocking themes: the nature and heterogeneity of the existing building stock (section 1.1), the strategies available to decarbonize it (section 1.2), and the role that digitization can play in supporting these strategies (sections 1.3–1.4).

1.1. Existing buildings: built environment as heritage

The built environment we inherited from the past can, in its broadest sense, be considered heritage in its entirety: every existing building embodies choices, techniques, and resources

invested by previous generations, and any renovation, whatever its scope, inevitably engages with this legacy rather than starting anew. This perspective is supported by critical heritage studies, which have progressively extended the core concept beyond the narrow set of assets formally designated as such. Through this wider lens, heritage is constituted by everything received from the past and carried forward into the present, tangible and intangible alike (Vecco, 2010; Blake, 2000), and its significance is a matter of social and cultural construction rather than an intrinsic property automatically conferred by age or style (Konsa, 2013; Graham & Howard, 2016). Within this interpretation, official designation does not necessarily create heritage value, but recognizes a condition that in principle extends to the entire inherited built environment (Harrison, 2012).

Despite the increasingly inclusive understanding of heritage, it remains neither possible nor useful to ignore the practical variety of the existing building stock, nor the consequent necessity of differentiating the approach adopted toward it. Buildings differ in age, constructive logic and features, and legal status. It is this last dimension that carries direct consequences for which interventions are admissible in practice.

At international level, this protection regime has been shaped by a continuous sequence of charters and conventions rather than by a single settled doctrine. The doctrinal framework was first formalized through the Athens Charter (ICOMOS, 1931/2011) and, more influentially, the Venice Charter (ICOMOS, 1964), which established material authenticity and minimal intervention as guiding principles. Later instruments progressively broadened this doctrine: the Council of Europe's Granada Convention (1985) extended protection specifically to architectural heritage; the Amsterdam Declaration (Congress on the European Architectural Heritage, 1975) introduced the principle of integrated conservation; the Nara

Document (ICOMOS/UNESCO, 1994) and the Kraków Charter (International Conference on Conservation, 2000) reconfigured the notion of authenticity toward context-specific readings; the Faro Convention (Council of Europe, 2005) reframed heritage as a societal resource; and, most recently, the Leeuwarden Declaration (Architects' Council of Europe, 2018) explicitly positioned heritage-led regeneration as a sustainability strategy in its own right. Protected heritage is subject to multiple national and international protection frameworks, including UNESCO's World Heritage Convention. At national level, in Italy, this apparatus was built on a legislative tradition that dates back to the beginning of the XX century. Since 1998, however, the decentralization of administrative functions to the regions initiated by Legislative Decree 112/1998 was followed by the systematic codification of heritage protection in the Codice dei Beni Culturali e del Paesaggio (Legislative Decree 42/2004), subsequently refined by two corrective decrees (Legislative Decree 156/2006; Legislative Decree 62/2008). This regulatory trajectory defines the legal conditions under which interventions on protected assets are admissible, depending on the age of the building, and explains why protected buildings are treated as a distinct case within European energy policy rather than being subject to its strictest requirements.

Although this apparatus originated around pre-modern monuments, the same protective logic has, over the past three decades, been extended to twentieth-century and post-war architecture, progressively narrowing the gap between historical and modern heritage in terms of formal recognition. The Council of Europe's Recommendation No. R(91)13 on the protection of the twentieth-century architectural heritage, the founding of Docomomo International in 1988 to document and safeguard the heritage of the Modern Movement (Guillet, 2007), and more recent, systematic inventories of significant modern buildings (Marsden & Spearritt, 2021) have all

contributed to treating modern heritage as a full instance of constrained heritage rather than as a separate, less codified category, even where its documentation depth and public appreciation still lag behind those of pre-modern monuments. By contrast, ordinary residential and non-residential buildings without any protective status constitute the numerically dominant share of the existing stock, and are themselves far from uniform: Annex I of the Energy Performance of Buildings Directive alone distinguishes single- and multi-family houses from offices, educational buildings, hospitals, hotels, and several other typologies (European Commission, 2010), a diversity mapped at European scale by comprehensive stock surveys such as the Buildings Performance Institute Europe's Europe's Buildings under the Microscope (BPIE, 2011). For this category, renovation is governed primarily by energy and safety regulation rather than by conservation doctrine, in the EU, principally the Energy Performance of Buildings Directive (Directive (EU) 2024/1275, recast).

These two regulatory logics, heritage protection and sustainability-driven renovation, do not always operate in alignment, and their interaction has produced an evolving tension. On constrained heritage, conservation requirements frequently limit or forbid the most effective envelope-level interventions, external insulation, façade replacement, or the alteration of window openings, creating a persistent conflict with energy performance targets (Elnagar et al., 2021). Despite this tension has been actively renegotiated from a conservative logic (Venice Charter, ICOMOS, 1964) to a readaptation logic (Leeuwarden Declaration, Architects' Council of Europe, 2018), European policy itself acknowledges the underlying conflict structurally: protected and historic buildings are largely exempted from the strictest requirements of the recast Energy Performance of Buildings Directive (Directive EU 2024/1275). Because international charters are not binding, however, the practical balance between

protection and performance is in fact struck at national level, and differently across Europe. This divergence means that instead of following a single European standard, individual renovation projects must resolve the trade-off between historic preservation and energy efficiency case by case.



Figure 1.1 – Heterogeneity of the built environment: Verona historic centre (left); multistorey residential buildings in Trento (right). Pictures by the author.

1.2. Decarbonization

Following the European Green Deal (European Commission, 2019), decarbonization is here understood as the systematic reduction of greenhouse gas emissions associated with a sector's energy use, materials, and processes, pursued with the aim of achieving economy-wide climate neutrality by 2050.

Applied to the built environment, the decarbonization objective can be pursued through several complementary and interdependent strategies, which recent reviews organize into a roughly sequential hierarchy: passive design measures acting on building form and envelope, improved thermal inertia, natural ventilation, and shading, to reduce demand before any active system is considered, consistently shown to lower both heating and cooling loads across a range of climates (Hu et al., 2023); the improvement of building envelopes and technical systems (insulation, glazing, HVAC, lighting); the integration of renewable energy generation, typically photovoltaic or solar-thermal, to cover residual demand; and the digital optimization of building operation through monitoring and predictive control (Akrofi & Okitasari, 2025).

Renovation of the existing stock occupies a distinctive position within this hierarchy, because most of the strategies above can be meaningfully deployed by intervening on buildings that already exist. This is reinforced by life-cycle and circular-economy considerations, which EU policy has begun to formalize beyond the scale of individual products, most recently through the Ecodesign for Sustainable Products Regulation, extending eco-design requirements toward the building components used in renovation (European Commission, ESPR). Demolition and reconstruction entail an immediate release of the carbon already embodied in the existing fabric and an acceleration of land consumption, whereas retaining and adapting existing structures preserves embodied carbon and allows urban densification to proceed

by extending existing volumes rather than consuming new soil, in line with the EU's "no net land take" target for 2050. Recent life-cycle assessments of renovation scenarios, however, complicate a purely favourable reading of this strategy: façade refurbishment can lower cumulative lifecycle emissions while simultaneously increasing material use and cost, and circular strategies, component reuse, material recovery, and design for disassembly, increasingly organized around modular, replaceable building components (Machado & Morioka, 2021), can offset a substantial share, but not all, of the additional material footprint that deep renovation entails (Zhang et al., 2025). Achieving decarbonization through renovation therefore requires the simultaneous management of operational and embodied carbon, rather than the optimization of operational energy performance alone (Zhang et al., 2025).

The literature on existing buildings distinguishes between several processes that commonly refer to as renovation (Shahi et al., 2020). Refurbishment denotes improving a building's existing conditions for its existing use, potentially including energy-efficient upgrades and renewable energy production. Retrofitting more specifically targets the addition of features or capacities absent at construction, typically concentrated on envelope, systems, and renewable integration. Rehabilitation addresses deteriorating or damaged buildings, often extending to structural elements. Adaptive reuse and conversion instead change a building's function altogether, maximizing the retention of existing material and structure. Finally, material reuse operates at component scale, recovering and repurposing individual elements across different buildings.

Even where individual strategies are technically well understood, their deployment at the scale required by EU targets is far from automatic. Deep renovation projects, those combining several of the strategies above to achieve

substantial performance gains, continue to face persistent technical, financial, and social barriers, including fragmented supply chains, uncertain returns on investment, and occupant resistance to prolonged or disruptive works (D'Oca et al., 2018).

These barriers do not fall evenly across the existing stock. While they are compounded on protected heritage by conservation constraints, unconstrained ordinary stock faces a different obstacle, less regulatory than logistical and economic: traditional on-site renovation is slow, disruptive to occupants, and difficult to standardize across a large building stock, where efficiency gains from repetition are precisely what conventional site-based methods struggle to capture. This mismatch between the scale of the renovation challenge and the artisanal, project-by-project nature of on-site work has motivated growing interest in industrialized, off-site approaches to retrofitting, in which prefabricated envelope and façade components, plug-and-play modular systems, or fully engineered façade units are manufactured under controlled conditions and installed with minimal on-site disruption (Malacarne et al., 2016; Du et al., 2019; Torres et al., 2021; Rovers et al., 2018). Such industrialized renovation packages report substantially compressed construction timelines relative to conventional retrofit, offering a credible route to reconciling deep renovation with occupied, repetitive building stock (Masera et al., 2014; Pernetti et al., 2021).

These advantages, however, come with their own set of limitations that continue to constrain uptake. Prefabricated solutions still carry significantly higher upfront costs than conventional retrofit, which are not always offset by the time savings achieved on site. Off-site manufacturing also demands a level of dimensional and geometric precision, both in the survey of the existing building and in the fabrication of components, that is difficult to guarantee across a heterogeneous and often poorly documented existing stock,

where minor discrepancies can compromise fit and installation. Realizing the benefits of industrialized retrofit therefore requires construction enterprises to adopt production models closer to manufacturing than to traditional site-based practice, entailing investments in design, tooling, and workflows that many actors in a fragmented supply chain are not yet equipped to make (Masera et al., 2014; Pernetti et al., 2021).
Across all the conditions of the existing stock, what varies is therefore not the ultimate objective, but the specific technical, regulatory, and informational requirements that a renovation process must satisfy at each phase.

1.3. Digitization

Digitization does not operate as a self-contained technical development. EU policy itself frames it alongside renovation as part of a single agenda for the built environment: the Renovation Wave strategy explicitly names sustainable renovation, digitization, and the protection of cultural heritage value as interdependent objectives rather than separate tracks (European Commission, COM 2020 662), positioning the sector's digital and ecological transformations as mutually reinforcing rather than competing priorities. Digitization of the built environment, in this sense, can be understood as the act of recording, representing, analysing or managing buildings, through the adoption of digital tools and techniques, a transformation the construction sector has undergone unevenly and comparatively late relative to other industries (Daniotti et al., 2020).
Before turning to individual methodologies adopted in the AEC sector, it is useful to distinguish the components that, in varying combinations, constitute any digitization strategy for the built environment: data acquisition and processing, i.e. the collection of geometric, material, and performance information about the existing building; the structuring of this

data into digital models, which can vary in geometric level of detail and semantic richness, from bi-dimensional drawings to parametric, information-rich models; and digital management, monitoring and sharing of information across the asset's life cycle, from design through operational management (facility management, maintenance, monitoring).

A literature review regarding digital technologies applied to construction confirms that it span a broad and heterogeneous spectrum (Manzoor et al., 2021). Digitization approaches exist that offer solutions oriented toward the urban scale and integrated with GIS systems and continuous management platforms based on digital twins, whose adoption in the construction sector nonetheless remains associated with significant technical and organisational challenges (Shahzad et al., 2022). Within the specific domain of existing building stock renovation, several authors frame digitization as a heterogeneous set of tools whose effective use depends on the purpose of the intervention process, rather than a single prescribed pathway (Cinquepalmi et al., 2023; Elagiry et al., 2020). In this context, Building Information Modelling (BIM) is a central component of this spectrum, and is examined separately below once the preceding stage of the process, data acquisition has been outlined.

Digital acquisition of the existing built environment

The main techniques employed for the digital acquisition of the existing built environment can be briefly and systematically outlined. Terrestrial laser scanning (TLS) captures geometry through ground-based laser scanning, producing high-density point clouds with millimetric precision and proving particularly well suited to the documentation of interiors and complex architectural elements (Valero, Bosché & Bueno, 2022; Conti et al., 2024). Digital photogrammetry, based on Structure from Motion (SfM) algorithms, reconstructs three-dimensional geometry from overlapping sets of photographic images

processed through automated correlation; it is generally more affordable than laser scanning, with performance that is comparable on geometries of moderate complexity (Remondino, 2011; Fassi et al., 2013). Aerial, drone-based photogrammetry (UAV/ortho-photogrammetry) extends this approach through remotely piloted aerial platforms, and is used above all for roofs, building envelopes, and sites that are difficult to access or extensive in scale (Gilmour & Stroulia, 2022). Mobile mapping and SLAM-based systems, including handheld or wearable laser scanners, acquire point clouds while in motion through Simultaneous Localization and Mapping techniques, reducing survey time relative to static TLS at the cost of generally lower accuracy (Sammartano & Spanò, 2018; Di Stefano et al., 2021). These techniques are not mutually exclusive: current practice frequently combines them, for instance pairing terrestrial laser scanning with drone-based photogrammetry, to balance accuracy, cost, and acquisition time according to the scale and purpose of the project.

The integration of survey data into an information model, commonly referred to as scan-to-BIM, constitutes the stage at which raw data acquired through the techniques above is structured into a semantically enriched model, a step that requires dedicated conversion procedures and remains an active area of methodological development (Quattrini et al., 2015; Sanhudo et al., 2020; Ursini et al. 2022). It is with this transition, from geometric acquisition to structured digital model, that BIM properly enters the discussion (Brumana, et al. 2022).

Building Information Modelling: from modelling to information management

Within the AEC sector specifically, BIM has emerged as the principal driver of this transition, serving both as a tool and as a methodology spanning multiple phases of the analysis, design and production process. It is formally standardised at international level through the ISO 19650 series (International

Organization for Standardization, 2018), which defines principles for organising and digitising information about buildings and civil engineering works across the delivery and operational phases of an asset. In Italy, this international framework is complemented by the national standard UNI 11337, which specifies digital management requirements for the domestic construction sector.

While BIM was originally developed for new construction, where the model can be built concurrently with, and as a direct driver of, the design and construction process, its application to existing buildings requires a fundamentally different logic: the model must be reconstructed retrospectively from survey data, and its reliability depends entirely on the acquisition and interpretation processes that generated it (Volk et al., 2014).

This retrospective condition has produced domain-specific declinations of BIM. Historic or Heritage Building Information Modelling (HBIM) extends BIM through libraries of parametric objects derived from historical architectural treatises, mapped onto laser-scanning or photogrammetric survey data, explicitly to support the documentation and conservation of heritage structures (Dore & Murphy, 2017; López et al., 2018). More recent developments have extended this strand both methodologically, refining the processes that translate survey data into semantic models (Croce et al. 2019; Brumana et al. 2022), and critically, highlighting the still-open limitations of the approach in terms of geometric accuracy, semantic richness, and interoperability (Radanovic, Khoshelham & Fraser, 2020; Ávila et al., 2024; Lovell, Davies & Hunt, 2023).

More broadly, the modelling of any pre-existing, non-heritage asset, here understood as Existing Building Information Modelling (EBIM), inherits the same retrospective logic without necessarily requiring the same conservation-oriented semantic apparatus, but introduces distinct challenges of scalability, since ordinary buildings are numerous, individually under-documented, and cannot always economically justify

the survey effort dedicated to a single monument (Sanhudo et al., 2018).
The potential of digitization for existing buildings is substantial, but it is not automatically realised (Habibi, 2017). The gap between technological availability and effective use is corroborated empirically: even where digital tools are formally available, their adoption across a fragmented renovation supply chain remains inconsistent, with practitioners reporting persistent organisational and process-level barriers rather than purely technical ones (Lasarte et al., 2021). Existing regulations and guidelines, ISO 19650 internationally and UNI 11337 in Italy, provide a framework for managing information requirements, but remain largely agnostic to the specific challenges of existing, as opposed to new, assets, leaving open the question of how much and what kind of information a given renovation purpose actually requires (Abualdenien & Borrmann, 2022). This open question is precisely where the intersection between digitization and decarbonization, discussed in the following section, becomes problematic in practice.

1.4. Decarbonization through digitization for the built environment

The three fields outlined so far are not independent. The heterogeneity of the existing stock is one of the reasons that makes a single decarbonization pathway insufficient. Digitization has been proposed, at policy level, as the connective infrastructure capable of absorbing this heterogeneity, providing the information base on which a differentiated renovation strategy can be grounded (European Commission, COM(2020) 662). Whether digitization practice actually delivers this remains, however, an open question.
Recent developments suggest the technical means are increasingly available: acquisition and processing tools continue to improve in accuracy and automation, and BIM is

progressively being coupled with complementary technologies, augmented and virtual reality, artificial intelligence and machine learning, to extend what a digital model can support beyond static documentation (Shahzad et al., 2022; Rashidi et al., 2024). At the same time, growing attention to the appropriate level of detail, development, and information need shows an awareness that models must be calibrated to their purpose rather than maximized indiscriminately (Abualdenien & Borrmann, 2022).

Two gaps, however, prevent this technical progress from translating into reliable practice. First, no standardized specification yet exists for models of existing buildings comparable to what design-stage BIM has achieved for new construction: the appropriate level of development is still negotiated case by case against the specific energy-modelling task at hand, rather than against a shared benchmark (Abualdenien & Borrmann, 2022; Jung et al., 2023; Stegnar & Cerovšek, 2019; Penjor et al., 2024). Second, and more critically, most proposed frameworks remain methodologically fragmented and untested across the whole renovation workflows: their benefits rarely withstand contact with the different actors, designers, energy modellers, contractors, facility managers, who must actually use them across a project's life cycle. This is corroborated empirically: even where digital tools are formally available, their adoption across a fragmented renovation supply chain remains inconsistent, with practitioners reporting persistent organisational and process-level barriers rather than purely technical ones (Lasarte et al., 2021; Daniotti et al., 2021; Doukari et al., 2024). It is this second gap, more than any shortage of technical capability, that limits digitization's ability to function as the connective infrastructure described above.

These reflections, together with the gaps identified above, allow the research questions that will guide the rest of this

thesis to be fixed, and are addressed in turn in the following chapter.

References chapter 1

Abualdenien, J., & Borrmann, A. (2022). Levels of detail, development, definition, and information need: A critical literature review. Journal of Information Technology in Construction, 27, 363–392. https://doi.org/10.36680/j.itcon.2022.018

Architects' Council of Europe. (2018). Leeuwarden Declaration: Statement on the adaptive re-use of the built heritage. Architects' Council of Europe.

Armijo, A., Elguezabal, P., Lasarte, N., & Weise, M. (2021). A methodology for the digitalization of the residential building renovation process through OpenBIM-based workflows. Applied Sciences, 11(21), 10429. https://doi.org/10.3390/app112110429

Ávila, F., Blanca-Hoyos, Á., Puertas, E., & Gallego, R. (2024). HBIM: Background, current trends, and future prospects. Applied Sciences, 14(23), 11191. https://doi.org/10.3390/app142311191

Blake, J. (2000). On Defining the Cultural Heritage. International and Comparative Law Quarterly, 49(1), 61–85. doi:10.1017/S002058930006396X

Brumana, R., Stanga, C., & Banfi, F. (2022). Models and scales for quality control: Toward the definition of specifications (GOA-LOG) for the generation and re-use of HBIM object libraries in a Common Data Environment. Applied Geomatics, 14(S1), 151–179. https://doi.org/10.1007/s12518-020-00351-2

Buildings Performance Institute Europe. (2011). Europe's buildings under the microscope: A country-by-country review of the energy performance of buildings. Buildings Performance Institute Europe (BPIE).

Cinquepalmi, F., Paris, S., Pennacchia, E., & Tiburcio, V. A. (2023). Efficiency and sustainability: The role of digitization in re-inhabiting the existing building stock. Energies, 16(9), 3613. https://doi.org/10.3390/en16093613

Congress on the European Architectural Heritage. (1975, October 21–25). Amsterdam Declaration. Council of Europe. https://rm.coe.int/090000168092ae41

Conti, A., Pagliaricci, G., Bonora, V., & Tucci, G. (2024). A comparison between terrestrial laser scanning and hand-held mobile mapping for the documentation of built heritage. The International Archives of the Photogrammetry, Remote Sensing and Spatial Information Sciences, XLVIII-2-W4-2024, 141–147. https://doi.org/10.5194/isprs-archives-XLVIII-2-W4-2024-141-2024

Council of Europe. (1985). Convention for the protection of the architectural heritage of Europe (Granada Convention). https://rm.coe.int/168007a087

Council of Europe. (1991). Recommendation No. R(91)13 on the protection of the twentieth-century architectural heritage. Committee of Ministers of the Council of Europe.

Council of Europe. (2005). Framework Convention on the value of cultural heritage for society (Faro Convention).

D'Oca, S., Ferrante, A., Ferrer, C., Pernetti, R., Gralka, A., Rizal, S., & Op 't Veld, P. (2018). Technical, financial, and social barriers and challenges in deep building renovation: Integration of lessons learned from the H2020 cluster projects. Buildings, 8(12), 174. https://doi.org/10.3390/buildings8120174

Daniotti, B., Bolognesi, C. M., Lupica Spagnolo, S., Pavan, A., Signorini, M., Ciuffreda, S., Mirarchi, C., Lucky, M. N., Andersson, B., Andersson, P., Valra, A., Madeddu, D., Chiappetti, J., Farina, D., O'Regan, B., O'Leidhin, E., Tahir, F., Mould, K., O'Donovan, S., … O'Sullivan, D. (2021). An interoperable BIM-based toolkit for efficient renovation in buildings. Buildings, 11(7), 271. https://doi.org/10.3390/buildings11070271

Daniotti, B., Pavan, A., Lupica Spagnolo, S., Caffi, V., Pasini, D., & Mirarchi, C. (2020). Evolution of the building sector due to digitalization. In B. Daniotti, A. Pavan, S. Lupica Spagnolo, V. Caffi, D. Pasini, & C. Mirarchi (Eds.), BIM-based collaborative building process management (pp. 1–16). Springer International Publishing. https://doi.org/10.1007/978-3-030-32889-4_1

Di Stefano, F., Chiappini, S., Gorreja, A., Balestra, M., & Pierdicca, R. (2021). Mobile 3D scan LiDAR: A literature review. Geomatics, Natural Hazards and Risk, 12(1), 2387–2429. https://doi.org/10.1080/19475705.2021.1964617

Directive (EU) 2024/1275 of the European Parliament and of the Council of 24 April 2024 on the energy performance of buildings (recast). Official Journal of the European Union.

Directive 2010/31/EU of the European Parliament and of the Council of 19 May 2010 on the energy performance of buildings. Official Journal of the European Union.

Dore, C., & Murphy, M. (2017). Current state of the art historic building information modelling. The International Archives of the Photogrammetry, Remote Sensing and Spatial Information Sciences, XLII-2-W5, 185–192.

Doukari, O., Kassem, M., Scoditti, E., Aguejdad, R., & Greenwood, D. (2024). A BIM based tool for evaluating building renovation strategies: The case of three demonstration sites in different European countries. Construction Innovation, 24(1), 365–383. https://doi.org/10.1108/CI-12-2022-0314

Du, H., Huang, P., & Jones, P. (2019). Modular facade retrofit with renewable energy technologies: The definition and current status in Europe. Energy and Buildings, 205, 109543. https://doi.org/10.1016/j.enbuild.2019.109543

Elagiry, M., Dugue, A., Costa, A., & Decorme, R. (2020). Digitalization tools for energy-efficient renovations. The 8th Annual International Sustainable Places Conference (SP2020) Proceedings, 9. https://doi.org/10.3390/proceedings2020065009

Elnagar, E., Munde, S., & Lemort, V. (2021). Energy efficiency measures applied to heritage retrofit buildings: A simulated student housing case study in Vienna. Heritage, 4(4), 3919–3937. https://doi.org/10.3390/heritage4040215

ENEA & CTI (2025). Rapporto Annuale sulla Certificazione Energetica degli Edifici 2025.

https://www.efficienzaenergetica.enea.it/pubblicazioni/rapporto-annuale-sulla-certificazione-energetica-degli-edifici/rapporto-annuale-sulla-certificazione-energetica-degli-edifici-2025.html

European Commission (2010). Directive 2010/31/EU on the energy performance of buildings.

European Commission (2019). The European Green Deal. COM (2019) 640 final. Publications Office of the European Union.

European Commission (2020). A Renovation Wave for Europe – greening our buildings, creating jobs, improving lives. COM (2020) 662 final). Publications Office of the European Union.

European Commission (2020). Report from the Commission to the European Parliament and the Council. COM (2020) 326 final. Publications Office of the European Union.

European Commission (2024). European Building Stock Observatory. Retrieved from https://energy.ec.europa.eu/topics/energy-efficiency/energy-performance-buildings/eu-building-stock-observatory_en#objective

European Commission (2024). Ecodesign for Sustainable Products Regulation (ESPR). Retrieved from https://commission.europa.eu/energy-climate-change-environment/standards-tools-and-labels/products-labelling-rules-and-requirements/ecodesign-sustainable-products-regulation_en

Fassi, F., Fregonese, L., Ackermann, S., & Troia, V. (2013). Comparison between laser scanning and automated 3D modelling techniques to reconstruct complex and extensive cultural heritage areas. The International Archives of the Photogrammetry, Remote Sensing and Spatial Information Sciences, XL-5/W1. https://doi.org/10.5194/isprsarchives-XL-5-W1-73-2013

Gilmour, L., & Stroulia, E. (2022). Ortho-photogrammetry for prefabricated energy-efficiency retrofits. Automation in Construction, 134, 104082. https://doi.org/10.1016/j.autcon.2021.104082

Graham, B., & Howard, P. (2016). Heritage and identity. In B. Graham & P. Howard (Eds.), The Routledge research companion to heritage and identity (pp. 1–15). Routledge.

Guillet, A. L. (2007). Docomomo International: Modernity as Heritage. Journal of Architectural Conservation, 13(2), 151–156. https://doi.org/10.1080/13556207.2007.10785002

Habibi, S. (2017). The promise of BIM for improving building performance. Energy and Buildings, 153, 525–548. https://doi.org/10.1016/j.enbuild.2017.08.009

Harrison, R. (2012). Heritage: Critical approaches. Routledge.

Hu, M., Zhang, K., Nguyen, Q., & Tasdizen, T. (2023). The effects of passive design on indoor thermal comfort and energy savings for residential buildings in hot climates: A systematic review. Urban Climate, 49, 101466. https://doi.org/10.1016/j.uclim.2023.101466

ICOMOS. (1994). The Nara document on authenticity. ICOMOS/UNESCO.

ICOMOS. (2011, November 11). The Athens Charter for the restoration of historic monuments – 1931. https://www.icomos.org/en/167-theathens-charter-for-the-restoration-of-historic-monuments

ICOMOS. (1964). The Venice Charter: International charter for the conservation and restoration of monuments and sites. https://www.icomos.org/en/participer/179-articles-enfrancais/ressources/charters-and-standards/157-thevenice-charter

International Conference on Conservation. (2000). Charter of Krakow. http://artalice.net/wp-content/uploads/2020/01/KRAKOV-CHARTER-2000.pdf

International Organization for Standardization. (2018). Organization and digitization of information about buildings and civil engineering works, including building information modelling (BIM) — Information management using building information modelling — Part 1: Concepts and principles (ISO 19650-1:2018).

ISTAT (2024). Rapporto annuale 2024 La situazione del Paese. https://www.istat.it/it/files/2024/05/Rapporto-Annuale-2024.pdf

Jung, D. E., Kim, S., Han, S., Yoo, S., Jeong, H., Lee, K. H., & Kim, J. (2023). Appropriate level of development of in-situ building information modeling for existing building energy modeling implementation. Journal of Building Engineering, 69, 106233. https://doi.org/10.1016/j.jobe.2023.106233

Konsa, K. (2013). Heritage as a socio-cultural construct: Problems of definition. Baltic Journal of Art History, 6, 125–151.

Lasarte, N., Elguezabal, P., Sagarna, M., Leon, I., & Otaduy, J. P. (2021). Challenges for Digitalisation in Building Renovation to Enhance the Efficiency of the Process: A Spanish Case Study. Sustainability, 13(21), 12139. https://doi.org/10.3390/su132112139

Legislative Decree 22 January 2004, n. 42. Codice dei beni culturali e del paesaggio, ai sensi dell'articolo 10 della legge 6 luglio 2002, n. 137. Gazzetta Ufficiale della Repubblica Italiana.

Legislative Decree 24 March 2006, n. 156. Disposizioni correttive ed integrative al decreto legislativo 22 gennaio 2004, n. 42. Gazzetta Ufficiale della Repubblica Italiana.

Legislative Decree 26 March 2008, n. 62. Ulteriori disposizioni integrative e correttive del decreto legislativo 22 gennaio 2004, n. 42. Gazzetta Ufficiale della Repubblica Italiana.

Legislative Decree 31 March 1998, n. 112. Conferimento di funzioni e compiti amministrativi dello Stato alle regioni ed agli enti locali, in attuazione del capo I della legge 15 marzo 1997, n. 59. Gazzetta Ufficiale della Repubblica Italiana.

López, F. J., Lerones, P. M., Llamas, J., Gómez-García-Bermejo, J., & Zalama, E. (2018). A review of heritage building information modeling (H-BIM). Multimodal Technologies and Interaction, 2(2), 21. https://doi.org/10.3390/mti2020021

Lovell, L. J., Davies, R. J., & Hunt, D. V. L. (2023). The application of historic building information modelling (HBIM) to cultural heritage: A review. Heritage, 6(10), 6691–6717. https://doi.org/10.3390/heritage6100350

Machado, N., & Morioka, S. N. (2021). Contributions of modularity to the circular economy: A systematic review of literature. Journal of

Building Engineering, 44, 103322. https://doi.org/10.1016/j.jobe.2021.103322

Malacarne, G., Monizza, G. P., Ratajczak, J., Krause, D., Benedetti, C., & Matt, D. T. (2016). Prefabricated timber façade for the energy refurbishment of the Italian building stock – The Ri.Fa.Re. project. Energy Procedia, 96, 788–799. https://doi.org/10.1016/j.egypro.2016.09.141

Manzoor, B., Othman, I., & Pomares, J. C. (2021). Digital technologies in the architecture, engineering and construction (AEC) industry—A bibliometric—qualitative literature review of research activities. International Journal of Environmental Research and Public Health, 18(11), 6135. https://doi.org/10.3390/ijerph18116135

Marsden, S., and Spearritt, P. (2021). The Twentieth-Century Historic Thematic Framework: A Tool for Assessing Heritage Places. Los Angeles: Getty Conservation Institute.

Masera, G., Iannaccone, G., & Salvalai, G. (2014). Retrofitting the existing envelope of residential buildings – Innovative technologies, performance assessment and design methods. In Advanced Building Skins Conference Proceedings of the 9th Energy Forum (pp. 987–994). Economic Forum. https://doi.org/10.13140/RG.2.1.2543.0887

Pernetti, R., Pinotti, R., & Lollini, R. (2021). Repository of deep renovation packages based on industrialized solutions: Definition and application. Sustainability, 13(11), 6412. https://doi.org/10.3390/su13116412

Penjor, T., Banihashemi, S., Hajirasouli, A., & Golzad, H. (2024). Heritage building information modeling (HBIM) for heritage conservation: Framework of challenges, gaps, and existing limitations of HBIM. Digital Applications in Archaeology and Cultural Heritage, 35, e00366. https://doi.org/10.1016/j.daach.2024.e00366

Quattrini, R., Malinverni, E. S., Clini, P., Nespeca, R., & Orlietti, E. (2015). From TLS to HBIM. High quality semantically-aware 3D modeling of complex architecture. The International Archives of the Photogrammetry, Remote Sensing and Spatial Information

Sciences, XL-5/W4, 367–374. https://doi.org/10.5194/isprsarchives-XL-5-W4-367-2015

Radanovic, M., Khoshelham, K., & Fraser, C. (2020). Geometric accuracy and semantic richness in heritage BIM: A review. Digital Applications in Archaeology and Cultural Heritage, 19, e00166. https://doi.org/10.1016/j.daach.2020.e00166

Rashidi, A., Sarvari, H., Chan, D. W. M., Olawumi, T. O., & Edwards, D. J. (2024). A systematic taxonomic review of the application of BIM and digital twins technologies in the construction industry. Engineering, Construction and Architectural Management. Advance online publication. https://doi.org/10.1108/ECAM-02-2024-0239

Remondino, F. (2011). Heritage recording and 3D modeling with photogrammetry and 3D scanning. Remote Sensing, 3(6), 1104–1138. https://doi.org/10.3390/rs3061104

Rovers, R., Lupíšek, A., Borodinecs, A., & Almeida, M. G. (2018). A guide into renovation package concepts for mass retrofit of different types of buildings with prefabricated elements for (n)ZEB performance.

Sammartano, G., & Spanò, A. (2018). Point clouds by SLAM-based mobile mapping systems: Accuracy and geometric content validation in multisensor survey and stand-alone acquisition. Applied Geomatics, 10(4), 317–339. https://doi.org/10.1007/s12518-018-0221-7

Sanhudo, L., Ramos, N. M. M., Martins, J. P., Almeida, R. M. S. F., Barreira, E., Simões, M. L., & Cardoso, V. (2020). A framework for in-situ geometric data acquisition using laser scanning for BIM modelling. Journal of Building Engineering, 28, 101073. https://doi.org/10.1016/j.jobe.2019.101073

Sanhudo, L., Ramos, N. M. M., Poças Martins, J., Almeida, R. M. S. F., Barreira, E., Simões, M. L., & Cardoso, V. (2018). Building information modeling for energy retrofitting – A review. Renewable and Sustainable Energy Reviews, 89, 249–260. https://doi.org/10.1016/j.rser.2018.03.064

Shahi, S., Esnaashary Esfahani, M., Bachmann, C., & Haas, C. (2020). A definition framework for building adaptation projects.

Sustainable Cities and Society, 63, 102345. https://doi.org/10.1016/j.scs.2020.102345

Shahzad, M., Shafiq, M. T., Douglas, D., & Kassem, M. (2022). Digital twins in built environments: An investigation of the characteristics, applications, and challenges. Buildings, 12(2), 120. https://doi.org/10.3390/buildings12020120

Stegnar, G., & Cerovšek, T. (2019). Information needs for progressive BIM methodology supporting the holistic energy renovation of office buildings. Energy, 173, 317–331. https://doi.org/10.1016/j.energy.2019.02.087

Torres, J., Garay-Martinez, R., Oregi, X., Torrens-Galdiz, I. J., Uriarte-Arrien, A., Pracucci, A., Casadei, O., Magnani, S., Arroyo, N., & Cea, A. M. (2021). Plug and play modular façade construction system for renovation for residential buildings. Buildings, 11(9), 419. https://doi.org/10.3390/buildings11090419

UNESCO. (2023). World Heritage. https://www.unesco.org/en/worldheritage

Valero, E., Bosché, F., & Bueno, M. (2022). Laser scanning for BIM. Journal of Information Technology in Construction, 27, 486–495. https://doi.org/10.36680/j.itcon.2022.023

Vecco, M. (2010). A definition of cultural heritage: From the tangible to the intangible. Journal of Cultural Heritage, 11(3), 321–324. https://doi.org/10.1016/j.culher.2010.01.006

Volk, R., Stengel, J., & Schultmann, F. (2014). Building information modeling (BIM) for existing buildings—Literature review and future needs. Automation in Construction, 38, 109–127. https://doi.org/10.1016/j.autcon.2013.10.023

Zhang, T., Yang, X., Wu, Z., Zhai, G., Doan, D. T., Sun, Q., & Gao, H. (2025). Application of building information modeling for energy efficiency: A systematic review. Buildings, 15(20), 3722. https://doi.org/10.3390/buildings15203722

2. Research questions

The considerations developed in the previous chapter converge on three research questions, each addressing a distinct stage of the acquisition-to-use chain that digitization for the built environment entails, and each investigated through the experimentation conducted on three case studies.

RQ1. *How does the methodology adopted for data acquisition affect the construction of digital models useful for supporting renovation processes?*

Digital acquisition techniques, including terrestrial laser scanning, photogrammetry, UAV-based survey, mobile mapping, differ substantially in precision, acquisition times, and cost. These differences do not remain confined to the survey stage: they propagate directly into the resulting digital model, shaping what that model can subsequently represent and support. Yet the relationship between a given acquisition methodology and the effectiveness of the model it produces is to be considered and analysed. RQ1 addresses this relationship directly, asking not simply which acquisition technique is most accurate in the abstract, but how the choice of methodology conditions the model that a renovation process actually receives. This question is investigated primarily through the first and third case studies (Chapter 3 and 5), where the geometric documentation of different building typologies isolates the acquisition-to-model link with comparatively few confounding variables.

RQ2. *What specific characteristics must a digital model have in order to support an energy retrofitting process in its various phases?*

Once a model exists, its usefulness is not automatic: the absence of a standardized specification for existing-building models means that the appropriate level of detail, development, and information content is still negotiated case by case rather than derived from a shared benchmark. This is

particularly consequential for energy retrofitting, a process that unfolds across distinct phases, such as diagnosis, scenario comparison, detailed design, each of which may require different information from the same underlying asset. RQ2 asks what characteristics, geometric, semantic, and organisational, a digital model must have to remain useful as a retrofit process moves through these phases, rather than being calibrated to only one of them. This question is investigated primarily through the second case study (Chapter 4), where the informative, multi-criteria comparison of retrofit scenarios for a modern heritage complex requires a model capable of supporting several evaluation criteria simultaneously.

RQ3. *How can the usability and interoperability of EBIM models be guaranteed for users with different skills and needs?*
Even a well-calibrated model is of limited value if it cannot remain legible and usable as it moves from the actor who produced it to the actors who must act on it, designers, energy modellers, contractors, facility managers, each approaching the model with different tools, expertise, and objectives. This is the gap identified as most critical in the preceding chapter: most proposed frameworks are validated, if at all, against a single use case, leaving open whether their benefits survive the handoff between different actors across a project's life cycle. RQ3 addresses this directly, asking how usability and interoperability can be guaranteed, rather than assumed, for users with different skills and needs. This question is investigated primarily through the third case study (Chapter 5), where a design-oriented, production-integrated workflow for a prefabricated retrofit requires the same model to be read and acted upon by designers and manufacturers alike.
Taken together, these three questions move from the origin of a digital model (RQ1), through its implementation to a specific renovation purpose (RQ2), to its utility across the different

actors who must use it once produced (RQ3), trying to give an answer to the gap highlighted in the previous chapter.

2.1. Structure of the case studies

The three case studies presented in Chapters 3 to 5 are organized to test these questions against different conditions of the existing stock and progressively more complex renovation objectives: from the geometric documentation of a single historical building, through the informative, multi-criteria comparison of retrofit scenarios for a modern heritage complex, to the design-oriented, production-integrated workflow required by a prefabricated retrofit of ordinary residential stock. Across the three, the same triad of acquisition, processing, and modelling phases is consistently examined, allowing the specific answers obtained in each context to be compared and, in conclusion, synthesized into a broader methodological framework for the development of digital models supporting the decarbonization of the built environment.

Disclaimer

This chapter is partially based on:

Maragno, A., Barbini, A., Bernardini, E., Chioni, C., Massari, G.A. (2024). *The measure for uncountable data from 3D digital survey. The case of the historical centre of Trento.*
In Bergamo F., Calandriello A., Ciammaichella M., Friso I., Gay F., Liva G., Monteleone C. (Eds.). *Measure/Out of Measure. Transitions. Proceedings of the 45th International Conference of Representation Disciplines Teachers*. Milano: FrancoAngeli.

Bernardini, E., Chioni, C., Massari, G. A., Vattano, S. (in press*). Four graphic dichotomies for a model.* In *Proceedings of eXploRA. Virtual journeys to discover Drawing's hidden layers*, 15 May 2026, Roma (Italy).

3. Geometric models to support historical heritage knowledge. A case study in Calliano (TN)

This chapter focuses on the first research question through the analysis of an instance of historical heritage. Specifically, it explores how data acquisition strategies influence the generation of digital models and, consequently, their applicability in renovation processes.
The content is organized into two distinct sections. The opening section establishes the theoretical framework, highlighting heritage knowledge as a prerequisite for any intervention on existing structures. It examines the concepts of architectural model and representation in relation to data acquisition and processing techniques, offering a critical reflection on both the nature of the information collected and the parameters used for its assessment.
The second section focuses on the *Casa Demartin* case study. This experimentation serves to investigate the direct impact of different survey choices on building representation and feature comprehension. By describing and comparing different workflows for data acquisition, processing and integration, and consistent results, this section evaluates appropriate strategies for historical assets. Through this analysis, the chapter discusses the potentials and limitations of digital representation methods in supporting knowledge-oriented approaches to the built heritage.
This case study originated as a didactic survey activity, later expanded into a master thesis cantered on structural renovation. Rather than developing a final design proposal, the current study investigates the specific conditions under which geometric models can effectively enhance the understanding of an existing building, providing essential foundation for future design phases.

3.1. Theoretical framework. From data acquisition to knowledge representation

3.1.1. Heritage knowledge: a prerequisite for initiating adaptation processes

Heritage buildings are complex, stratified organisms, shaped by a continuous succession of human interventions, environmental factors, and the passage of time. Investigating these structures often reveals significant challenges, such as a lack of documentation, uncertainty regarding original construction techniques, discrepancies between archival designs and actual execution, or the presence of undocumented modifications. These gaps inevitably hinder a comprehensive understanding of a building's true characteristics, structural behaviour, and state of conservation. Before initiating any design activity, it is essential to establish a targeted framework of knowledge regarding the object of intervention. Within this knowledge framework, it is possible to identify at least three primary knowledge practices involving an increasing level of depth: description, measurement, and classification (Massari, 1998; Barbini, 2024). Description is derived from direct observation or existing documentation and it is used to identify distinct, measurable properties. Measurement evaluates the specific intensity of a single property across different objects (Cunietti, 1979). Classification links objects together based on common attributes, organizing them into homogeneous categories (Monti, 1988). Representation, intended both as conceptual, theoretical framework and as graphic, visual expression (Ugo 1994), serves as a primary tool to operationalize these practices. The process of representing itself, in fact, not only implies the act of describing, measuring, and classifying, but also materializes and communicates their results. This interpretation of representation as a tool to imitate and reveal an object's true essence introduces a built-in paradox: while

depictions of reality are deeply dissimilar from how things actually stand, they function as a practical facsimile of it, even though the congruence between the model and the physical object inevitably remains imperfect (Geymonat & Giorello, 1980).

Regarding architectural objects, representation entails the recording and reconstruction of spatial forms through models that create a scientific link between the physical object and specific measurement units (Ugo, 1994). In this context, the concept of "form" extends beyond mere volumetric configuration to encompass the combination of dimensions and the specific ways an object exists in space, including its relationships with history and the surrounding context (Ugo, 1994; Migliari 2003). Since 'form' consists of multifaceted layers, establishing a precise scientific correspondence between the physical object, the model, and its representation necessitates the prior definition of dimensions, measurement units, and the logical structures that ensure consistency in the final depiction (Massari, 1998).

Generally, any tangible or intangible phenomenon can be represented through countless features. These attributes can be quantitative, implying direct measurements and counting of intrinsic properties, or qualitative, artificially defining comparable and classifiable non-numerical, descriptive characteristics (de Rubertis, 1995; Barbini, 2024). The formalization and synthesis of these attributes provide the very foundation for building models. As theoretical devices, models operate to fix the relationships between reality and its cognitive interpretations (Geymonat & Giorello, 1980). Depending on the adopted approach, they can fulfil various functions, such as explanation, demonstration, operational guidance, discovery, simulation, or the forecasting of specific phenomena (Barbini, 2024). Due to the variety of scopes these devices can cover, they can range from highly rigorous scientific structure, such as mathematical models, that

rationally abstract physical phenomena and empirical data, to symbolic frameworks grounded in metaphysical or meta-rational language, such as myths (Ugo, 1994). Regardless of a model's specific goal or nature, however, it must inherently address two fundamental motivations of theoretical elaboration: the synthesis of knowledge into a unified structure and the clarity of explanatory frameworks (Delattre, 1981). Ultimately, to be defined as such, any model must rely on recognizable elements and intelligible rules, thereby ensuring its reproducibility and reusability for multiple investigative purposes (Massari, 2005).

3.1.2. Geometric models of existing buildings. Acquisition methods, evaluation parameters and possible outputs for heritage knowledge

Models constitute thus an operative syntax, providing a structured methodology for organizing elements and regulating their internal relationships. To translate built environments, typically perceived as a continuous physical reality, into functional models useful for the hermeneutical process, it is necessary to operate a critical discretization. As the fundamental mathematical language for spatial measurability, geometry represents the primary tool for decoding, analysing, and representing architectural organisms (Torsello, 1988). Through this process of abstraction, the heterogeneous features of built spaces can be transformed into a coherent system of numerical and graphic information, highlighting both specific building elements and the structural whole (Docci, 1993). Primitive geometric entities, including points, lines, surfaces, and volumes, enable the communication of space through their inherent schematic nature, defining the object in both qualitative and quantitative terms (De Carlo, 2011).
Operatively, architectural recording and discretization is implemented through a variety of survey techniques, which

can be fundamentally categorized based on their approach (direct or indirect), the nature of acquired data (qualitative or quantitative), spatial reach (global or punctual), and their impact on the fabric (invasive or non-destructive) (Torsello, 1988). Among discrete representations of architecture, point-based models typically coincide with the first result of elaboration of acquired data. They represent therefore the most straightforward output to generate, though their structural properties vary significantly depending on whether they originate from selective measurement techniques or automated digital acquisitions. Traditional techniques, such as longimetric and topographic surveys, adopt a punctual logic for harvesting specific coordinates and dimensions. Their application requires rigorous methodological planning and a deliberate selection of datasets, involving significant operational time. Direct longimetric surveys generate discrete datasets constrained to bidimensional planes, which require subsequent cognitive and graphical translation to schematize three-dimensional shapes. Topographic surveys capture a limited set of points coordinates directly within a three-dimensional reference frame (Figure 3.1).
Conversely, digital innovative tools, such as laser scanners and mobile LiDAR sensors integrated into portable devices, supports the harvesting of extensive datasets within restricted operational timeframes (Maragno et al., 2024; Chioni et al., 2023; Vacca, 2023). These result in high-density, three-dimensional point clouds organized into three-dimensional spaces. Similarly massive acquisition of photosets can be operated through digital cameras. In this case, resulting dense point clouds do not coincide directly with the raw output of the acquisition phase but derive from the photomodelling process (Figure 3.1).

However, the use of high-precision instruments and automatic elaboration processes does not ensure the transition from raw empirical data to effective architectural models, as knowledge does not simply emerge from the passive accumulation of information (Massari, 2005). The increasing accessibility of these digital tools instead demands a critical reflection on the explicit purpose of information relative to the survey objectives (Sultan, 2021; Barbini, 2024). For the act of documentation to remain meaningful, it must involve an intentional selection and an attribution of value (Ugo 1998). Consequently, data acquisition cannot be treated as a mechanical task independent of the object, but must be understood as a critical operation. Furthermore, an objective-oriented assessment of data is essential to move beyond mere volume and evaluate its qualitative essence (Cannarozzo & Salerno 1991; Massari 1998) and functional utility (Radanovic et al. 2020). Digital overabundance also complicates issues of long-term management, leaving heritage data vulnerable to technological obsolescence and format interoperability gaps (Guercio 2013; Weston 2013; Maragno 2024).

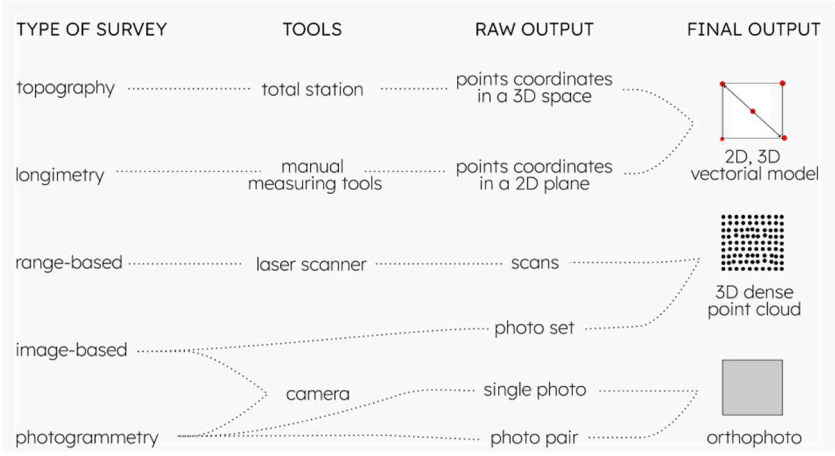

Figure 3.1 – Synthesis of possible acquisition techniques and respective results.

To address these challenges, as a first step it is possible to select some quantitative and qualitative features for the evaluation of the collected data. This assessment serves a twofold purpose: an a priori framework to guide the initial survey design by determining the actual necessity of massive data collection and an a posteriori application to analyse existing datasets for sustainable reuse (Maragno, 2024).
Given that diverse techniques frequently are used to document only partially overlapping fragments of the built environment, it is appropriate to evaluate specific parameters relative to the overarching survey objectives rather than the physical object alone. While each case study possesses unique characteristics requiring specific reflection, the use of calibrated parameters reduces arbitrary decision-making and informs the workflow across various phases. In this perspective, specific parameters that could be evaluated are metric reliability, geometric accuracy and density (Table 3.1).
Metric reliability indicates the possibility of deriving accurate measurements from acquired data. It can be verified by comparing a virtual measurement extracted from the acquired data against direct topographic or longimetric controls. Geometrical accuracy highlights the capability to extract realistic proportions, maintains geometric relationships among surveyed objects, and recognizes 3D geometries representing actual shapes. It provides qualitative scores to assess how faithfully the resulting model represents physical surfaces. Finally, density represents the richness of the data within a constant and predefined volume from a quantitative, therefore objective point of view.
Metric reliability, geometric accuracy and density of point clouds resulting from scans or photomodelling are a direct function of instrument settings and precision, and the quality of the acquisition and processing phases.

Table 3.1 – Quantitative and qualitative parameters to evaluate data acquired from 3D digital survey.

	Parameter	Description	Evaluation Criteria
Quantitative	Density	Represents the richness of the data depending on the "mass" of the data itself. It strongly influences visual fidelity and, in part, geometric accuracy.	Expressed as a numerical value, it indicates the number of points within a constant and predefined unit of volume (a sphere).
	Metric Reliability	Indicates the possibility of obtaining accurate measurements from the numerical model.	Expressed as a numerical value, it indicates the deviation (cm) from a dataset acquired and validated through a different method (e.g., topographic).
Qualitative	Geometric Accuracy	Expresses the possibility of obtaining realistic proportions of the surveyed objects, maintaining spatial relationships between them, and recognizing 3D geometries representative of the real shapes.	It can be expressed through scores. The minimum value indicates that it is not possible to identify the object's geometries; the maximum value indicates that they can be defined in detail.

It is worth highlighting that even scoring high metric reliability and geometric accuracy, point-based models do not automatically contain qualitative data, such as semantic information, if not supported by advanced semantic segmentation. Additionally, these kinds of discrete models present a notable limitation upon closer inspection, since they lack inherent structural detail. Changing the viewer orientation or zooming in, even the densest point cloud loses resolution, dissolving back into isolated points that do not allow for the recognition of architectural elements' precise edges (Barbini, 2024).

In light of these limitations, to achieve functional architectural knowledge, discrete models such as point clouds need to be transformed into continuous surface or solid-based models. Nevertheless, the initial digital datasets represent the primary, indispensable foundation for any subsequent geometric reconstruction. As the direct metric links to the physical reality of the building, they preserve unedited architectural complexities that continuous models might otherwise oversimplify. Consequently, dense discrete models deserve rigorous, standalone methodological attention, not merely as temporary intermediate steps, but as the primary repository of authentic spatial truth for built heritage.

3.2. Contextualisation. *Casa Demartin*, a historical landmark of the Vallagarina

Casa Demartin, historically known as Palazzo Pilosi, represents one of the most significant architectural expressions of the Renaissance in Calliano (Trento), within the Vallagarina valley (Dal Pra, 2009; Bottura, 2012). Commissioned in 1514 by Fabiano Pilosi, the building integrates seamlessly into the urban fabric, interacting directly with the public sphere through a prominent ground-floor portico (Figure 3.2).

At the end of the XVIII Century, the building passed to the Menegatti family, becoming a pharmacy on the ground floor. At the same time, the Demartin family rented a room in the same palace, starting a commercial business. This sharing of the building between the two families continued until the mid-nineteenth century, when Menegatti sold the entire palace to Demartin.

Today, the building consists of a single structure organized across three floors above ground, plus a basement and an attic, with a garden located at the rear. The portico consists of three semi-circular arches, supported by two central octagonal columns and corner pillars, and is made of white ammonitic limestone and *scaglia veneta* stone.



Figure 3.2 – Casa Demartin, the main façade with polychrome fresco and three-arch portico. Picture by LAMARC.

This covered entrance leads to two large rooms covered by barrel vault with lunettes, connected by segmental arch openings with splayed jambs (Figure 3.3). Inside, the ground floor preserves highly interesting vaulted rooms, which were likely intended from the very beginning for service and storage purposes. The basement houses a vaulted cellar, accessible via a stone staircase (Figure 3.3). The first floor, designed as a piano nobile, features a U-shaped gallery covered by a barrel vault with lunettes, facing the main facade through large windows (Figure 3.3). Throughout the 1960s, this floor underwent significant functional adaptation into a residential space, driven by the needs of the Demartin family. This marked profound structural and technical transformations of the building's original fabric and systems. The second floor

consists of a spacious hallway opening onto storage rooms and two east-facing balconies. The ceiling of these utility rooms is made of wooden floors, which show significant deformations (Figure 3.3). The third floor coincides with the building's attic, which finishes with a wooden roof structure, reinforced and partially replaced in the 1990s.

Over the centuries, extensive transformations have turned *Casa Demartin* into a highly stratified complex that nonetheless retains a legible core layout across its basement, three main floors, and attic. Its structure, decoration, and spatial organization reflect the progressive social and political consolidation of the commissioning family, offering a valuable insight into the architectural and construction evolution between the late Middle Ages and the Renaissance within the Trentino context.

Due to its complex geometry and its architectural values, the building serves as an ideal testbed, demanding for highly accurate representation. Through the investigation of this case study, key research questions emerge regarding the metric reliability, geometric accuracy, and visual fidelity required for the comprehension of historical heritage. This experimentation highlights thus how diverse data acquisition methodologies fundamentally shape architectural interpretation, demonstrating that geometric models function as interpretive theoretical devices rather than simple descriptive records. Grounded in this dialectic between mechanical data accumulation and intentional selection, the experimentation presented in the following paragraph aims to investigate operational approaches for transitioning from the empirical complexity of the physical asset to the structured synthesis of the virtual model. To address the challenges of digital overabundance and critical discretization, the methodological framework will evaluate two factors: the integrability of multi-source, heterogeneous datasets and the metric accuracy of the results.

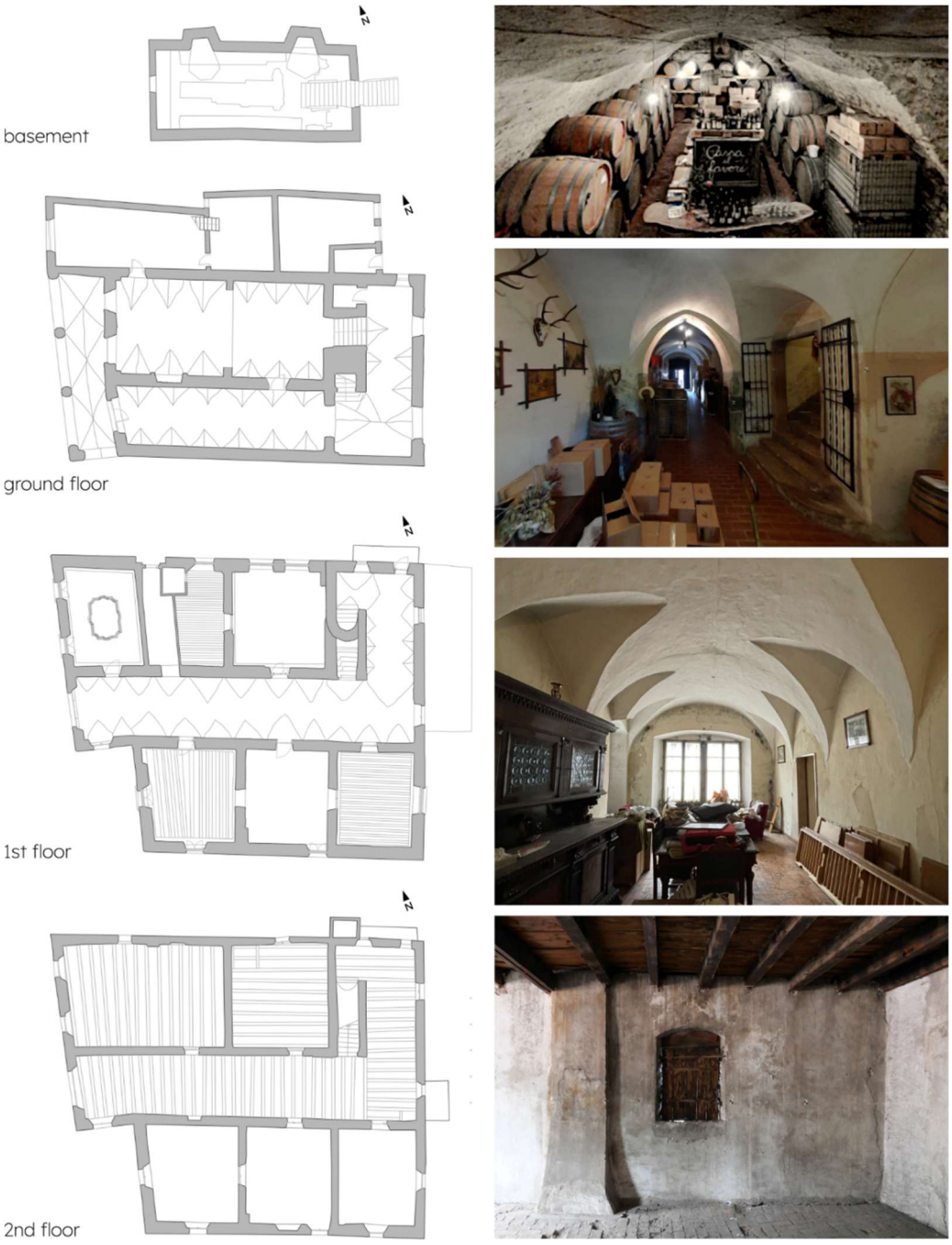

Figure 3.3 – Overview of the four main floors of Casa Demartin.
Elaborated by the author based on LAMARC materials.

3.3. Workflow. Knowledge for the evaluation of appropriate modelling strategies

Moving from the theoretical framework to an operative application, this section illustrates the empirical investigation conducted on *Casa Demartin*, detailing the diverse acquisition and processing workflows implemented and consistent results. Subsequently, the experimental techniques adopted are evaluated critically through the lens of parameters introduced in the previous section (Figure 3.4).

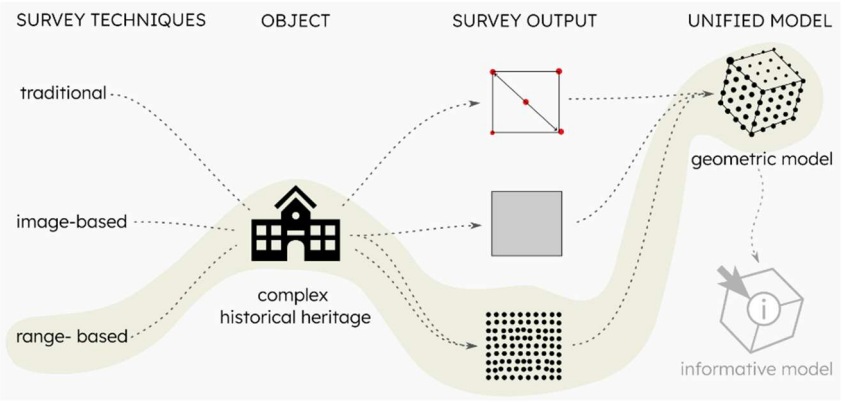

Figure 3.4 – Graphic synthesis of the applied workflow and chapter focus.

3.3.1. Data acquisition, processing and integration

The acquisition activities for this case study were conducted partly within the framework of the Architectural Survey course (A.Y. 2024/2025), and partly during an experimental campaign aimed at comparing traditional and innovative surveying methodologies (Table 3.2).

The primary framework for the building survey was established in the context of the didactic campaign. The educational workshop activities were conducted over a four-day period, totalling approximately 30 hours. The participants were organized into 21 groups of two or three people. Each group was assigned the survey of a portion of the building, employing various techniques and instruments.

Table 3.2 – Overview of acquisition campaigns conducted on the case study.

Type of campaign		Type of survey	Used instruments	Acquired data
Didactic		Topographic	TOPCON GPT 1001	**15** stations **247** points
		Image-based	Canon EOS 600D	**1248** photos
			Ricoh Theta V	**34** 3D photos **5** 3D videos
			3DEye system, Sony ILCE 6000	**610** photos
			TLS Faro S120	**26** scans
	Experimental	Range-based	MLS Gexcel Heron Twin Color	**1** scan **90** control points **90** 3D photos

Different methodologies adopted were alternately complementary, to ensure data completeness, and overlapping, in order to compare instrument precision and the accuracy of results. The operative division of the building into distinct portions was subordinated to the identification of common references across the various working groups, thus allowing the subsequent integration of independently recorded datasets.
In the following paragraphs a short overview of the activities carried out during the didactic survey campaign is presented.

Topographic survey. To ensure integrability and spatial consistency across heterogeneous datasets acquired during both the didactic and experimental campaigns, the methodological framework relies on a traditional topographic network. This provides a unique, mathematically rigorous 3D

reference frame. A topographic total station[1] was used to establish a net of 15 primary stations distributed across the basement, ground, first, and second floors (Figure 3.5). A dataset consisting of 247 discrete points was recorded across the primary three-story structure and the accessible external areas (Figure 3.6). This provides the essential topographic skeleton upon which all subsequent acquisition and processing activities were anchored.



Figure 3.5 – The topographic net. Stations 1000, 8000, 13000 and 14000 allow the connection among the three main floors. Elaborated by the author based on LAMARC materials.

[1] The total station used for this study is a Topcon GPT-1001, part of the equipment supplied by the LAMARC laboratory.

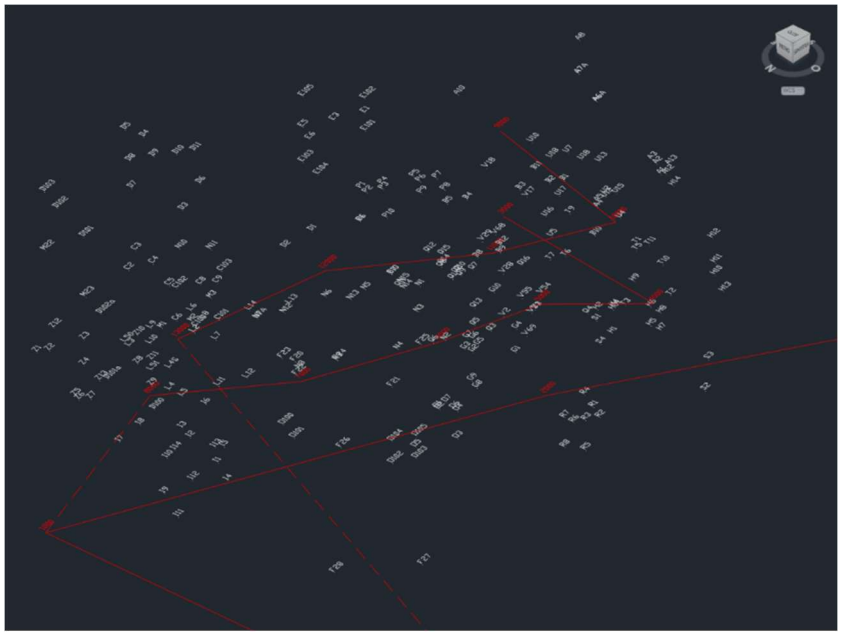

Figure 3.6 – The result of topographic survey in the 3D vectorial space. In red, the topographic stations. In grey the 247 recorded points. Elaborated by the author based on LAMARC materials.

Direct longimetric survey. Operating through a logic of useful reference planes, seamless across the whole building, levelled horizontal and vertical profiles were established, using laser levels, plumb lines, and physical benchmarks. Spatial boundaries and irregularities were traced using trilateration networks and local Cartesian coordinate grids (x, y) to map complex architectural elements like masonry deformations and vaults. These operations were initially supported by preliminary 2D proportionated but yet schematical hand-drawings, then enriched with alpha-numerical information derived from measurements (Figure 3.7 and Figure 3.8).

Once the measurements acquired and verified, they were individually transposed to the digital environment, based on the topographic network, and then integrated across the

different spaces, converging into a three-dimensional vectorial model[2] (Figure 3.9).

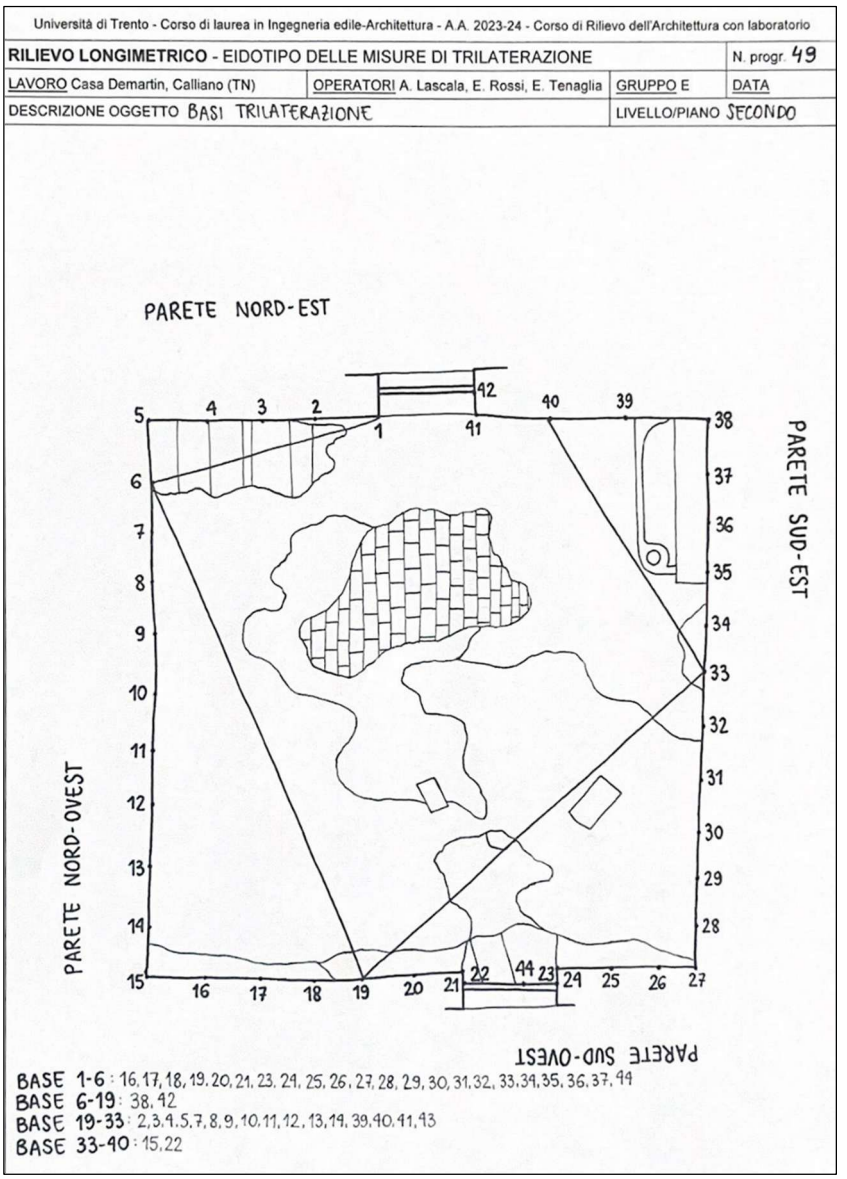

Figure 3.7 – Hand-drawn eidotype of the trilateration measurements showing the survey control points and trilateration bases used for the metric recording of one of the rooms of Casa Demartin. Students drawing.

[2] The digital environment used for the vectorial reconstruction of the case study is Autodesk AutoCAD 2024.

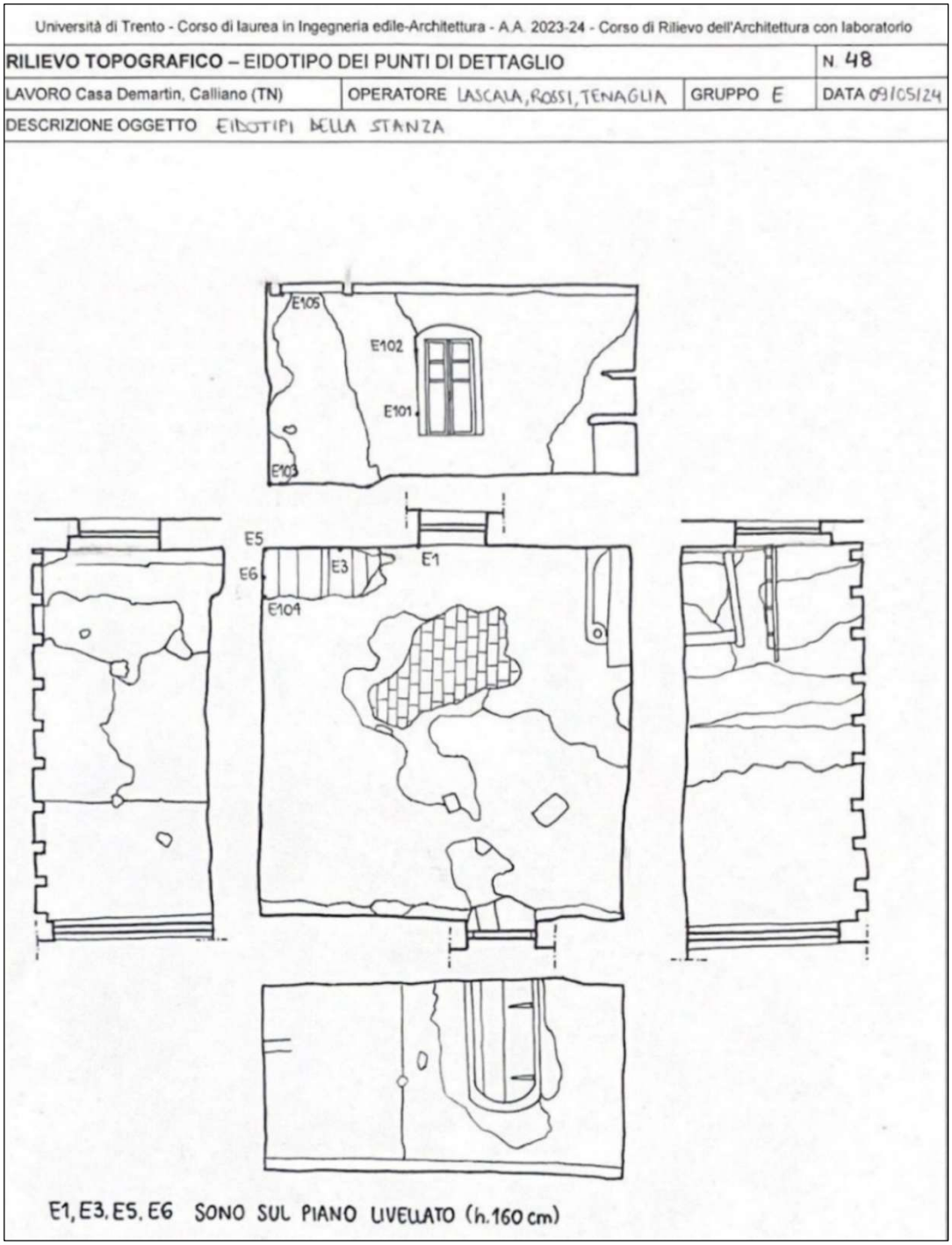

Figure 3.8 – Hand-drawn eidotype of one of the surveyed rooms of Casa Demartin showing the location of detail points recorded during the topographic survey. Students drawing.

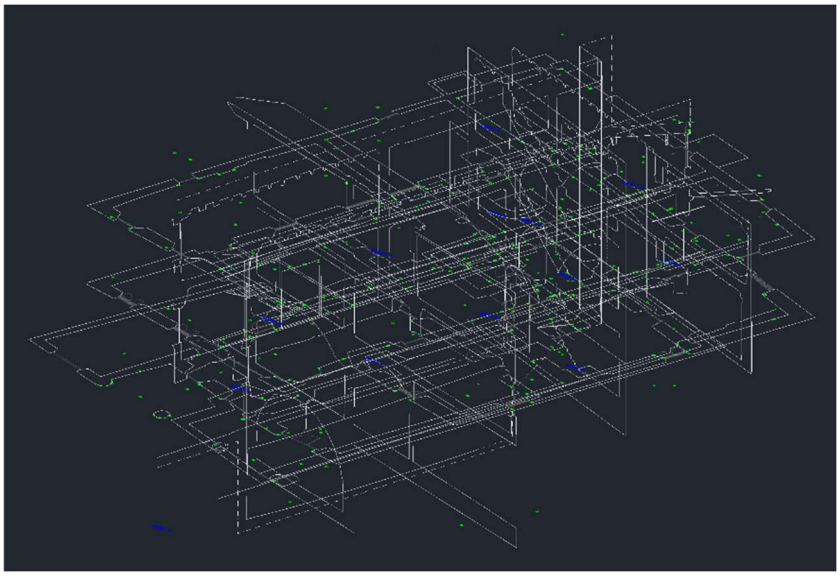

Figure 3.9 - The vectorial model resulting from the integration of traditional survey activities. Elaborated by the author based on LAMARC materials.

Range-based acquisitions through TLS. To integrate punctual representations generated from the topographic and longimetric survey, a high-precision range-based 3D dataset was acquired through a static laser scanner[3]. Across all accessible rooms, the TLS acquisition comprised 26 independent scans completed over an operational timeframe of approximately 12 hours. The acquired scans were registered and merged using topographic reference coordinates, then segmented and cleaned with noise-reduction filters to eliminate points outside the volume of interest. The final processing step involved integrating the georeferenced, clean point cloud into the vector model generated from traditional survey activities. Merging three-dimensional data into the 2d-based model allowed the assessment of manually acquired measures and the enrichment of vertical and horizontal sections.

[3] The TLS FARO Focus3D S120 was used for the survey; the instrument was supplied and operated by Geom. Alberto Leoni.

Image-based acquisitions. To enrich the final model and optimize its graphic readability, image-based data acquisition was deployed across two distinct operational scales: 2D planar digital rectification and multi-image 3D photomodelling.

Planar photogrammetry was implemented to capture and document specific, highly significant flat surfaces. This process utilized an analytical digital photo-rectification method, leveraging control points registered within the primary topographic survey to eliminate perspective distortion[4]. The digitally rectified photoplanes were thus georeferenced and integrated into the 3D vectorial model derived from the longimetric survey. The high-precision orthophotos served for the extraction of detailed elevation drawings and as a metric backdrop for direct measurements.

Multi-image photomodelling was applied for capturing both the complex internal environments and external facades of *Casa Demartin*. The utilized equipment consists of reflex and mirrorless digital cameras alongside tripods to guarantee stability and prevent motion blur in poorly lit interiors. To achieve a complete vertical coverage and safely capture high-altitude imagery of the upper facade elevations, the 3Deye system was used. It consists of a digital camera fixed on a telescopic pole, equipped with a gimbal and a remote-controlled device. Dense datasets were obtained capturing hundreds of photographs of internal rooms, ceilings, external façades from multiple, shifting viewpoints, maintaining a strict image overlap of at least 60–70% across all visible surfaces. By using processing software[5], automatic tie-point matching was executed and high-density, photorealistic 3D point clouds are reconstructed. These were then scaled and georeferenced using the topographic control point network. The resulting dense point clouds were thus integrated with the same digital

[4] RDF free software was used for 2D photogrammetry.

[5] Agisoft Metashape and 3DF Zephyr were used for photomodelling.

environment of the topographic points and laser scanner point clouds, establishing a unified, multi-source digital asset (Figure 3.10).



Figure 3.10 – The vectorial resulting model obtained from the integration of traditional survey acquisition and point clouds resulting from TLS scans and photomodelling. Elaborated by the author based on LAMARC materials.

Architectural detail recording. In addition, localized physical features, timber floor deflections, and mouldings were documented using needle profilographs, callipers, and tactile frottage techniques, while surface finishes were systematically classified using the standardized Natural Colour System (NCS).

The experimental campaign. Subsequently the experimental campaign was conducted, consisting in the acquisition through a backpack-based MLS[6]. The system comprises three core integrated components. A dual LiDAR sensor, consisting of two 32-channel laser scanners, one aligned horizontally and

[6] The survey was carried out using the HERON TWIN Color mobile mapping system, developed and supplied by Gexcel S.r.l.; data acquisition was performed by Arch. Giorgia Rossi (Gexcel).

the other tilted vertically, to capture comprehensive spatial elevation profiles within an operational range of 120 to 300 meters. A panoramic RGB camera system equipped with four synchronized lenses, supporting 4K video streaming and high-resolution 8K single-shot image capture. A handheld mobile device interface running a dedicated application connected via Wi-Fi to track real-time trajectory paths and facilitate local control point registration.

The continuous survey trajectory encompassed a complete external loop around the building perimeter, followed directly by sequential walkthroughs of the basement and upper residential floors (Figure 3.11). To optimize multi-source data integration the path included the passage toward windows and structural openings, ensuring geometric continuity with potential external aerial datasets, such as those derivable from Unmanned Aerial Vehicle (UAV) photogrammetry.

Concurrently, 90 control points and panoramic photos were captured along the path to anchor, align, and georeference the resulting spatial data (Figure 3.12). The acquisition took about 30 minutes.

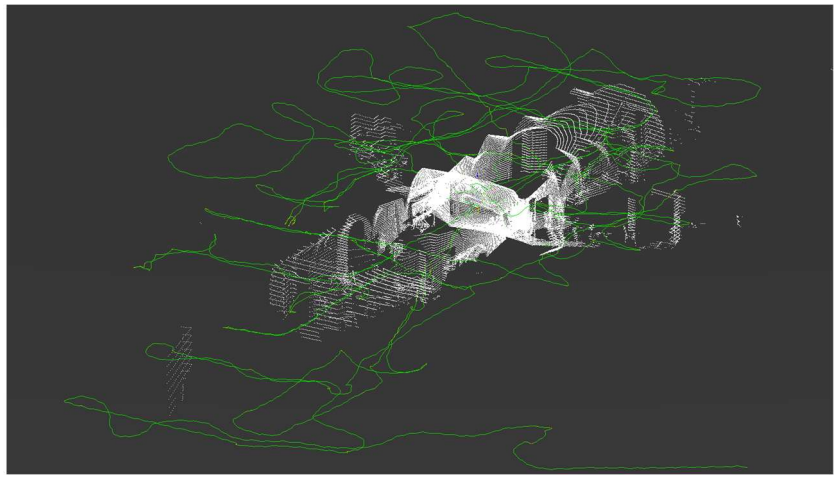

Figure 3.11 – The trajectory followed during the MLS acquisition, processed within the dedicated digital environment. Image by Gexcel.

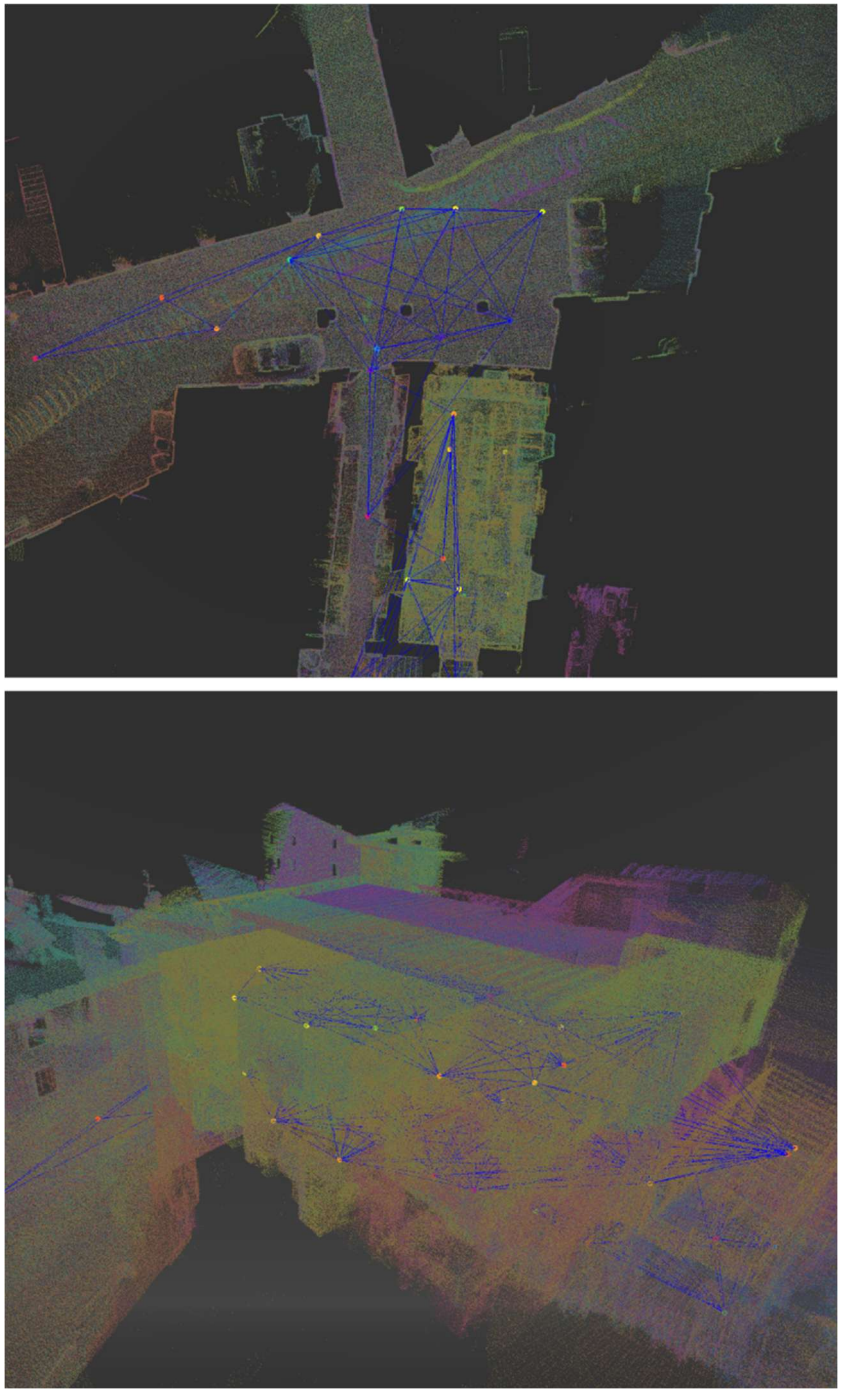

Figure 3.12 – 2D and 3D views of the net generated through the MLS acquisition. Images by Gexcel.

The elaboration of MLS data was performed in a dedicated digital environment[7] which allows to combine the SLAM trajectory information with the scanned data, generating the georeferenced point cloud.
In the processing phase the panoramic captures were used to provide greater details, including colour, to be transferred to the point cloud (Figure 3.13).
The resulting point cloud was cleaned and segmented to eliminate unnecessary data.
A fundamental challenge in MLS is the accumulation of drift error over time. Because SLAM technology estimates the sensor's position consistently to the trajectory, minor local discrepancies inevitably propagate throughout the survey. This cumulative error induces remarkable global geometric deformations and metric inconsistencies within the final 3D point cloud. This distortion is particularly pronounced when traversing vast distances without fixed reference targets, or when operating within homogeneous environments that lack the morphological variations necessary for feature tracking.



Figure 3.13 – The point cloud resulting from the MLS acquisition. Elaborated by the author based on Gexcel materials.

[7] Gexcel's proprietary software, Reconstructor, was used to compute the scanner trajectory and integrate the spatial and colorimetric data.

To mitigate drift propagation and anchor the dynamic tracking alignment, it is possible to act corrective strategies both during the fieldwork phase and the processing one. A primary corrective measure was applied during the acquisition phase by returning repeatedly to previously scanned spatial nodes. By re-identifying familiar environmental geometries, the SLAM algorithm can automatically compute scan-to-scan correspondences and retroactively adjust a significant portion of the accumulated trajectory error. Furthermore, the integration acquired through different tools acts as a corrective strategy in processing the acquired scans. Fusing the dynamic MLS trajectory with stable external spatial constraints, such as topographic coordinates or static TLS datasets, introduces high-precision spatial anchors that successfully curtail global drift and stabilize the absolute orientation of the architectural model.

To evaluate the potential optimization due to the corrective processing strategy, during the experimentation, the MLS data underwent two different processing workflows. The first processing run was based exclusively on the topographic network. The scan was registered using the reconstructed trajectory (Figure 3.14, 1a) and then adjusted to the reference topographic network through rigid transformations (Figure 3.14, 1c). The second processing workflow was based both on topographic points and on three selected scans acquired through TLS. This allowed for the parametric optimization of the trajectory before the points registration (Figure 3.14, 2a) and thus for a re-shape of the point cloud (Figure 3.14, 2b) not meant as merely rigid transformation. The second workflow requires more computation time of the scan, but is supposed to allow for more precise registration.

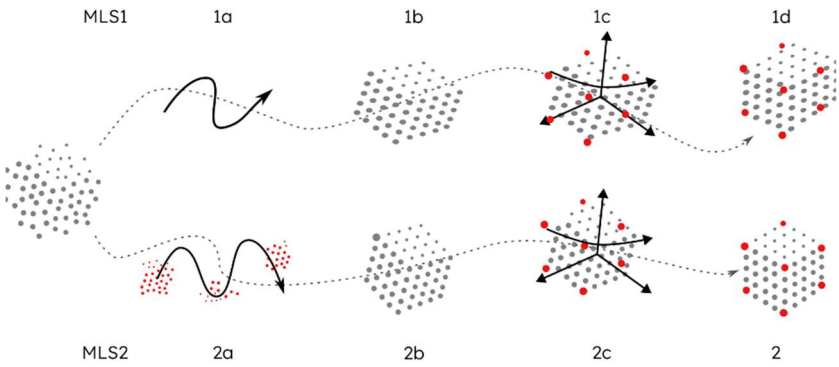

Figure 3.14 – The two processing workflows applied to the data acquired with the mobile scanner.

3.3.2. Evaluation and comparative assessment of technical workflows

The primary objective of this experimentation is not to evaluate the replaceability of established surveying methodologies, but rather to critically assess the capabilities and limitations of innovative ones within a real-world architectural context. To achieve this, the mobile dataset was directly compared against data captured concurrently via topography and TLS, which reliability is deeply recognized both in literature and current practice. The comparative analysis focused on the parameters defined in the theoretic framework, namely density, metric reliability and geometric accuracy.

In terms of density, the point clouds generated from both mobile workflows (MLS1, resulting from the topography-only processing, and MLS2, derived from the TLS-constrained processing) were individually benchmarked against the TLS dataset.

The metric reliability of the scans was evaluated by cross-referencing distances against the topographic control points, specifically comparing TLS–topographic, MLS1–topographic,

and MLS2–topographic datasets, and alongside direct scan-to-scan metric comparisons, MLS1–TLS and MLS2–TLS.
Furthermore, the geometric accuracy was validated through a comprehensive surface-to-surface deviation analysis between MLS1–TLS and MLS2–TLS.
Given the significant computational weight of the acquired datasets, the comparative analysis was restricted to a limited sample of the whole building. The selected volume is a second-floor room, referred to as 'Room E' after the team that conducted the survey activities in this space (Figure 3.15).



Figure 3.15 – From the top to below, TLS, MLS1 and MLS2 point clouds of the sample space used for the analysis, "room E".
Elaborated by the author based on Gexcel materials.

Table 3.3 – Comparison of general features of the three point clouds.

	TLS	MLS1	MLS2
N. of points	690.181.440	170.321.563	158.257.610
Acquisition time	12 h	30 min	30 min
Processing time	4 h	6 h	8 h

Spatial density analysis

As first, to evaluate the qualitative differences between the point clouds, a comparison based on the spatial density of the points was performed. The procedure consists of calculating the density by counting the number of neighbouring points N within a spherical radius R around each point. The returned parameter is the volumetric density, which is the number of points per unit volume, in this case a sphere radius equal to r= 0.1 m. A comparison of the results obtained for the three point clouds is summarized in Table 3.4, while individual results are reported in form of graphs below.

The point cloud acquired with the TLS shows an average density of 5,809,938.5 pt/m³, with an extremely high standard deviation of 13,631,229 pt/m³. This confirms that most of the points are concentrated in areas very close to the instrument, while the density drops drastically as the distance increases. In fact, 86.5% of the TLS points fall into the lower range (238 – 7.3 million pt/m³), where the density is high and the acquisition is detailed. The percentages in the higher ranges drop rapidly.

The cloud resulting from the first processing of the MLS1 acquisition has an average density of 284,929.88 pt/m³, with a standard deviation of 87,559.06 pt/m³. The distribution is compact and regular, over 89% of the MLS1 points are distributed between 7.3 and 21.9 million pt/m³, with a clear peak (60.8%) in the 14.6 – 21.9 million pt/m³ range, indicating a regular coverage favoured by the movement of the sensor along the path. The very high-density component is completely absent, indicating a uniform coverage that is less intensive on details.

The average density of MLS2 cloud is 272,889.91 pt/m³, with a standard deviation of 82,605.91 pt/m³. The density distribution is significantly concentrated in the last range, between 21.9 and 29.1 million pt/m³, containing 47.87% of the points.

Table 3.4 – Comparison of main density ranges and relative percentages.

Density [pts/m³]	TLS [%]	MLS1 [%]	MLS2 [%]
238 – 7.3M	**86.5**	1.8	1.1
7.3M – 14.6M	5.8	28.2	13.9
14.6M – 21.9M	2.7	**60.8**	27.2
21.9M– 29.1M	1.6	6.1	**47.9**
> 29.1M	3.5	3.1	8.8

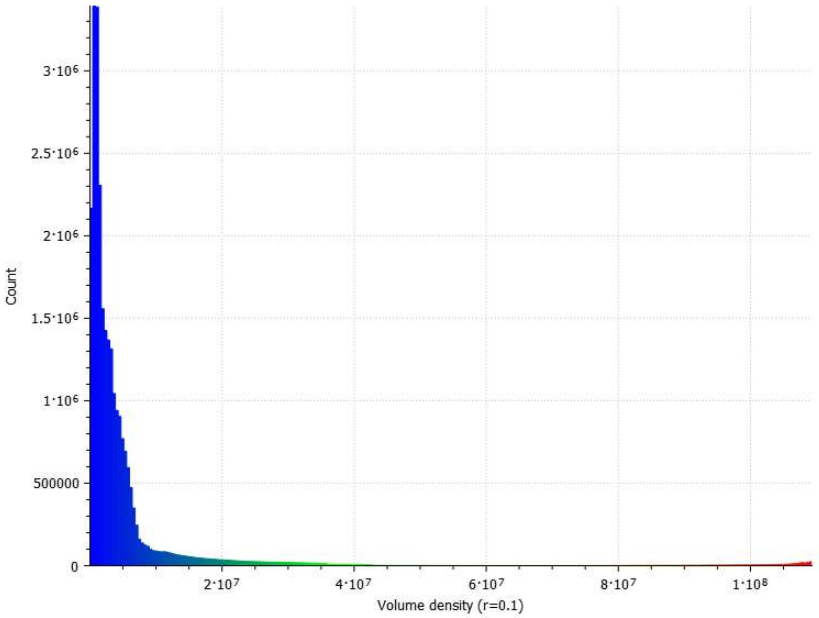

Figure 3.16 – Distribution of points density within the TLS point cloud.

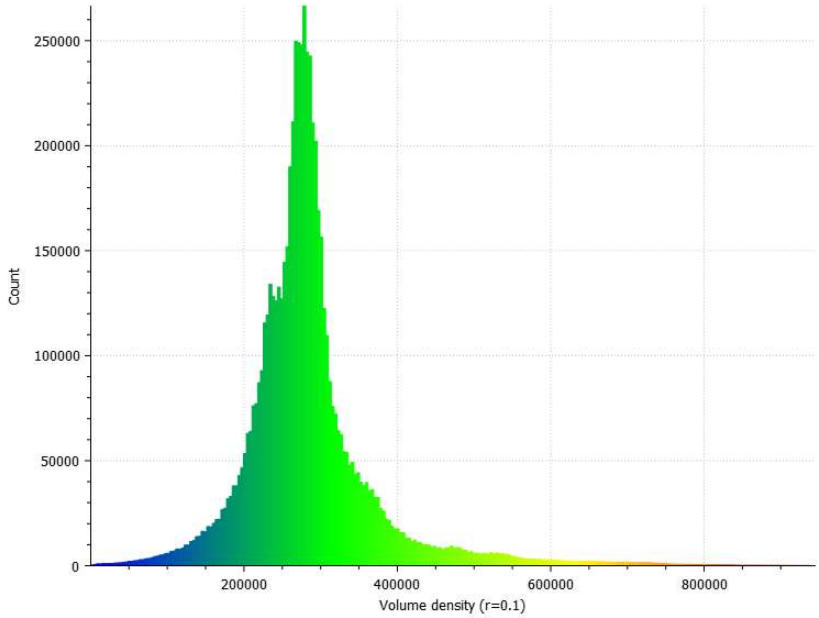

Figure 3.17 – Distribution of points density within the MLS1 point cloud.

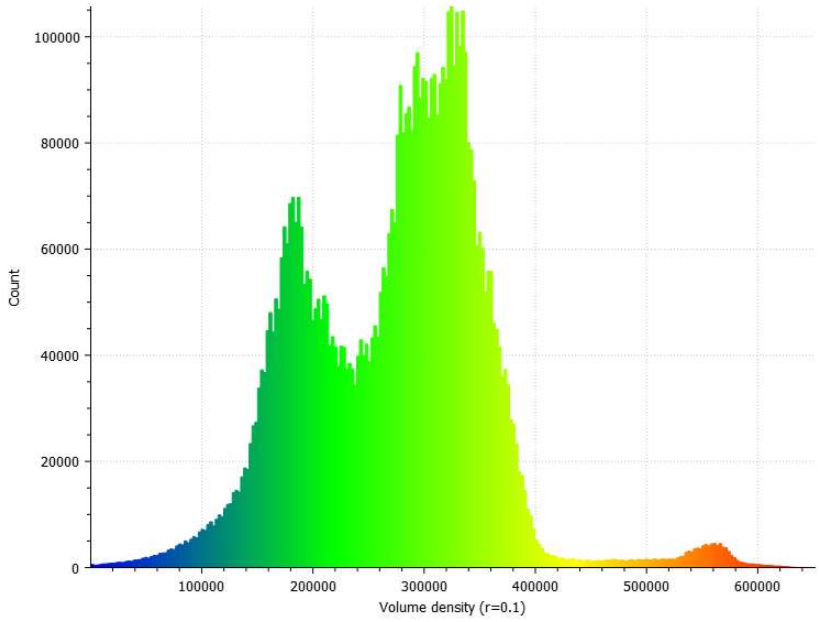

Figure 3.18 – Distribution of points density within the MLS2 point cloud.

Point to point distance

Since the topographic survey constitutes an independent metric reference of high reliability, it was adopted as a validation base for the point clouds acquired via TLS and MLS. The calculation of point-to-point distance allowed to verify the geometric consistency and alignment of the three datasets with respect to the topographic points surveyed in the sample room 'E'. This analysis was carried out computing the clouds distance from the topographic points, setting the dense clouds as the reference surfaces.

The comparative analysis indicates that the majority of topographic points (20 in the sample room) deviate from the TLS point cloud by less than 5 cm (Table 3.5). When evaluating the MLS1 cloud against the same topographic baseline, a similar trend emerges: the vast majority of points display most deviations below 7 cm. As evidenced by the table (Table 3.6), only two points exceed a 5.5 cm threshold. This minor discrepancy confirms a satisfactory spatial consistency between the MLS1 dataset and the topographic survey, representing a positive outcome for a comparison between heterogeneous scanning systems. The analysis of MLS2 point cloud reveals a substantial increase in metric accuracy, with the majority of points exhibiting a deviation of less than 2 cm from the topographic benchmarks (Table 3.7).

Table 3.5 – Distance of the TLS point cloud from topographic points.

N. of point	Min distance [cm]	Max distance [cm]
10	0.16	0.42
6	0.42	0.68
2	1.20	1.46
2	4.32	4.57

Table 3.6 – Distance of the MLS1 point cloud from topographic points.

N. of point	Min distance [cm]	Max distance [cm]
4	0.51	0.57
2	0.64	0.70
2	1.03	1.09
2	1.81	1.88
2	2.07	2.14
2	3.38	3.45
2	3.58	3.64
2	5.21	5.28
2	5.34	5.41

Table 3.7 – Distance of the MLS2 point cloud from topographic points.

N. of point	Min distance [cm]	Max distance [cm]
2	0.20	0.29
2	0.39	0.48
4	0.58	0.68
2	0.68	0.77
4	1.25	1.35
2	1.54	1.63
4	1.63	1.73

Cloud to cloud distance

The TLS cloud was then used as a global reference and compared with the MLS1 and MLS2 clouds, again focusing on the sample room 'E'. The absolute point-to-point distances were calculated in order to evaluate the accuracy and metric consistency of the mobile datasets. The analysis was carried out splitting the distances in their three-dimensional components, along the X, Y, and Z axes, in order to better evaluate the accuracy of results. The comparison between MLS1 and TLS clouds reveals that the distance between points varies from a minimum of 0.07 mm to a maximum of 80 cm (Figure 3.19). This maximum value, however, can be considered as a singular anomaly, to be attributed to the positioning of

the TLS, beneath which no points are acquired, and the presence of movable furniture, which may have been shifted between the two scans. Table 3.8 presents the progressive distribution, highlighting how the points are distributed within the individual discrepancy ranges.
The increase in accuracy due to the optimization process is clearly demonstrated by the values of the same analysis carried out on the MLS2 cloud (Figure 3.20). Compared to the first data processing, the comparison highlights substantial improvements. The progressive percentage (Table 3.9) confirms the quality of the optimization: most of the discrepancies are concentrated in the first two ranges (<1 cm and <5 cm), while the subsequent classes show a sharp decrease in the number of points with larger errors.

Table 3.8 – Distance of the MLS1 point cloud from the TLS point cloud.

TLS- MLS1 Distance [cm]	N. of points	Percentage [%]
< 1	647.050	9,6
< 5	**3.155.459**	**46,8**
<10	**2.396.325**	**35,6**
<20	363.102	5,3

Table 3.9 – Distance of the MLS2 point cloud from the TLS point cloud.

TLS-MLS2 Distance [cm]	N. of points	Percentage [%]
< 1	**2.640.412**	**42,3**
< 5	**2.939.420**	**47,1**
<10	301.166	4,8
<20	243.017	3,9

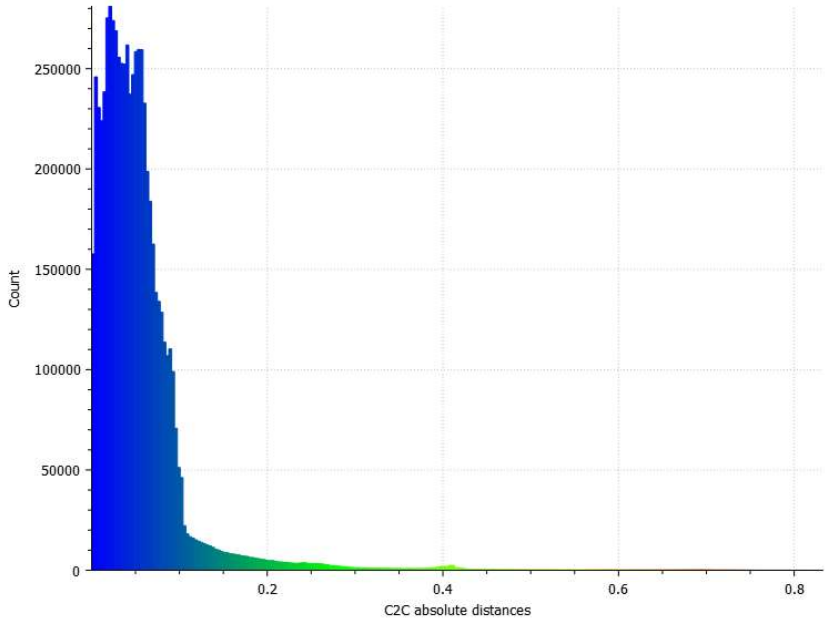

Figure 3.19 – Distribution of the distances of MLS1 points from the TLS point cloud.

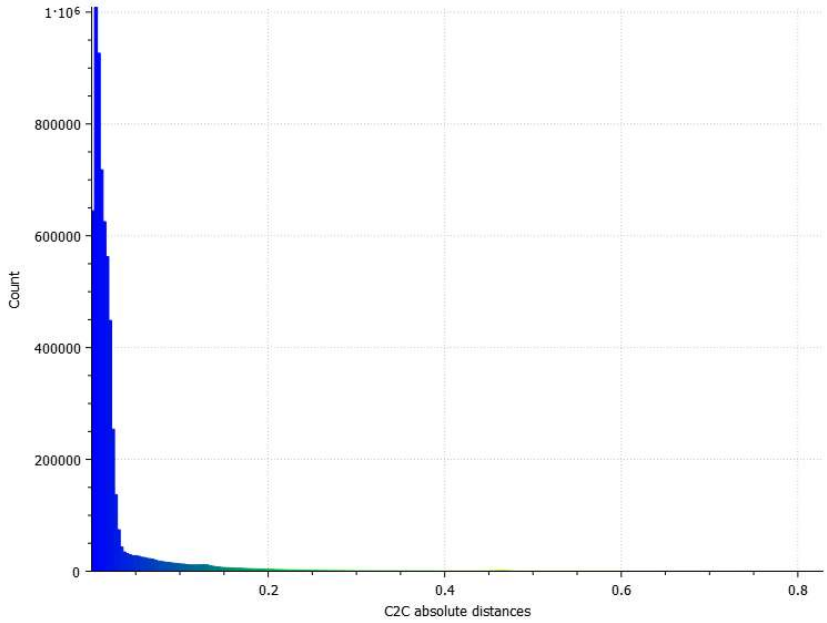

Figure 3.20 – Distribution of the distances of MLS2 points from the TLS point cloud.

The comparison between the MLS and TLS point clouds was extended to the analysis of horizontal and vertical sections, in order to evaluate the presence of local deviations and verify the geometric consistency of the two datasets (Table 3.10 and Table 3.11). Five vertical section (two longitudinal and three transversal), and three horizontal ones are taken into account (Figure 3.21).

The analysis of the five vertical cross-sections (A-A, B-B, C-C, D-D, E-E) of MLS1 point cloud revealed that standard deviations are higher in those sections that cut transversally the wooden timber, and lower where the geometry is less complex. The percentage of points with a deviation under 5 cm varied significantly, ranging from 33% to 97%. The maximum deviation reaches 80 cm in section A-A (Figure 3.22), but as in the global cloud-to-cloud analysis, this peak value does not indicate acquisition errors and is negligible, as it relates to the TLS setup area or displaced objects.

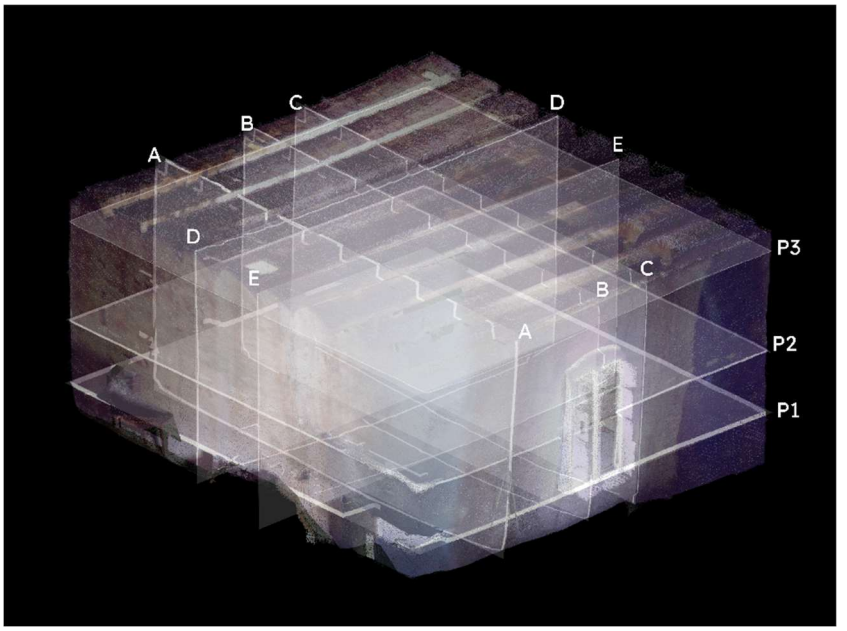

Figure 3.21 – Horizontal and vertical sections analysed on the sample space, room E. Elaborated by the author based on Gexcel materials.

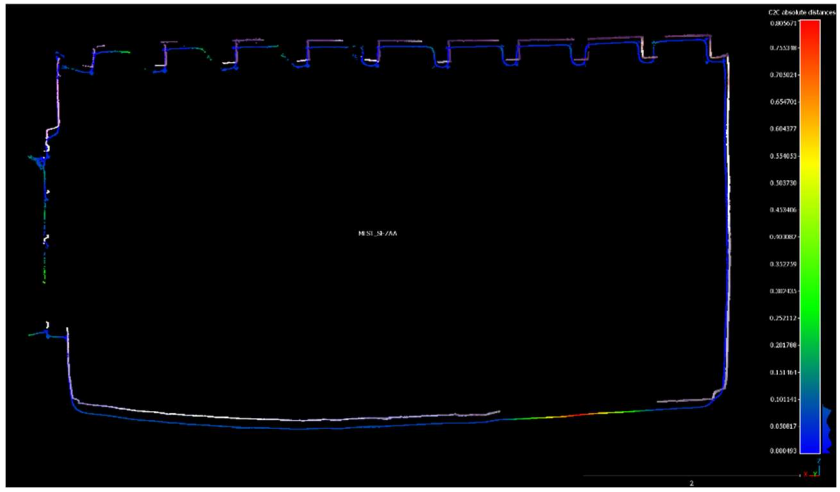

Figure 3.22 – Comparison of section AA between MLS1 and TLS point clouds.

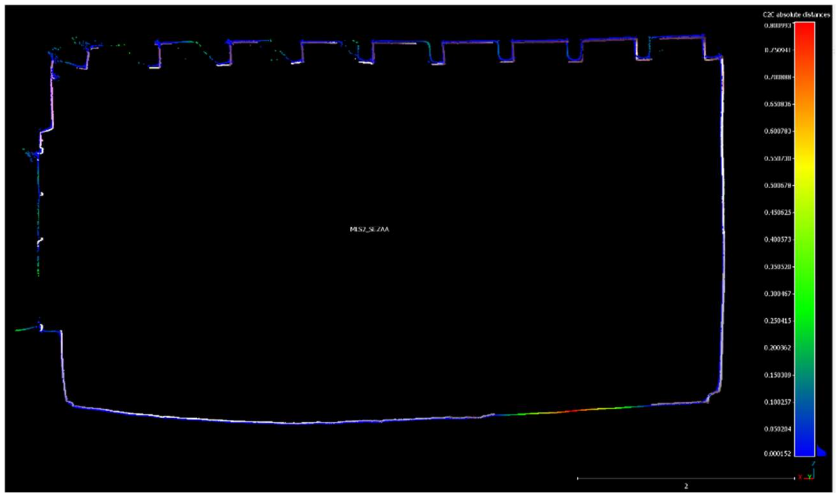

Figure 3.23 – Comparison of section AA between MLS2 and TLS point clouds.

The same methodology was applied to three horizontal cross-sections: P1 at floor level, P2 at the openings, and P3 near the ceiling. Statistical analysis confirmed that the error margin in these sections is very low, suggesting strong planimetric consistency between the two point clouds, with planimetric errors being significantly lower than altimetric ones. The three horizontal sections demonstrate a stable behaviour, with low

mean deviations ranging between 4.3 cm and 8.1 cm, and with tight standard deviations. The percentage of points within the 5 cm threshold exceed 60% across all horizontal sections, reaching 71.2% in P2 and 71.6% in P3, confirming good data consistency. Maximum distances reach 1.05 m in section P1, locally affected by obstacles such as furniture, and 1.00 m in P3, where accuracy is likely reduced by the proximity to the ceiling. In summary, the horizontal sections show a more stable distribution and lower mean deviations (4–8 cm) than the vertical ones, with over 70% of points within 5 cm in two out of three cases.

The results obtained with the MLS2 point cloud highlight a significant improvement in the altimetric component (Figure 3.23). The percentage of points with a deviation under 5 cm, which previously dropped below 40%, is now consistently above 85%, reaching nearly 98% in sections A-A and D-D. Mean deviations decreased across all sections, often falling below 3–4 cm. Standard deviations are generally lower, indicating greater internal consistency in error distribution. Maximum distances remain comparable to values obtained with MLS1, but are less significant as they represent isolated, sporadic points. Indeed, this analysis highlights that, despite achieving good overall metric reliability, geometric accuracy remains problematic for dynamic acquisitions. The representative image of section A-A shows a significant approximation of the squared timber cross-section, which compromises the recognition of its actual geometry (Figure 3.24).

Table 3.10 – Local distribution of the distances of MLS1 points from the TLS point cloud in sections.

Section	N. of points	Mean [m]	Std. dev. [m]	%< 5 cm	Max distance [m]
AA	12400	0.0753	0.1212	96.96%	0.8056
BB	11661	0.0586	0.0790	57.67%	0.4669
CC	32973	0.0508	0.0335	49.11%	0.2365
DD	13487	0.0571	0.0283	33.68%	0.2965
EE	7245	0.0618	0.0487	48.76%	0.3814
P1	83796	0.0816	0.1112	62.42%	1.054
P2	42744	0.0472	0.0552	71.22%	0.36
P3	14612	0.043984	0.021470	71.60%	1.004

Table 3.11 – Local distribution of the distances of MLS2 points from the TLS point cloud in sections.

Section	N. of points	Mean [m]	Std. dev. [m]	%< 5 cm	Max distance [m]
AA	10939	0.0429	0.1154	97.57%	0.8009
BB	11661	0.0363	0.0850	86.07%	0.4717
CC	26591	0.0170	0.0231	94.86%	0.2593
DD	13487	0.0145	0.0189	97.64%	0.2300
EE	6335	0.0265	0.0536	90.41%	0.4124
P1	79896	0.040272	0.08522	80.62%	1.002
P2	38122	0.015066	0.02045	95.87%	0.269
P3	5337	0.012871	0.00846	99.83%	0.070

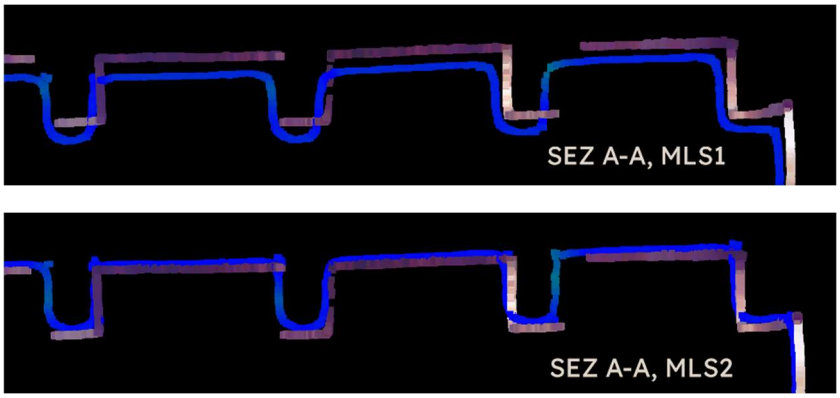

Figure 3.24 – Detail of section A-A that shows the improvement in the restitution of 'z' values in MLS2. Geometric accuracy remains poor in both clouds, as shown by the squared timber profile edges approximated to rounded edges.

Global qualitative comparison of the acquisition and processing methodologies and relative results.

The comparative experimentation provides a comprehensive overview of the operational trade-offs, capabilities, and structural limitations inherent to the evaluated surveying methodologies. When assessing acquisition efficiency, mobile laser scanning represents a major paradigm shift. Both MLS workflows required only 30 minutes of field activity compared to the 12.5 hours demanded by traditional TLS setups, effectively reducing on-site capturing time by over 95 per cent. However, this field efficiency shifts the computational burden onto the post-processing phase. Processing times increase from 4 hours for TLS to 6 hours for MLS1 (topography-only) and 8 hours for MLS2 (TLS-constrained), highlighting the computational weight required by trajectory optimization algorithms.

From a qualitative perspective, the resulting point clouds exhibit fundamentally different spatial structures. TLS, characterised by an average density twenty times higher than mobile alternatives, offers unparalleled local detail. Nonetheless, its massive standard deviation underscores an uneven point distribution, with data density dropping

drastically away from the instrument stations. MLS1 provides a highly regular and compact density distribution, with nearly 90 per cent of its points clustered in the intermediate ranges (7.3–21.9 million pt/m³). It lacks, however, the capacity to capture very high-density local geometries. MLS2 bridges this gap. The trajectory optimization process yields an efficient point redistribution, concentrating nearly 48 per cent of its data within the high-density range (21.9–29.1 million pt/m³) and drastically mitigating the noise observed in the first iteration. While TLS maintains a much higher and more detailed density, MLS2 provides good distribution and regularity, making it more suitable for complex, large-scale surveys.

The distance from the topographic references calculated for the TLS and both the MLS datasets yielded highly satisfactory results. The errors observed across the three compared clouds are generally constrained within a few centimetres, remaining well within standard instrumental and operational tolerances. Most notably, the analysis of the optimised dataset highlights a stark improvement over the first processing iteration. Restricting the vast majority of deviations to under 2 cm, the optimization process significantly enhanced the spatial alignment of the MLS data.

The results of local distances analysis in cross sections demonstrate that the MLS2 point cloud optimization effectively reduced altimetric errors and substantially enhanced survey accuracy. Vertical sections now exhibit much more consistent behaviour, resolving the pronounced Z-axis deviations observed in the first processing phase. Similarly, statistical analysis of the distance distribution between the optimized MLS2 and TLS clouds shows a clear improvement, particularly in planimetric precision. Overall, the optimization guaranteed high planimetric precision, making the MLS2 dataset fully comparable to the TLS reference. The behaviour of the horizontal sections confirms excellent geometric

consistency, with errors generally lower than those in the vertical sections. This is due to odometric stability along the plane and a more regular coverage of the moving sensor.
The 2D analysis highlights that the MLS survey guarantees excellent planimetric consistency and overall metric reliability. In contrast, elevation data shows less homogeneity, though it remains well within acceptable tolerance thresholds.
The multi-dimensional metric validation confirms that while raw mobile data can achieve satisfactory global consistency, optimization is imperative for rigorous architectural applications. Ultimately, a critical limitation remains regarding local geometric accuracy. Despite the acceptable metric reliability achieved globally by MLS2, dynamic data capture tends to introduce a structural approximation of complex elements, such as the edge roundedness observed in squared timber profiles.
In this light, integrating a dynamic acquisition framework with a limited number of strategically selected static scans to act as rigid constraints emerges as a highly effective operational compromise. Whilst this hybrid approach does not inherently resolve the issues of lower spatial density or local geometric approximation, it guarantees a substantial improvement in overall metric reliability. Consequently, whilst traditional TLS remains indispensable for heritage contexts demanding strict geometric fidelity and fine architectural detailing, the optimised, TLS-constrained MLS workflow proves to be a highly reliable and computationally viable methodology for large-scale architectural inventories.

3.4. Answer to the RQ. Considerations on the case Calliano study

The Calliano case study demonstrates that the construction of a geometric model is not determined solely by the performance of individual surveying technologies, but by the acquisition strategy adopted and by the way heterogeneous

datasets are integrated throughout the processing workflow. This directly addresses RQ1 by showing that data acquisition is not an independent preliminary operation: it conditions the characteristics, reliability, and ultimately the usefulness of the digital model for subsequent renovation activities.

Within this framework, the integration of Terrestrial Laser Scanning, Mobile Laser Scanning, and traditional topographic control proved essential to obtain a complete and metrically reliable representation of the building. Combining static and mobile acquisition significantly improved both the efficiency of the survey workflow and the quality of the resulting model. While mobile scanning enabled rapid documentation of extensive and otherwise inaccessible spaces, the introduction of targeted TLS acquisitions on morphologically complex areas, such as corner joints and vertical distribution systems, provided high-precision spatial references that reduced global drift, corrected local distortions, and substantially increased the overall reliability of the integrated point cloud.

The resulting workflow produced a geometric model suitable for high-accuracy metric documentation and advanced architectural analyses. At the same time, the experimentation demonstrates that the level of metric reliability required is not constant throughout a renovation process. Achieving the highest level of accuracy required considerable processing time and specialist expertise, yet such precision would only become indispensable during the detailed design or communication stages of a renovation project. For preliminary analyses aimed at understanding building behaviour or supporting early design decisions, the lower level of accuracy obtained during the initial MLS processing would have been sufficient. Consequently, the study suggests that acquisition strategies should pursue a level of accuracy commensurate with the information requirements of the specific renovation phase, rather than maximising precision independently of the intended application.

References chapter 3

Barbini, A. (2024) Built Heritage Interface Models Multipurpose information access and data exchange. Doctoral Thesis, Massari, G. (Supervision). Department of Civil, Environmental and Mechanical Engineering, University of Trento

Bottura, V. (1991). Calliano: villaggio illustre alla sinistra dell'Adige. Documentazione fotografica di: archivio centro catalogazione servizio beni culturali (P.A.T.) G. Zotta Giorgio Moser Collezioni private. Calliano (TN): Casa editrice Comune di Calliano (TN).

Cannarozzo M.L., Salerno R. (1991). Fotografie e misura. Milano: Cluva, CittàStudi.

Chioni, C., Maragno, A., Pianegonda, A., Ciolli, M., Favargiotti, S., & Massari, G. A. (2023). Low-Cost 3D Virtual and Dynamic Reconstruction Approach for Urban Forests: The Mesiano University Park. Sustainability, 15(19), Articolo 19.

Conti, A., Pagliaricci, G., Bonora, V., & Tucci, G. (2024). A Comparison Between Terrestrial Laser Scanning And Hand-Held Mobile Mapping For The Documentation Of Built Heritage. The International Archives of the Photogrammetry, Remote Sensing and Spatial Information Sciences, XLVIII-2-W4-2024, 141–147. ISPRS / CIPA
 10th International Workshop 3D-ARCH «3D Virtual Reconstruction and Visualization of Complex Architectures» - 21–23 February 2024, Siena, Italy.

Croce, V., Caroti, G., Piemonte, A., & Bevilacqua, M. G. (2019). Geomatics for Cultural Heritage conservation: Integrated survey and 3D modeling. IMEKO TC-4 International Conference on Metrology for Archaeology and Cultural Heritage Florence, Italy, December 4-6, 2019

Cunietti, M. (1979). Misurabilità e misura nell'analisi cartografica. In Torsello, B. P. (Ed.), Misura e conservazione: tecniche di rilevamento. Cluva libreria editrice.

Dal Prà, L., & Borrelli, L. (2009). Tra affreschi, stemmi ed archivi: palazzo Pilosi (ora casa Demartin) di Calliano al tempo dell'imperatore Massimiliano I d'Asburgo.

De Carlo, L. (2011) Il digitale per la de-costruzione geometrica della forma. In Albisinni, P., De Carlo (Eds.) Architettura, disegno, modello. Gangemi editore, ROMA, pp. 77-86.

de Rubertis, R. (1995). Riflessioni sulle nuove tendenze. XY – Dimensioni del Disegno, 23-24-25, 6-14.

de Rubertis R. (1998). Editoriale. In XY. Dimensioni del Disegno, 32-33, p. 3.

Delattre, P. (1981). "Teoria/modello", lemma. Enciclopedia Einaudi, 14, 148. Torino.

Di Stefano, F., Chiappini, S., Gorreja, A., Balestra, M., & Pierdicca, R. (2021). Mobile 3D scan LiDAR: A literature review. Geomatics, Natural Hazards and Risk, 12(1), 2387–2429.

Docci M., (1993). Rilevare per conoscere. Il rilievo di Santa Barbara dei Librari in largo dei Librari a Roma. XY dimensioni del disegno Numero. Dossier rilievo 17-18-19 pp. 84-85.

Duan, R., Feng, Y., & Wen, C.-Y. (2022). Deep Pose Graph-Matching-Based Loop Closure Detection for Semantic Visual SLAM. Sustainability, 14(19), 11864.

Geymonat, G. & Giorello, G., (1980). "Modello", lemma. Enciclopedia Einaudi, 9, 399. Torino.

Guercio M. (2013). Conservare il digitale. Principi, metodi e procedure per la conservazione a lungo termine di documenti digitali. Roma-Bari: Editori Laterza.

Leon, I., Pérez, J. J., & Senderos, M. (2020). Advanced Techniques for Fast and Accurate Heritage Digitisation in Multiple Case Studies. Sustainability, 12(15), 6068.

Li, Y., Zhao, L., Chen, Y., Zhang, N., Fan, H., & Zhang, Z. (2023). 3D LiDAR and multi-technology collaboration for preservation of built heritage in China: A review. International Journal of Applied Earth Observation and Geoinformation, 116, 103156.

Maragno, A, Barbini, A, Bernardini, E, Chioni, C, (2024) "Other Stories. Virtual Reconstruction of Different Design Hypotheses for Piazza d'Arogno in Trento" in Stilo, F., Castiglione, V., Cazzaro, I., Ceracchi, M., Natta, F., Pileri, M., Pizzonia, L., Tomalini, A.,

Tomasella, N., Trivi, M. B. (a cura di), eXplo Я A UID 2024. Virtual Journeys to discover inaccesible heritages, Alghero: PUBLICA, 2024, p. 533-545.

Maragno, A, Barbini, A, Bernardini, E, Chioni, C, Massari, G.A., (2024) The Measure for Uncountable data from 3D Digital Survey. The Case of the Historical Centre of Trento. In Bergamo, F., Calandriello, A., Ciammaichella, M., Friso, I., Gay, F., Liva, G., Monteleone, C. (a cura di), Measure / Out of Measure. Transitions. Proceedings of the 45th International Conference of Representation Disciplines Teachers, Milano, Franco Angeli, 2024, pp. 1679-1698.

Massari G.A. (1998). Misurare Interpretare Conoscere. In XY Dimensioni del Disegno, 32-33, pp. 5-18.

Massari G.A. (2005). Del rigore della misura. XY Dimensioni del disegno. Rappresentazione e verità, 9, 47, pp. 105-116.

Matrone, F., Lingua, A., Pierdicca, R., Malinverni, E. S., Paolanti, M., Grilli, E., Remondino, F., Murtiyoso, A., & Landes, T. (2020). A Benchmark For Large-Scale Heritage Point Cloud Semantic Segmentation. The International Archives of the Photogrammetry, Remote Sensing and Spatial Information Sciences, XLIII-B2-2020, 1419–1426.

Migliari R. (2003). Geometria dei modelli: rappresentazione grafica e informatica per l'architettura e per il design. Roma: Edizioni Kappa.

Monti, C. (1998). Scienza, Tecnologia e Misura. XY – Dimensioni del Disegno, 32, 5-18.

O'Donnell, J., Truong-Hong, L., Boyle, N., Corry, E., Cao, J., & Laefer, D. F. (2019). LiDAR point-cloud mapping of building façades for building energy performance simulation. Automation in Construction, 107, 102905.

Pepe, M., Alfio, V. S., Costantino, D., & Herban, S. (2022). Rapid and Accurate Production of 3D Point Cloud via Latest-Generation Sensors in the Field of Cultural Heritage: A Comparison between SLAM and Spherical Videogrammetry. Heritage, 5(3), 1910-1928.

Puente, I., González-Jorge, H., Riveiro, B., Arias, P. (2013). Accuracy verification of the Lynx Mobile Mapper system, Optics & Laser Technology, Volume 45, 2013, 578-586.

Radanovic M., Khoshelham K., Fraser C. (2020). Geometric Accuracy and Semantic Richness in Heritage BIM: A Review. In Digital Applications in Archaeology and Cultural Heritage, 19. https://doi.org/10.1016/j.daach.2020.e00166.

Remondino, F. (2011). Heritage Recording and 3D Modeling with Photogrammetry and 3D Scanning. Remote Sensing, 3(6), 1104-1138.

Remondino, F. (2011). 3D surveying and modelling of complex architectural sites and heritage objects. DISEGNARECON, 4(8), 90–98.

Sammartano, G., & Spanò, A. (2018). Point clouds by SLAM-based mobile mapping systems: Accuracy and geometric content validation in multisensor survey and stand-alone acquisition. Applied Geomatics, 10(4), 317–339.

Szrek, A., Romańczukiewicz, K., Kujawa, P., & Trybała, P. (2024). Comparison of TLS and SLAM technologies for 3D reconstruction of objects with different geometries. IOP Conference Series: Earth and Environmental Science, 1295(1), 012012.

Sultan, C., De Wolf, C., Bocken, N. (2021). 'Circular Digital Built Environment: An Emerging Framework', Sustainability, 13(11), 6348.

Torsello, B. P. (1988). La materia del restauro: tecniche e teorie analitiche. Marsilio Editore.

Ugo, V. (1994). Fondamenti della rappresentazione architettonica. Società Editrice Esculapio.

Ugo V. (1998). Misura-interpretazione-conoscenza-interpretazione-misura: circolo vizioso, o virtuoso? In XY. Dimensioni del Disegno, 32-33, pp. 19-24.

Ulvi, A., & Yiğit, A. Y. (2022). Comparison of the Wearable Mobile Laser Scanner (WMLS) with Other Point Cloud Data Collection Methods in Cultural Heritage: A Case Study of Diokaisareia. Journal on Computing and Cultural Heritage, 15(4), 1–19.

Vacca G. (2023). 3D Survey with Apple LiDAR Sensor - Test and Assessment for Architectural and Cultural Heritage. In Heritage, 6, pp. 1476-1501. https://doi.org/10.3390/heritage6020080.

Valacchi F. (2023). La verità di carta. A cosa servono gli archivi? Perugia: Graphe.it.

Valacchi F. (2006). La memoria integrata nell'era digitale. Continuità archivistica e innovazione tecnologica. San Miniato PI: Archilab.

Valero, E., Bosché, F., & Bueno, M. (2022). Laser scanning for BIM. Journal of Information Technology in Construction, 27, 486–495.

Yang, S., Xu, S., & Huang, W. (2022). 3D Point Cloud for Cultural Heritage: A Scientometric Survey. Remote Sensing, 14(21), 5542.

Yogender, Raghavendra, S., & Kushwaha, S. K. P. (2020). Role of Ground Control Points (GCPs) in Integration of Terrestrial Laser Scanner (TLS) and Close-range Photogrammetry (CRP). In J. K. Ghosh & I. da Silva (A c. Di), Applications of Geomatics in Civil Engineering, Springer, 531–537.

Weston P.G. (2013). Digital curation. Nuove opportunità per bibliotecari e archivisti. In P.G. Weston, Il libro, gli archivi e la memoria digitale. Milano: Unicopli.

Disclaimer

This chapter is partially based on:

Bernardini, E., Palmero-Sánchez, P.L., De-Juan-Ripoll, C. Rodrigo-Catalán, P. (2026) *Integrating Eco-Design Strategies in the Energy Retrofitting of Mid-20th Century Heritage Buildings: The Case of Antonio Rueda's Housing Complex*. In *Applied Sciences*, v. 2026, 16, n. 2 pp. 1-26.

4. Informative models to support modern heritage reuse. A case study in Valencia

The case study presented in this chapter, an example of modern heritage, specifically addresses the second and third research questions, focusing on the specific characteristics a digital model must possess to support an energy retrofitting process and how the usability and interoperability of informative models can be guaranteed for actors with diverse skills and needs.

The chapter is structured in two main parts. The first part introduces the theoretical framework underlying the research, discussing the intersection of heritage conservation, ecodesign principles, and multi-criteria performance simulations as core vectors for the decarbonization of the late-modern built stock. Particular attention is given to the integration of Building Information Modelling (BIM) with Building Energy Modelling (BEM) protocols, reflecting on how quantitative metrics and qualitative heritage values can be balanced and represented within a standardized level of information need.

The second part presents the Grupo Antonio Rueda housing complex in Valencia. This case study investigates how an integrated workflow, encompassing data modelling, performance simulation, and multi-criteria synthesis, can support the comparative assessment of passive envelope enhancements and active volumetric modifications. The analysis evaluates optimization trajectories for modern residential heritage, discussing the role of simulation-based decision systems in managing the architectural and environmental trade-offs of multi-family assets. Rather than finalizing a closed design, the study validates an automated framework for scenario profiling. It defines how informative models can deliver the multi-parameter comparisons essential for large-scale social housing modernization.

4.1. Theoretical framework. Multi-criteria performance simulation for ecodesign assessment in architectural retrofitting

Architectural heritage represents an essential component of urban historical and cultural identity, materializing the evolution of technical expertise, architectural paradigms, and social values over time. This heterogeneous stock encompasses both historical monuments and century-old buildings, and late-modern heritage (Martínez-Molina et al., 2016). Adapting these assets to contemporary uses and standards ensures their continued relevance within today's lifestyle and international requirements. In this perspective, the European policy framework has shifted its focus from target-setting to active delivery. Driven by the European Green Deal for 2030 (European Commission, 2019) and its implementation via the Clean Industrial Deal, energy efficiency serves as a core lever for competitiveness, affordability, and security (Berg et al., 2017). These objectives place both new and existing buildings, including culturally significant assets, at the centre of practical decarbonization pathways. Concretely, this orientation is reinforced by near-term EU priorities promoting large-scale renovation, affordable energy-efficient housing, and circular economy principles (European Commission, 2024). Broadly, these initiatives align with the 2030 Agenda for Sustainable Development and are backed by the Horizon Europe Work Programme 2025, which funds research and innovation actions addressing sustainable renovation, decarbonization of the built environment, and the integration of circular design principles in buildings.

This regulatory impulse is further compounded by the growing demand for affordable housing within contemporary urban fabrics, driving a paradigm shift toward prioritizing renovation, adaptive reuse, and volumetric extensions over greenfield development. In alignment with the EU's target of 'no net land take' by 2050, urban densification via the strategic

expansion of existing assets has emerged as a core sustainability trajectory. Demolition and ex-novo reconstruction induce an immediate upfront release of embodied carbon and accelerates biodiversity loss through soil sealing. Retaining existing structures can preserve a substantial share of the embodied carbon already invested in the built fabric while avoiding some emissions associated with demolition and new construction. By optimizing and expanding these existing volumes, cities can absorb demographic growth and mitigate housing shortages while drastically shrinking the life-cycle carbon footprint per capita.
Achieving these environmental goals, however, fundamentally requires safeguarding material authenticity and architectural integrity (ICOMOS, 1964). While traditional conservation associates authenticity primarily with preserving original materials, contemporary theory extends this concept beyond mere materiality to encompass spatial configuration, constructive logic, and the cultural significance of the ensemble. Consequently, while interventions on existing buildings inherently drive technical and morphological optimization, they simultaneously risk compromising other multi-dimensional architectural values. This critical conflict explains why protected and historic structures are frequently exempt from the strictest Energy Performance of Buildings Directive (EPBD) requirements (European Commission, 2024). To resolve this issue, the EU's post-2030 trajectory toward mid-century climate neutrality emphasizes that renovation, circularity, and high-quality design must advance together rather than as opposing trade-offs (European Commission, 2024). In this light, a growing research consensus favours narrowing the gap between heritage protection and energy efficiency, advocating for reversible, context-aware, and staged measures that fully respect both material and structural integrity (Elnagar et al., 2021).

To bridge the gap between these political mandates and the tangible reality of historic buildings, ecodesign has evolved from a conceptual approach into a well-established methodological framework formally recognized by the International Organization for Standardization (ISO). According to ISO 14006:2020, ecodesign is defined as "a systematic approach which considers environmental aspects in the design and development of products with the aim of reducing environmental impacts throughout their life cycle." This formalization provides a foundation for its application in architectural rehabilitation. By embedding environmental foresight directly into the early stages of heritage-oriented interventions, ecodesign-oriented approaches allow to pursue substantial energy gains without compromising intrinsic historical values. In heritage contexts, this systematic methodology relies on three pillars. Passive design strategies such as improving thermal inertia, enhancing natural ventilation, and integrating context-appropriate shading systems drastically reduce operational energy demand while maintaining the visual and material coherence of the historic envelope (Hu et al., 2023). Component modularity, adopting interventions that are designed to be adaptable and circular; modular windows, prefabricated façade panels, and service systems can be individually upgraded or replaced, extending the useful life of the building fabric in alignment with the circular economy (Machado & Morioka, 2021). Reversibility ensures that interventions remain respectful and non-invasive, guaranteeing that contemporary additions can be removed or altered in the future without damaging or degrading the original structural substrate (Liang et al., 2023).

To operationalize these ecodesign principles and bridge the gap between heritage preservation and climate neutrality, recent research has increasingly relied on advanced digital and simulation-based tools. Within this context, digitization through Building Information Modelling has emerged as a

methodological framework capable of consolidating the heterogeneous geometric, material, and environmental data required for heritage retrofitting into cohesive parametric models (Jung et al., 2023; Zhang et al., 2025). While this methodology traditionally supports a multidimensional project development approach, integrating spatial modelling (3D), time management (4D), and cost control (5D), it can be extended to incorporate additional specialized dimensions. Specifically, the sixth dimension (6D BIM) focuses on sustainability, lifecycle environmental performance, and energy efficiency (Montiel-Santiago et al., 2020). The operationalization of 6D BIM is achieved by linking the parametric environment with Building Energy Modelling (BEM) tools, enabling simulations that quantify a building's thermal behaviour and evaluate design alternatives (Azhar et al., 2012). This digital integration establishes an empirical framework where the constructive, environmental, and management attributes of an intervention are verified through measurable evidence, providing the necessary computational workflow to deploy passive design, component modularity, and reversibility within heritage-oriented practices. Despite the expanding literature and experimental research on digital tools to improve energy retrofitting, current methodologies exhibit critical research gaps when applied to modern architectural heritage (Sanhudo, 2018). Most studies focus either on pre-20th-century historic monuments or on isolated, singular buildings (Piselli, 2020; Veerendra, 2024). This leaves the specific challenges of mid-century complexes, characterized by repetitive modular construction, severely deficient thermal envelopes, and strict heritage constraints, largely underexplored. Furthermore, existing evaluation methods tend to analyse energy demand or carbon emissions in isolation, omitting interlinked trade-offs such as indoor daylight performance, qualitative reversibility criteria, or the socio-

spatial implications of volumetric extensions (Angileri et al., 2024).

Finally, although BIM and BEM tools are increasingly applied to heritage assets, their utility is frequently restricted to single-parameter simulations (Montiel-Santiago et al., 2020). They rarely form part of a comprehensive, automated decision-support workflow.

Collectively, these limitations reveal a distinct research gap, the absence of an integrated, multi-criteria methodology capable of simultaneously assessing energy efficiency, operational carbon, lighting quality, and intervention invasiveness within a single, replicable framework tailored to modern residential complexes.

To bridge these gaps, a comprehensive ecodesign assessment methodology can be implemented by embedding diverse quantitative and qualitative metrics within a unified digital environment. Under this framework, HBIM, EBIM, and BEM tools function not merely as descriptive modelling instruments, but as a multi-criteria decision-support system designed to evaluate comparative retrofitting scenarios, encompassing reversible, passive, and volumetric intervention strategies.

In alignment with ISO 19650-1:2018, for conducting this kind of explorative analysis, the Level of Information Need should not be arbitrarily maximized. Instead, it should be selectively structured around the specific technical requirements of the energy simulations and decision-making objectives. To ensure that hypothetical interventions are simultaneously effective, environmentally coherent, and compatible with conservation constraints, the methodology proposed in this study operationalizes four distinct evaluation criteria.

Annual Energy Use Intensity (EUI), a quantitative indicator expressing the total operational energy consumed by the building over one year, normalized by its gross floor area [kWh/(m^2·year)] (AIA, n.d.). This metric aggregates all operational vectors (heating, cooling, ventilation, lighting, and

appliances) according to international standards, isolating the building's operational demand from the embodied impacts of its materials.

Operational carbon [$kgCO_2$\e] translates operational energy consumption into direct environmental impacts by calculating the greenhouse gas emissions associated with the building's use phase. Generated by synthesizing spatial geometry, thermal envelope characteristics, HVAC efficiency, and site-specific meteorological files (ASHRAE, n.d.), the calculation multiplies each energy vector by its specific carbon intensity emission factor, allowing designers to prioritize absolute footprint reductions over raw energy savings.

Lighting performance analysis, evaluates solar radiation utilization and indoor illuminance quality through metrics such as the Daylight Factor, Daylight Autonomy (DA), and Useful Daylight Illuminance (UDI). Based on the radiosity method and the European standard UNE-EN 17037:2020, the simulation environment applies standardized performance thresholds derived from the LEED v5 Indoor Environmental Quality framework (USGBC, n.d.). In Mediterranean contexts, balancing natural light is vital, as opening dimensions and passive lighting strategies directly modulate visual well-being, artificial lighting runtime, and cooling thermal loads.

Finally, socio-architectural and conservation factors address evolving domestic patterns and heritage values. This framework supplements quantitative simulation data with qualitative constraints. These include the modification of the interior usable surface, the physical disruption or invasiveness experienced by residents during construction, and the irreversible alteration of the historic façade.

Embedding these multi-criteria metrics within the BIM environment models serves as a centralized repository that interprets, integrates, and reconciles legacy archival data with contemporary simulation outputs, ensuring strict information traceability across the entire intervention lifecycle.

Table 4.1 – Quantitative and qualitative parameters to evaluate data acquired from 3D digital survey.

	Parameter	Description	Measurement
Quantitative	Annual Energy Use Intensity (EUI)	Aggregates all operational energy vectors over one year, isolated from the embodied impacts of materials.	AEUI [kWh/m^2·year] = (Heating + Cooling + Interior Lighting + Exterior Lighting + Interior equipment + Exterior equipment + Water Systems + Refrigeration + Generators) [KWh/m^2]
	Operational carbon	Translates operational energy consumption into greenhouse gas emissions by multiplying each energy vector by its specific carbon intensity emission factor.	Operational Carbon = Σ (Energy Consumption$_i$ × Emission Factor$_i$) i = 1 to n [kg CO_2e]
	Lighting performance analysis	Evaluates solar radiation utilization and indoor illuminance quality to balance visual well-being, artificial lighting runtime, and cooling thermal loads.	Daylight Factor (%)
Qualitative	Socio-architectural factors	Addresses evolving domestic patterns and heritage values, including interior surface modification, resident disruption/invasiveness, and irreversible façade alteration.	Expressed through an assessment score (e.g., high / medium / low)

4.2. Contextualisation. Antonio Rueda's Housing Complex

The empirical validation of the proposed EBIM framework is conducted on the Grupo Antonio Rueda housing complex, located in the Tres Forques district of Valencia, Spain. Designed by the architects Vicente Valls Abad, Joaquín García Sanz, and Luis Marés Feliu, and built between 1969 and 1972, the complex was promoted by the Obra Sindical del Hogar as part of a major state-led effort to provide high-quality, low-cost social housing during Spain's post-war urban expansion (Mengual, 2016; Tortosa Garcia, 2017; Reig Navarro, 2024).

Due to its architectural and urban value, innovative construction techniques, the complex has been recognized and listed in the DOCOMOMO Ibérico Register, positioning it as a significant milestone of modern architectural heritage in the Mediterranean region. The neighbourhood is characterized by a high-density urban fabric composed of different building typologies. This case study focuses specifically on the eight-story linear blocks, classified as the A8-3 typology (Figure 4.1 and 4.2), which constitutes the dominant residential unit within the entire development. Planimetrically, each block houses 560 compact apartments, with an average usable floor area of approximately 76 m^2 per unit. The architectural design layout positions the apartments symmetrically along an East-West longitudinal axis. This specific orientation was deliberately chosen to maximize natural daylight distribution and leverage cross-ventilation, a crucial passive cooling mechanism within the warm Mediterranean climate context.



Figure 4.1 – Site plan of Antonio Rueda urban block. The colours distinguish the different building typologies.

Figure 4.2 – Pictures of Antonio Rueda neighbourhood. From the top left, the A2-4 and B2-3 blocks, below, the A8-3 and the A4-3 blocks.



At the ground level, the buildings feature an open-pilotis or portico system designed to promote pedestrian permeability and connect the communal outdoor spaces. However, this architectural feature introduces a severe, continuous thermal bridge beneath the first-floor apartments, which are directly exposed to the outdoor microclimate.

From a technical standpoint, the Grupo Antonio Rueda complex embodies the transition towards industrialization and prefabrication that characterized late-modern architecture. The structural framework consists of a reinforced concrete frame with unidirectional floor slabs. The vertical envelope is particularly innovative for its time, utilizing rendered Ytong[1] modular cellular concrete blocks as external infill panels. While these cellular concrete components offered advanced thermal and structural performance compared to traditional solid brick masonry in the 1970s, they currently exhibit significant physical degradation and fail to meet contemporary energy efficiency requirements. The original fenestration system represents the most critical weak point in the building envelope. The windows consist of galvanized steel or non-thermally broken aluminium frames equipped with single-pane glazing (typically 4 mm thickness), supplemented by external adjustable louvers for solar protection. To establish a numerical baseline for the energy simulation, the current thermal transmittances (U values) of the existing envelope components were calculated and cross-referenced against the maximum thresholds mandated by the current Spanish building code for the Mediterranean climatic zone, DB-HE1 (Table 4.2).

[1] Load-bearing and insulating autoclaved aerated concrete (AAC) blocks.

Table 4.2 – Comparison between actual transmittances and those established as maximum values by DB-HE1 Spanish regulation.

	Thermal transmittances U [W/m²K]	
Components	Existing Building	DB-HE1, Climatic Zone B3
Perimetral walls	0.93	1
Roof	0.81	0.65
Slabs	1.54	0.65
Windows	5.70	4.20

The experimental construction techniques and socio-spatial characteristics of the Grupo Antonio Rueda complex make it an interesting environment for addressing the second research questions. The modularity and repetitive geometric nature of the A8-3 blocks provide a baseline to test how a digital model can structure information. Due to the frequent unease of access, residential sites often require moving from archival records to simulations. This case study, being based on information desumed from archive documentations, also represents a testbed on how to define the minimum necessary Level of Information Need (ISO 19650). It determines which semantic parameters should be embedded in the BIM environment to support energy forecasting without unnecessary over-modelling.

Moreover, large-scale social housing retrofits inherently involve a wide range of stakeholders, from environmental engineers to municipal decision-makers and residents. By utilizing this complex, multi-family asset, the research can evaluate how data can be translated into intuitive, multi-criteria comparison dashboards. This ensures that highly technical environmental outputs remain legible, usable, and actionable for non-expert users involved in public housing renovation strategies.

4.3. Workflow. Informative modelling to support the comparison of renovation strategies

The proposed methodological framework is structured around an integrated digital workflow designed to align retrofitting requirements with performance simulations (Figure 4.3). This approach transitions from archival data collection and interpretation to multi-dimensional parametric modelling, concluding with the comparison of a set of multi-criteria potential retrofitting alternatives rooted in ecodesign principles. By linking historical conservation constraints with predictive environmental simulations, this workflow bypasses traditional single-parameter evaluations, establishing an automated decision-support framework that targets the reduction of operational Energy Use Intensity (EUI), mitigation of operational carbon and enhancement of indoor socio-spatial liveability. Operationalizing these objectives within a digital environment, the replicability of the process was taken into account. The first step implicates the establishment of quantitative and qualitative metrics aligned with ISO 19650-1:2018 Level of Information Need protocols. Then, development of an informative model embedding legacy material and semantic attributes was carried out, integrating the aforementioned parameters. Subsequentially, the processing and extraction of analytical data via integrated interoperable engines took place. Finally, it was possible to achieve scenario profiling by executing a comparison to evaluate alternative design interventions.

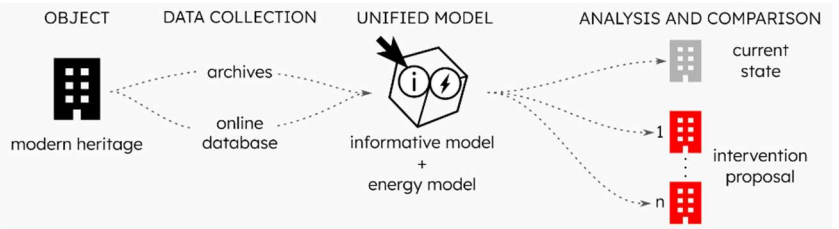

Figure 4.3 – The diagram outlines the data pipeline applied for modern heritage buildings.

4.3.1. Existing building modelling

This section describes the operative data integration into a BIM environment and adopted procedures to construct the digital baseline. To establish the spatial framework of the case study, the two-dimensional documents of the Grupo Antonio Rueda residential complex were collected, using the original 1960s architectural drawings and DOCOMO's online archive as primary sources. These archival records were translated into the three-dimensional virtual space, providing a geometric base for the development of the case study informative model. The current physical condition and use of the building were verified, providing a foundation for the digital modelling process.

The model was then semantically enriched by incorporating multi-layered material assemblies for all primary building components, including external envelopes, internal partitions, horizontal slabs, roofing systems, and fenestration. To allow the evaluation and subsequent comparative analysis of the proposed retrofitting interventions key thermophysical properties were embedded within each material layer, according to the criteria established in the previous section. These parameters comprise thermal conductivity (λ [W/m·K]) density (ρ [kg/m^3]), and specific heat capacity (c [J/kg·K]). Given the exploratory scope of this research, these attributes were primarily derived from manufacturer technical datasheets corresponding to the materials originally deployed, or selected from standard commercial analogues when exact matches were unavailable. Information on the specific use of each space and a characterization of the plants were added for each space of the building. Furthermore, the actual geographic location of the complex was set so that all calculations could be based on real climate data from the Valencia metropolitan area (Figure 4.4).

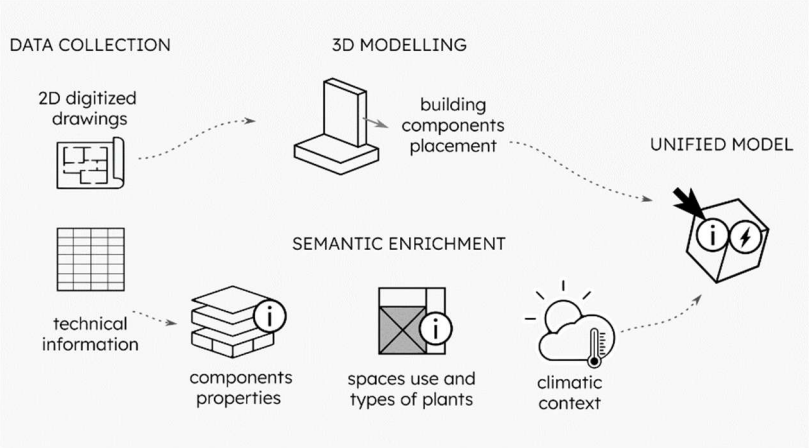

Figure 4.4 – Workflow diagram illustrating the generation of a unified model through data collection, 3d modelling, and semantic enrichment.

Once the model representing the current conditions was completed, it served as the basis for generating energy model (Figure 4.5). Once the building's energy model was generated, it was exported to Autodesk Insight in gbXML format, that ensures seamless data exchange and allows mapping the thermophysical properties of materials, such as component thickness and thermal transmittance. This has enabled energy analyses to be carried out that incorporate real geometric construction and climatic aspects of the building, facilitating the accurate assessment of the building's energy consumption and carbon footprint in global and detailed terms according to the building's facilities or construction materials. The assumptions that are used for energy simulations are based on ASHRAE standards. Through the Insight plug-in, the building's annual EUI, divided into different consumption ranges, and operational carbon that quantifies the CO_2 equivalent emissions associated with energy consumption during the use and operation of a building, were calculated. Before to expose the results, it is necessary to clarify that the analysis of energy consumption and lighting in buildings

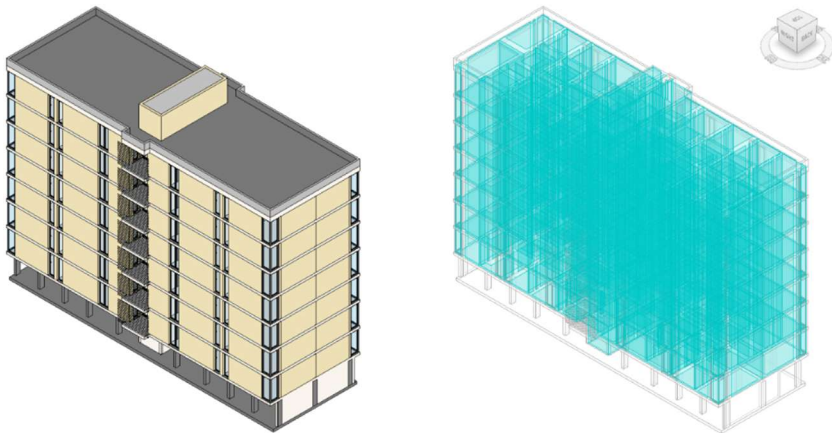

Figure 4.5 – On the left, 3D informative model of the building; on the right the analytical spaces of the energy model in Revit 2024.

conducted directly through the BIM model, although offering meaningful insights, remains a theoretical simulation study.

As such, it presents the typical limitations of this type of approach, which in this case include the following. The construction characteristics of the building's façades have been determined through observation, thickness measurements, and consultation of the technical documentation of the original project carried out in the mid-1960s. It has therefore not been possible to carry out on-site tests of transmittance, infiltration, or humidity, which introduces uncertainty into the results. The software does not allow for the incorporation of the effect of vegetation or microclimatic phenomena, restricting the analysis of passive bioclimatic strategies. The thermal properties of the windows must be selected from a list of predefined windows in the software used. Although the Autodesk Insight and EnergyPlus databases are extensive, they do not always accurately reproduce the original construction solutions of the complex, limiting the accuracy of the model. The software used does not consider relevant thermal bridges in buildings with exposed concrete structures, resulting in an underestimation of energy losses.

Finally, the study focuses on a single block (A8-3), so the results do not represent the total complexity of the neighbourhood or its typological, volumetric, and orientation variations.

4.3.2. Energy analysis and design hypothesis

The preliminary evaluation of the building's energy model, conducted on the linear block type A8-3 reveals a heavy dependence on fossil fuels and an elevated energy intensity (Figure 4.6).

The annual consumption obtained through digital simulation was 305.59 kWh/m², indicating that the building has a high energy intensity, typical of mid-20th century residential architecture. This value can be disaggregated for the residential interior spaces isolating distinct end-use demands, demonstrating that summer cooling constitutes the dominant energy requirement at 77.89% of the total load. This pronounced requirement reflects the severe thermal loads of the Mediterranean summer compounded by the inadequate insulation of the building envelope. Conversely, artificial lighting accounts for 13.39%, while internal electrical appliances represent a demand of 6.85%.



Figure 4.6 – Insight results for the existing building case study. Operational carbon and Annual Energy Use Intensity components are highlighted.

Finally, space heating presents a minor demand of 1.87%, a consequence of both the mild winter climate of the region and the compensatory effect of direct solar gains (Table 4.3).
The operational carbon analysis shows an annual consumption of 122.502 $kgCO_2e$, with a clear predominance of fossil fuel consumption over electricity consumption. This emission profile exhibits an acute imbalance toward fossil-fuel vectors, which account for 72.6% of the total footprint, whereas electricity consumption accounts for the remaining 27.3% (Table 4.4).
Concurrently with the thermal analysis, the daylight performance simulation was performed on a representative floor to evaluate solar radiation utilization and indoor illuminance patterns. The internal luminance evaluations were calibrated to the autumn equinox on September 21, selecting 9:00 am and 3:00 pm as representative temporal benchmarks. At these specific times, the sun's low and relatively horizontal incidence promotes deep horizontal penetration of direct solar rays through the façade openings.

Table 4.3 – Annual Energy Use Intensity of the existing building and relative contributions expressed in kWh/m² and in percentage.

Annual Energy Use Intensity [kWh/m²]	305.59	
Cooling	238.02	77.89%
Interior lighting	40.91	13,38%
Interior equipment	20.94	6.85%
Heating	5.72	1.87%

Table 4.4 – Operational carbon of the existing building and relative contributions expressed in $kgCO_2e$ and in percentage.

Annual Operational Carbon [$kgCO_2e$]	122.502	
Electricity	33,492.20	27.3%
Fossil fuel	89,009.81	72.6%

This geometric condition introduces noticeable glare phenomena that compromise visual well-being and threaten compliance with the indoor environmental tolerances dictated by the European standard UNE-EN 17037:2020. The simulation results reveal an uneven and highly fragmented distribution of natural light across the domestic units. In peripheral zones near the exterior envelope, direct sunlight causes illuminance levels to spike up to 6000 lux, represented graphically by intense yellow shades that denote high glare vulnerability.
In contrast, internal rooms and deep core spaces lack sufficient illumination, with values regularly dropping below 1200 lux (Figure 4.7 and Figure 4.8). This sharp decline stems from a low window-to-wall ratio and internal partitions that obstruct the deep propagation of natural light. The resulting lighting map depicts an abrupt and disproportionate transition between over-illuminated perimeters and dark central cores.

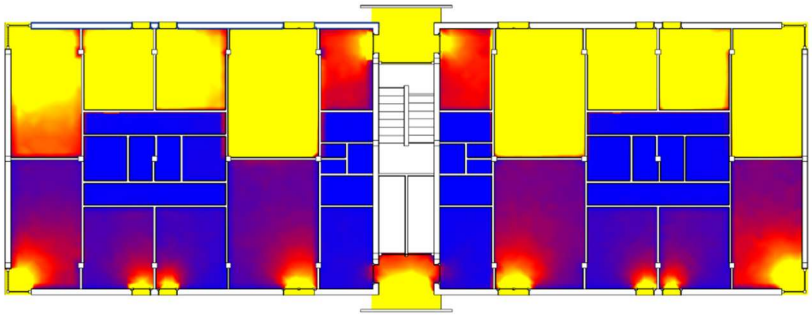

Value	Color below value
Max	RAL 1026
1076	RAL 1026
972	RGB 255-204-0
864	RGB 255-153-0
756	RGB 255-102-0
648	RGB 255-051-0
540	Red
432	RGB 204-000-0
324	RGB 153-000-1
216	RGB 102-000-1
108	RGB 051-000-2
0	Blue

Figure 4.7 – Lighting analysis expressed in lux (9/21, 9:00 am).

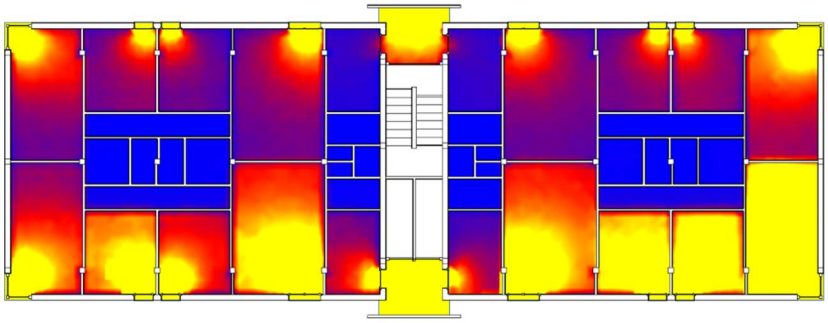

Value	Color below value
Max	RAL 1026
1076	RAL 1026
972	RGB 255-204-0
864	RGB 255-153-0
756	RGB 255-102-0
648	RGB 255-051-0
540	Red
432	RGB 204-000-0
324	RGB 153-000-1
216	RGB 102-000-1
108	RGB 051-000-2
0	Blue

Figure 4.8 – Lighting analysis expressed in lux (9/21, 3:00 pm).

4.3.3. Hypothesis of intervention

In light of the thermal and visual performance deficits identified in the baseline diagnostic phase, this study establishes a structured framework of alternative retrofitting scenarios designed to mitigate the building's operational vulnerabilities. To establish a structured multi-criteria comparison of the proposed retrofitting strategies, the methodological framework differentiates between scenarios that preserve the existing built volumes and those that require structural or spatial modifications. This taxonomy defines a gradient spanning from non-invasive, conservative preservation to active volumetric interventions. The first category of interventions focuses exclusively on passive and fabric-first optimization strategies that maintain the baseline usable floor area intact, thereby mitigating spatial disruption for the inhabitants. The second category of the proposed framework encompasses active interventions that expand the existing volumetric boundaries of the building fabric to address both spatial obsolescence and energetic inefficiency.

Interventions Without Modifying Usable Floor Area

Case 1 implicates the complete replacement of the original single-paned fenestration system with a modern, high-performance assembly. This intervention incorporates sliding frames for their specific geometric adaptability to varied domestic layouts, featuring double-glazing units integrated into thermally broken aluminium frames. Under this configuration, the simulated thermal U (W/m^2K) of the window assembly drops (Table 4.5). As the case study is located in a Mediterranean region, where the main impact is related to cooling demand, the low-emission glass will be placed on the exterior surface to reduce solar heat gain. Sliding frames were selected for their adaptability to various interior layouts.

Table 4.5 – Comparison between new windows transmittances, actual ones, and those established as maximum values by DB-HE1 Spanish regulation.

Component	Transmittances U [W/m²K]		
	Proposed intervention	Existing building	DB-HE1, climatic zone B3
Windows	1.53	5.70	4.20

The upgrade of the glazed components directly reduces both operational carbon emissions and the annual Energy Use Intensity (EUI). This decarbonization is entirely attributable to the fossil fuel component, which drops, while the electricity-related share remains constant (Table 4.6).
Similarly, the decline in annual EUI is primarily driven by mitigated cooling demand, supplemented by a minor reduction in heating requirements, whereas energy consumption for interior lighting and equipment remains unchanged. Although this fabric modification does not meet the strict criteria for total material reversibility, it preserves the architectural appearance and rhythm of the original façade and does not implicate disturbance for residents.

Table 4.6 – Operational carbon and annual EUI comparison of consumption between current state and case 1.

	Current state	Case 1
Operational Carbon total [kgCO_2e]	**122,502.00**	**118,723.44**
%	0.00%	–3.18%
Annual Operational Carbon—electricity	33,492.19	33,492.19
Annual Operational Carbon—fossil fuel	89,009.81	85,231.25
Annual EUI [kwh/m²]	**305.59**	**295.12**
%	0.00%	–3.55%
Heating	5.72	3.99
Cooling	238.02	229.28
Interior lighting	40.91	40.91
Interior equipment	20.94	20.94

Case 2 expands the thermal envelope optimization through the application of an external thermal insulation system across the vertical facades, combined with a structural and material upgrade of the horizontal roof. The roof intervention involves laying high-density insulation beneath a new paving layer, which simultaneously resolves thermal deficiencies and enhances the functional utility of the rooftop as a shared recreational space for residents. This insulation strategy improves the thermal resistance of the envelope, reducing the vertical wall and the roof transmittance (Table 4.7).

Concurrently the annual Energy Use Intensity (EUI) decreases, a reduction primarily driven by mitigated cooling demand, followed by successive savings in heating demand. Conversely, energy consumption for interior lighting and equipment grows slightly. While this intervention preserves the building's original architectural aesthetics, it cannot be classified as materially reversible and entails minor, temporary disruption for the residents.

The addition of external insulation to the perimeter walls and the roof yields a marked decrease in operational carbon emissions. This environmental improvement is partially driven by a reduction in the fossil-fuel component, whereas the electricity-related share exhibits an increase (Table 4.8).

Table 4.7 – Comparison between new components, actual ones, and those established as maximum values by DB-HE1 Spanish regulation.

Component	Transmittances U [W/m²K]		
	Proposed intervention	Existing building	DB-HE1, climatic zone B3
Perimetral walls	0.19	0.93	1.00
Roof	0.20	0.81	0.65

Table 4.8 – Operational Carbon and Annual EUI comparison of consumption between current state and Case 2.

	Current state	Case 2
Operational Carbon total [kgCO_2e]	**122,502.00**	**115,866.33**
%	0.00%	–5.73%
Annual Operational Carbon—electricity	33,492.19	34,333.94
Annual Operational Carbon—fossil fuel	89,009.81	81,532.39
Annual EUI [kwh/m^2]	**305.59**	**287.35**
%	0.00%	–26.35%
Heating	5.72	2.65
Cooling	238.02	221.10
Interior lighting	40.91	41.73
Interior equipment	20.94	21.88

Case 3 addresses solar heat gain and daylight quality through the systematic integration of dynamic solar shading devices at the façade openings (Figure 4.9). This scenario involves replacing the degraded and largely inoperable original blinds with external sliding shutters equipped with horizontal slats, specifically engineered to shield the highly exposed east- and west-facing fenestrations. From a conservation standpoint, this shading system represents a highly reversible and non-invasive approach that aligns with the core principles of circular ecodesign, offering a flexible mechanism to mitigate the extreme summer glare and thermal stress identified in the baseline simulation.

The installation of solar shading systems yields a notable reduction in operational carbon emissions, a decrease driven exclusively by lower fossil fuel consumption. This passive strategy simultaneously minimizes the annual Energy Use Intensity (EUI), an efficiency gain primarily achieved through mitigated space cooling demands.

Conversely, the introduction of shading elements leads to a marginal increase in annual heating loads due to reduced winter solar heat gains, alongside a slight rise in electricity consumption for interior lighting and building equipment.

From a preservation and logistical perspective, this retrofit scenario represents a fully reversible intervention that exerts no impact on the original architectural aesthetics of the building while ensuring zero structural or spatial disruption for the residents (Table 4.9).

Table 4.9 – Operational Carbon and Annual EUI comparison of consumption between current state and Case 3.

	Current state	Case 3
Operational Carbon total [kgCO_2e]	122,502.00	122,179.42
%	0.00%	–0.26%
Annual Operational Carbon—electricity	33,492.19	33,501.44
Annual Operational Carbon—fossil fuel	89,009.81	88,677.97
Annual EUI [kwh/m^2]	305.59	304.76
%	0.00%	0.27%
Heating	5.72	6.19
Cooling	238.02	236.70
Interior lighting	40.91	40.93
Interior equipment	20.94	20.95

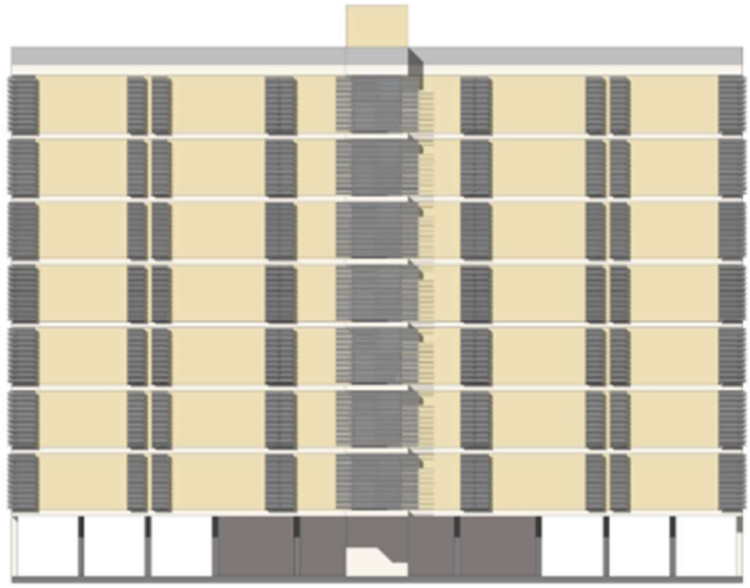

Figure 4.9 – The building main façade with new solar shading elements.

Case 4 introduces a continuous ventilated façade skin supported by an independent metal substructure that extends vertically down to the ground level (Figure 4.10). The hydrothermal optimization achieved by this system is primarily governed by its breathability and passive cooling dynamics. The continuous air cavity serves as a physical barrier that interrupts direct solar radiation and mitigates sensible heat accumulation within the primary masonry mass, while concurrently driving heat removal via the chimney effect. Furthermore, this architectural cavity isolates the historical reinforced concrete framework from driving rain and accelerates moisture evaporation during highly humid seasons. The installation of a continuous façade skin yields a significant reduction in operational carbon emissions, a decrease driven exclusively by lower fossil fuel consumption (Table 4.10). This envelope intervention simultaneously minimizes the annual Energy Use Intensity (EUI), an efficiency gain primarily achieved through mitigated space cooling demands. Additionally, both the space heating loads and the electricity consumption for interior lighting and building equipment experience a concurrent decrease.

Table 4.10 – Operational Carbon and Annual EUI comparison of consumption between current state and Case 4.

	Current state	Case 4
Operational Carbon total [$kgCO_2e$]	122,502.00	106,385.08
%	0.00%	–15.15%
Annual Operational Carbon—electricity	33,492.19	33,929.00
Annual Operational Carbon—fossil fuel	89,009.81	72,456.08
Annual EUI [kwh/m^2]	305.59	257.67
%	0.00%	–18.59%
Heating	5.72	4.22
Cooling	238.02	191.60
Interior lighting	40.91	40.72
Interior equipment	20.94	21.13

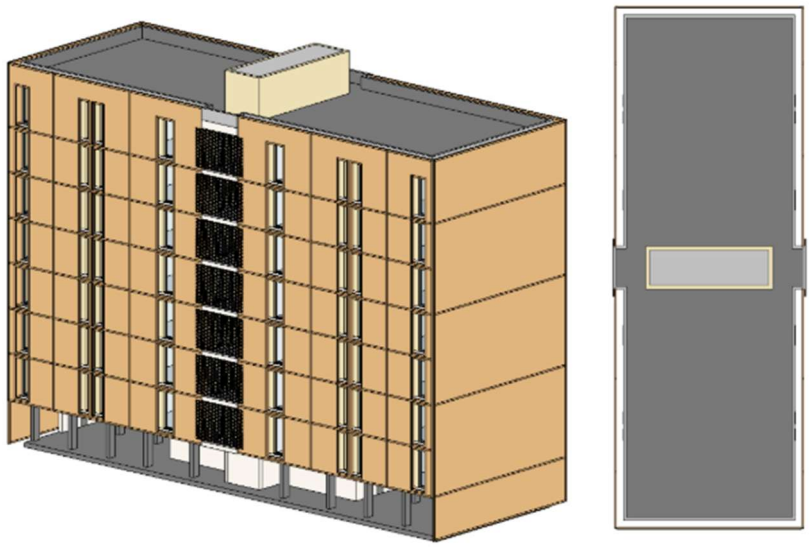

Figure 4.10 – On the left, installation of a continuous façade skin; on the right, roof flat detailing ventilated façade system.

From a conservation standpoint, this ventilated envelope represents a structurally independent and highly reversible solution that directly satisfies circular ecodesign criteria.

Interventions with modifications to usable floor area.

Driven by the current requirement to expand the built area within the existing site boundaries, the subsequent interventions maximize the usable floor area, as quantified in Table 4.11.

Case 5 utilizes prefabricated tray terraces to physically expand the domestic floor area of each residential unit by shifting the position of the exterior thermal envelope outward (Figure 4.11).

Table 4.11 – Modifications to usable floor area case by case.

	Case 5	Case 6	Case 7	Case 8
Area [m^2]	1832.01	1932.54	1613.35	1633.7
%	20.11%	24.27%	9.29%	10.42%

The depth of the east and west façade-facing rooms is extended by 90 cm on floors one through three, and by 150 cm on floors four through eight. This variable depth gradient is calibrated to safeguard the logistical functions of the open pilotis ground floor while preventing root or canopy interference with trees. In conjunction with this spatial reconfiguration, new fenestration units are integrated into the expanded envelope to introduce direct natural light and passive cross-ventilation into the kitchen spaces. Because this scenario implies a complete renovation of the vertical perimeter, it inherently absorbs the material upgrades defined in Case 1 and Case 2 to guarantee compliance with contemporary technical standards.

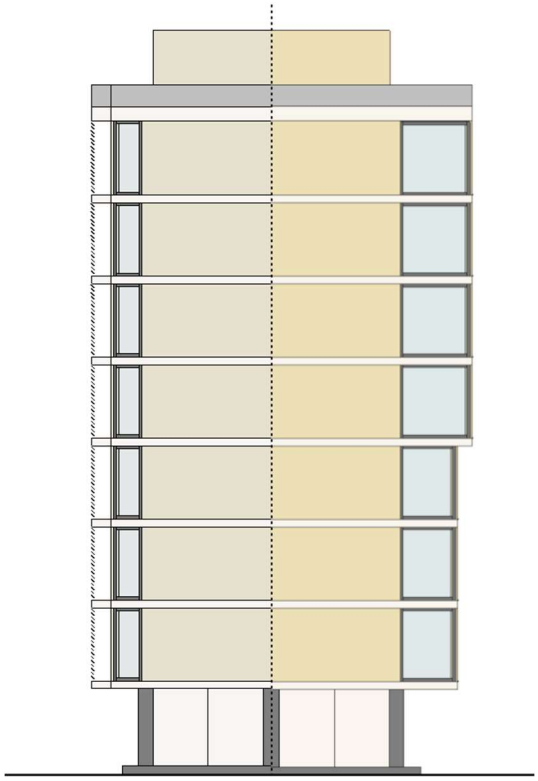

Figure 4.11 – On the left, the current building profile, compared to the tray terraces on the right.

Increasing the depth of façade-facing rooms inherently expands the built area, resulting in a corresponding increase in operational carbon emissions (Table 4.12). This upward trend is primarily driven by the fossil-fuel component, whereas the electricity-related share exhibits a more moderate growth. Conversely, the annual Energy Use Intensity (EUI) decreases, an efficiency improvement predominantly achieved through reduced space heating demands.
This thermal benefit is balanced by a concurrent increase in energy consumption for space cooling, interior lighting, and building equipment. From a conservation perspective, this structural expansion alters the formal character of the building, resulting in a highly invasive intervention that impacts both the architectural aesthetics of the façade and the daily routine of the residents.

Table 4.12 – Operational Carbon and Annual EUI comparison of consumption between current state and Case 5.

	Current state	Case 5
Operational Carbon total [kgCO_2e]	**122,502.00**	**153,493.19**
%	0.00%	20.19%
Annual Operational Carbon—electricity	33,492.19	42,946.72
Annual Operational Carbon—fossil fuel	89,009.81	110,546.47
Annual EUI [kwh/m^2]	**305.59**	**304.89**
%	0.00%	-0.23%
Heating	5.72	2.09
Cooling	238.02	239.45
Interior lighting	40.91	41.47
Interior equipment	20.94	21.89

Case 6 evaluates a vertical densification strategy through the addition of a two-story rooftop extension, introducing 16 new residential units that replicate the original typological layout. To support this added volume, the horizontal roof structure undergoes a comprehensive structural and thermal upgrade, utilizing thick high-density insulation to improve the global

energy performance of the underlying block. To maintain architectural and environmental continuity, the new residential levels replicate the integrated fenestration and insulation metrics established in Case 1 and Case 2.
The operational carbon emissions exhibit an increase, an outcome anticipated due to the expanded surface area. This upward trend is partially driven by the fossil-fuel component, while the electricity-related share concurrently expands (Table 4.13). Conversely, the reduction in annual Energy Use Intensity (EUI) is primarily achieved through a substantial decline in cooling loads, supplemented by further decreases in space heating demands. Additionally, energy consumption for interior lighting and building equipment experiences a minor decrease. Although this intervention results in a change to the volume, it neither compromises the overall character of the building nor generates an excessive disturbance for its residents.

Table 4.13 – Operational Carbon and Annual EUI comparison of consumption between current state and Case 6.

	Current state	Case 6
Operational Carbon total [kgCO_2e]	**122,502.00**	**136,288.28**
%	0.00%	10.12%
Annual Operational Carbon—electricity	33,492.19	36,419.31
Annual Operational Carbon—fossil fuel	89,009.81	99,868.97
Annual EUI [kwh/m²]	**305.59**	**255.10**
%	0.00%	–19.79%
Heating	5.72	4.08
Cooling	238.02	200.65
Interior lighting	40.91	33.43
Interior equipment	20.94	16.93

Case 7 examines the adaptive reuse of the open ground floor through the insertion of eight new habitable units designed to serve as community coworking spaces or flexible temporary rentals for the neighbourhood. While this structural filling of the pilotis does not directly optimize the thermodynamic

behaviour of the upper residential floors, it establishes an empirical model for maximizing urban footprint efficiency amid pressing municipal housing shortages. This ground-floor activation implements the high-performance window frames and insulated wall systems of Case 1 and Case 2, ensuring that the newly enclosed spaces satisfy modern regulatory comfort standards while stabilizing the building's lower thermal boundary.

The addition of eight ground-floor dwellings inherently expands the total floor area, resulting in an expected increase in operational carbon emissions. This upward trend is partially driven by the fossil-fuel component, while the electricity-related share concurrently expands (Table 4.14). Concurrently, the annual Energy Use Intensity (EUI) decreases, an efficiency improvement predominantly driven by a significant decline in space cooling loads, followed by secondary reductions in space heating demands. Conversely, energy consumption for interior lighting and building equipment experiences a marginal decrease. From an architectural perspective, this intervention generates a profound aesthetic impact, as it fails to liberate the ground-floor plane as originally intended in the initial design.

Table 4.14 – Operational Carbon and EUI comparison of consumption between current state and Case 7.

	Current state	Case 7
Operational Carbon total [kgCO_2e]	**122,502.00**	**128,919.92**
%	0.00%	4.98%
Annual Operational Carbon—electricity	33,492.19	36,771.83
Annual Operational Carbon—fossil fuel	89,009.81	92,148.08
Annual EUI [kwh/m^2]	**305.59**	**290.31**
%	0.00%	–5.26%
Heating	5.72	3.09
Cooling	238.02	225.62
Interior lighting	40.91	40.66
Interior equipment	20.94	20.94

However, from a logistical and structural standpoint, it does not impose excessive disruption on the residents and can be classified as a partially reversible modification.

Case 8 proposes a modular and flexible retrofitting strategy characterized by the attachment of industrialized plug-in pods that expand individual domestic floor areas according to evolving family demographics and changing user needs (Figure 4.12). Similar to the preceding spatial expansions, this modular system operates as a comprehensive envelope upgrade by embedding the high-performance building envelope metrics of Case 1 and Case 2 into the prefabricated components. Capitalizing on the newly established exterior perimeter, this modular intervention replicates the spatial optimization of Case 5 by inserting dedicated windows that provide direct natural light and mechanical-free ventilation to the kitchen zones.
The incorporation of modular extensions on the principal façades inherently expands the total built area, resulting in a predictable increase in operational carbon emissions. This upward trend is partially driven by the fossil fuel component (Table 4.15).
Concurrently, the annual Energy Use Intensity (EUI) increases, an expansion predominantly driven by heightened space cooling demands, which outweigh the sequential reductions achieved in space heating requirements. Additionally, energy consumption for interior lighting and building equipment experiences a minor increase. From an architectural perspective, the supplemental floor area significantly alters the formal character of the building, constituting a substantially more invasive intervention than previous scenarios. Consequently, this structural modification generates a higher level of disruption for the residents and must be classified as a materially non-reversible intervention.

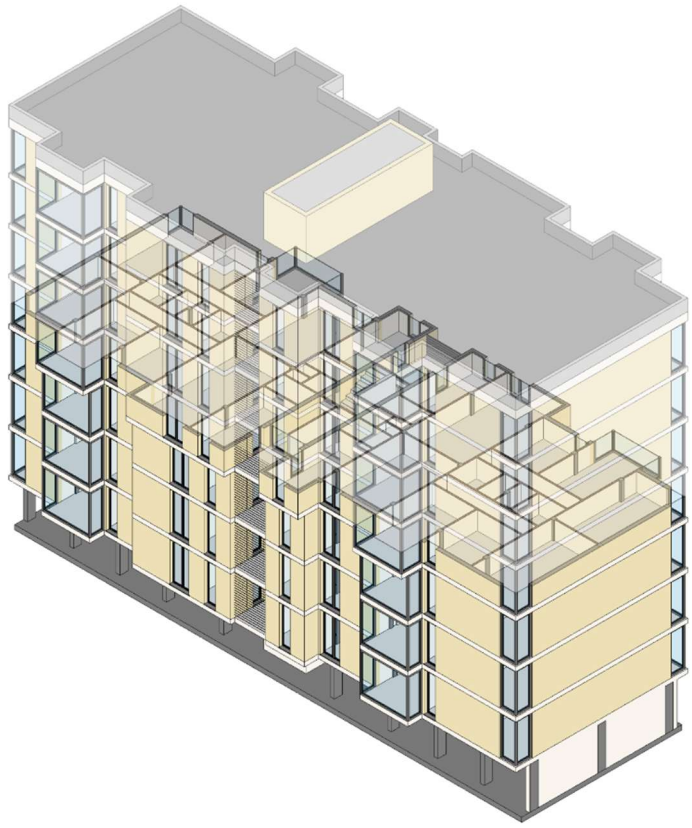

Figure 4.12 – Modular intervention to extend floor areas.

Table 4.15 – Operational Carbon and EUI comparison of consumption between current state and Case 8.

	Current state	Case 8
Operational Carbon total [kgCO_2e]	**122,502.00**	**154,238.42**
%	0.00%	20.58%
Annual Operational Carbon—electricity	33,492.19	37,756.44
Annual Operational Carbon—fossil fuel	89,009.81	116,481.97
Annual EUI [kwh/m^2]	**305.59**	**411.06**
%	0.00%	25.66%
Heating	5.72	2.98
Cooling	238.02	334.82
Interior lighting	40.91	47.87
Interior equipment	20.94	25.38

Lighting Analysis Results

The predictive simulation of indoor daylighting performance highlights the distinct luminous behaviours of the evaluated retrofitting scenarios, differentiating between geometrically invariant passive interventions and volumetric alterations.
For Cases 1, 2, 6, and 7, the lighting analysis yields results closely aligned with current conditions, as these specific interventions preserve the original façade openings that primarily dictate solar incidence. In the morning simulations configured at 9:00 a.m., daylight distribution remains evenly spread across the three evaluated illuminance bands, with each range accounting for approximately 30% to 36% of the useful floor area. Conversely, the afternoon simulations at 3:00 p.m. reflect the high solar exposure of the west-facing orientation, causing the mid-range illuminance band, defined between 300 and 1,076 lux, to become dominant and encompass 41.47% of the total evaluated surface area.
Case 3 modifies these baseline patterns through the integration of external sliding shutters equipped with horizontal slats. This passive shading strategy significantly expands the indoor areas characterized by low solar incidence, between 0 and 300 lux, which grow to encompass 61.26% of the total floor plane. This configuration directly mitigates over-illumination, shrinking the zones exposed to high and medium radiation to 16.21% and 22.53%, respectively, relative to the alternative interventions.
In Case 4, which involves the application of a continuous ventilated façade system, the absolute window surface area is held constant, yet the increased depth of the envelope modifies the solar incidence angles at the aperture reveals. Consequently, the 9:00 a.m. metric shows a 6.70% increase in floor area falling below 300 lux and a concurrent 5.82% decrease in spaces exceeding 1,076 lux. This architectural screening effect is further amplified at 3:00 p.m., where the

low-illuminance areas expand by 20.53% and the over-illuminated zones decrease by 9.26%.
The volumetric reconfigurations evaluate alternative spatial and luminous trade-offs. The deeper internal spaces introduced in Case 5 reveal an increased polarization of light intensities at 9:00 a.m., with high-intensity zones expanding to 37.40% of the area, while mid-range values decrease by 12.52% relative to the baseline. At 3:00 p.m., this spatial extension induces a 9.31% shift in mid-range illuminance and an 11.39% increase in areas below 300 lux.
Finally, in Case 8, the creation of new terraces and expanded glazed surface areas increases the floor area exposed to intensities above 1,076 lux by 7.72% at 9:00 a.m. and by 12.17% at 3:00 p.m., whereas low- and mid-range illuminance bands experience minor fluctuations under 5%.

4.3.4. Quantitative and qualitative assessment of comparative modern heritage retrofitting scenarios

This section provides an integrated assessment of the proposed retrofitting interventions by synthesizing the quantitative results of the annual Energy Use Intensity, operational carbon emissions, and indoor luminous behaviour analyses. Beyond these primary environmental performance indicators, the discussion incorporates qualitative socio-architectural vectors linked to contemporary living needs. Specifically, it addresses the modification of interior usable floor surfaces, the physiological invasiveness of each intervention during the construction phase, and the degree to which the historic architectural fabric is irreversibly altered. Synthesizing these interlinked criteria offers a comprehensive understanding of the divergent performance trajectories of the proposed scenarios, framing the critical trade-offs between environmental optimization and architectural quality. The combined datasets derived from the annual EUI and operational carbon simulations (Figure 4.13 and 4.14), alongside the daylighting calculations (Figure 4.15 and 4.16),

highlight the distinct behaviours of the proposed interventions, establishing a comparative framework for their environmental performance and heritage preservation implications.

The first group of strategies, comprising the envelope-focused passive interventions (Cases 1–4), maintains absolute geometric invariance and preserves the existing window-to-wall ratios of the modern complex. The predictive simulations demonstrate that the most substantial reductions in both annual EUI and operational carbon are achieved via fabric-first envelope upgrades.

This is most apparent in Case 4, where the continuous ventilated façade skin delivers optimal thermodynamic returns, followed closely by the external insulation system evaluated in Case 2. While the independent impacts of Case 1 and Case 3 remain relatively modest, these passive measures are highly compatible with incremental, cumulative deployment strategies to maximize systemic efficiency.

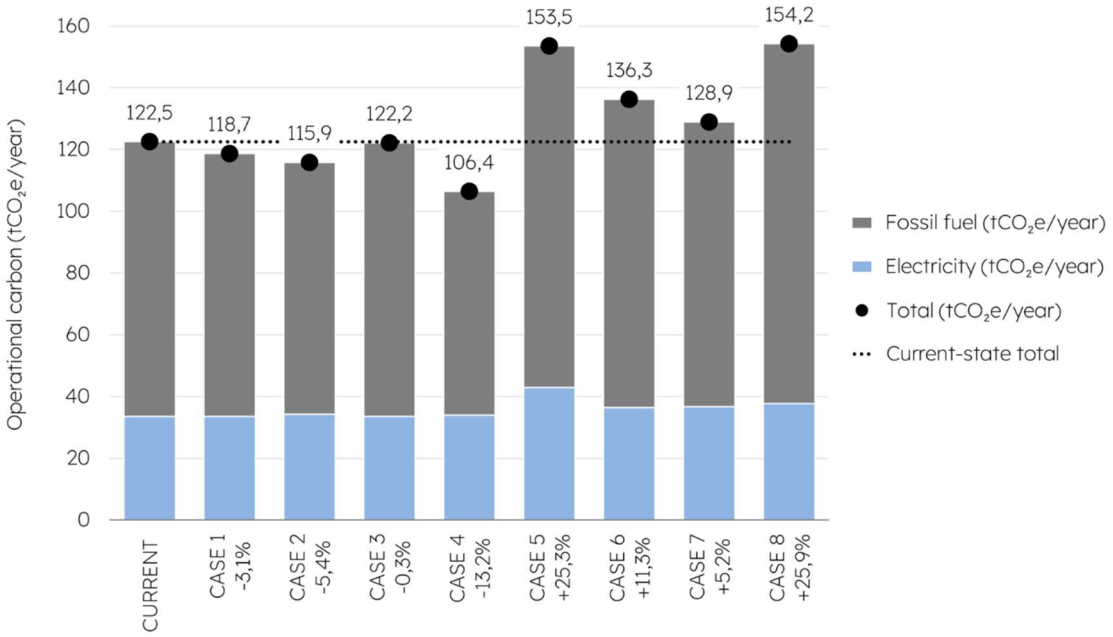

Figure 4.13 – Operational carbon kgCO_2e (electricity and fossil fuel) case by case.

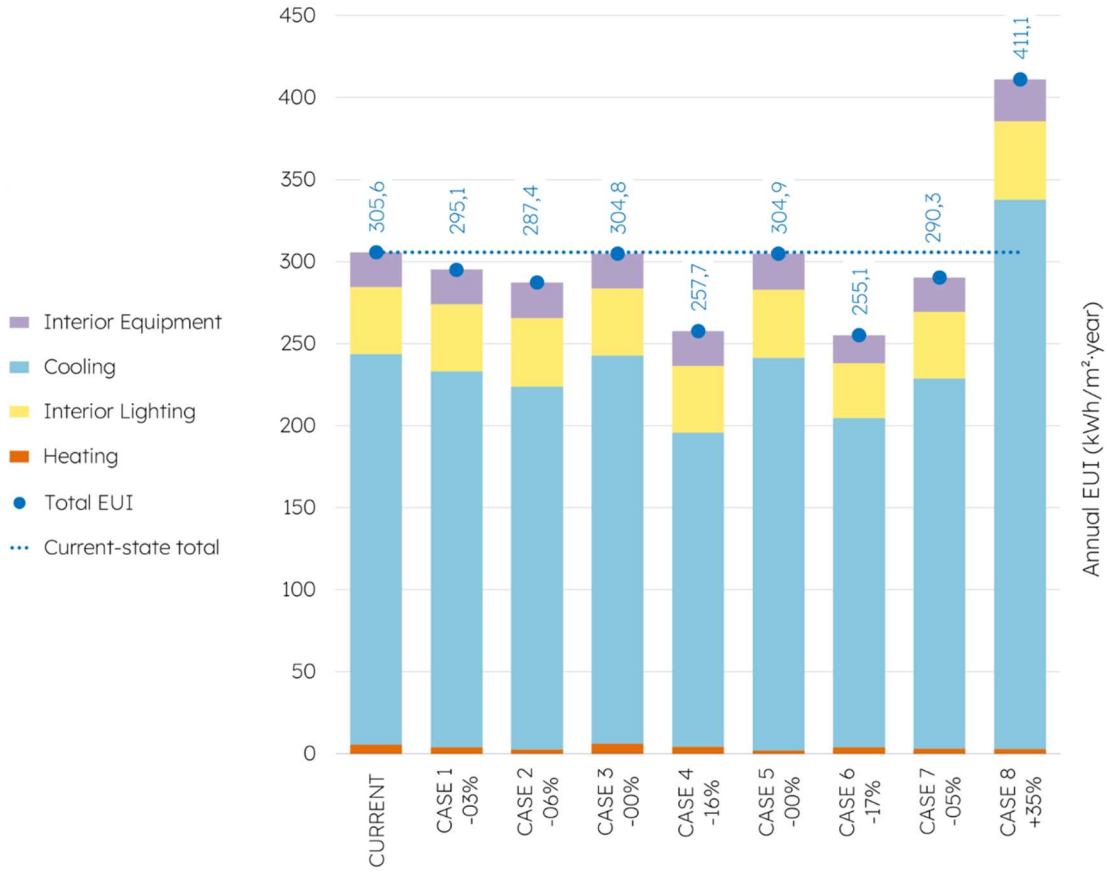

Figure 4.14 – Annual EUI KWh/m² case by case.

Crucially, the components and materials selected for these retrofits can accurately replicate the authentic tectonic rhythm of the heritage façade, ensuring negligible aesthetic impact while safeguarding architectural authenticity. They are also minimally invasive for the residents, as the construction workflows can be carried out entirely from the building exterior; conversely, these preservation-led options fail to provide the additional habitable floor area required to combat urban housing obsolescence.

Because these passive strategies do not adjust the external opening boundaries, indoor daylighting patterns remain aligned with the baseline diagnostic conditions. This geometric consistency perpetuates a distinct spatial duality between the

highly illuminated peripheral zones, where maximum daylight levels approach 6,000 lux, and the deep central cores, which consistently remain under 1,200 lux. The relatively homogeneous light distribution recorded during the morning simulations at 9:00 a.m. contrasts with the wider data dispersion observed at 3:00 p.m., which is induced by direct western solar exposure.

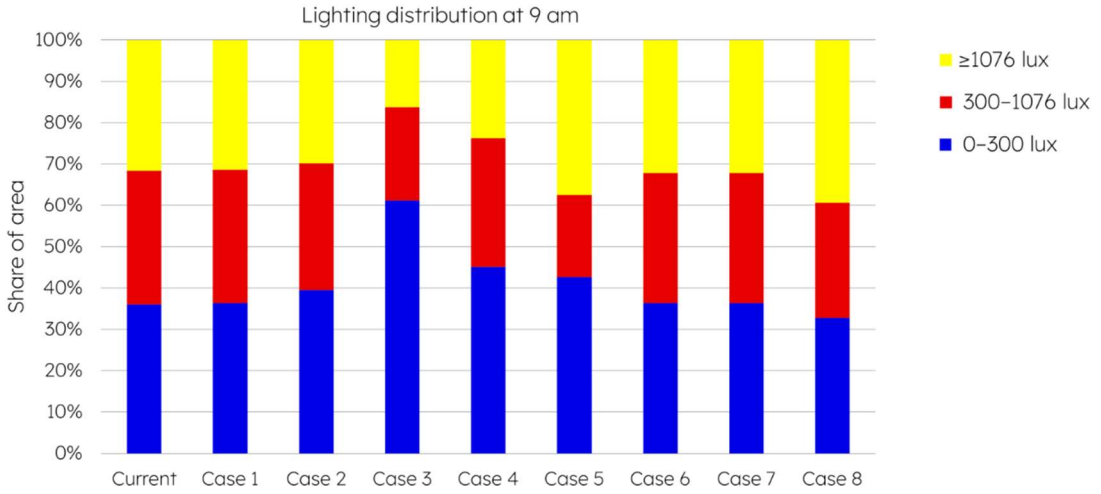

Figure 4.15 – Lighting intensity distribution at 9 a.m., 09/21.

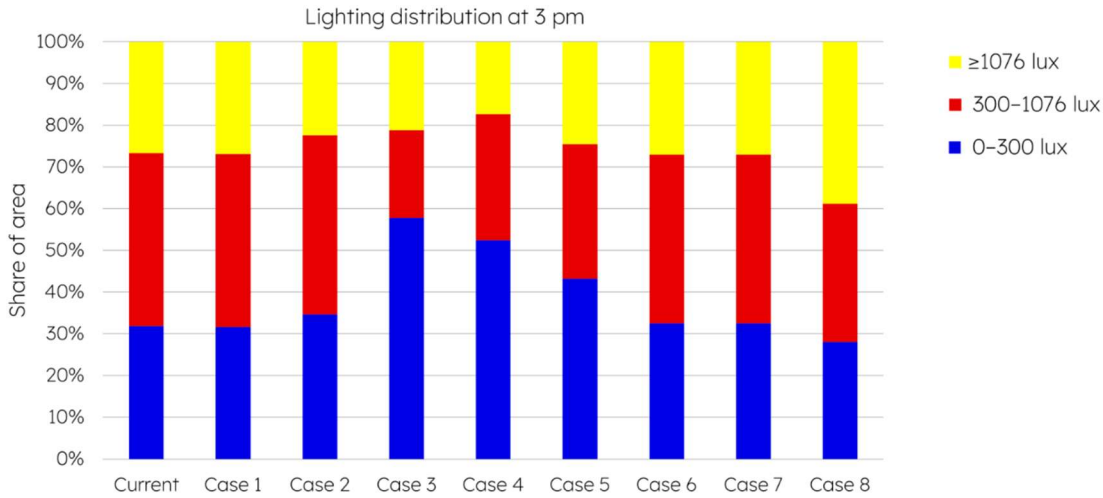

Figure 4.16 – Lighting intensity distribution at 3 p.m., 09/21.

Nevertheless, the transitions between over-illuminated zones exceeding 1,076 lux and medium-range spaces between 300 and 1,076 lux remain balanced across these cases, confirming that maintaining geometric invariance safeguards stable, predictable indoor luminous conditions.

The second group of proposed interventions introduces volumetric variations that structurally alter the building envelope to expand the usable interior area, adjust glazing ratios, or enclose open spaces. These active interventions generate highly heterogeneous energy and lighting behaviours. Within this category, the vertical densification evaluated in Case 6 maximizes habitable square meters and achieves the most significant operational carbon reduction among the volumetric scenarios, though it induces a corresponding increase in raw annual energy intensity. Case 7 exhibits a comparable performance trend, though it yields slightly less pronounced environmental savings and imposes a severe architectural impact by enclosing the open ground-floor pilotis, thereby disrupting the intended public permeability and spatial flow of the original master plan.

Volumetric modifications likewise complicate the interaction between daylight availability and thermal behaviour. While expanded glazing configurations and reconfigured façades successfully deepen natural light penetration into the newly added spaces, they simultaneously amplify solar incidence. This effect is particularly pronounced in the afternoon simulations, leading to elevated summer solar heat gains that increase thermal loads and potentially raise cooling energy consumption. Cases 5 and 8 exemplify these systemic trade-offs, as both scenarios heavily modify the formal architectural expression of the façade while yielding limited performance benefits. Case 5 achieves only a marginal reduction in annual EUI, whereas Case 8 demonstrates poor efficiency gains across both EUI and operational carbon metrics, failing to

justify the high physical invasiveness and material irreversibility of its prefabricated plug-in components.
Ultimately, this comparative analysis indicates that passive, envelope-first retrofits constitute the most balanced and context-compatible trajectory for this modern heritage case study. They combine high cumulative efficiency potential, minimal tenant disturbance, and stable daylighting behaviour while allowing the preservation of the building's original architectural features. By contrast, while volumetric strategies successfully provide necessary usable floor area extensions and enhance localized daylight availability, they introduce unfavourable interactions between expanded glazing surfaces, increased solar heat gains, and irreversible morphological transformations that compromise the integrity of the historic façade.

4.4. Answer to the RQ. Considerations on the Antonio Rueda case study

The Antonio Rueda case study answers Research Question 2 by identifying the characteristics that a digital model should possess to support an energy renovation process throughout the initial design phases. These characteristics were found to be contingent upon the specific phase and objective of the preliminary analysis, rather than upon developing a single optimal configuration.
The results show that embedding thermophysical attributes within the building components, was sufficient to generate early-stage forecasting from archival sources alone, without recourse to destructive on-site testing. The semantic enrichment was not limited to material properties: the parallel integration of space-specific use profiles and plant characterizations proved equally necessary, since energy demand and internal comfort conditions cannot be inferred from envelope performance alone. Likewise, anchoring the model to the actual geographic location of the complex

allowed all subsequent calculations to be grounded in real climate data for the Valencia metropolitan area, rather than in generic or default weather assumptions. The coupling of this informative model with interoperable BEM engines, via open formats such as gbXML, enabled the simultaneous processing of competing quantitative and qualitative parameters, thereby exposing trade-offs that would otherwise have remained concealed within a single-parameter evaluation.

Most notably, those passive interventions yielding the most favourable thermodynamic and daylighting performance were also found to be the least capable of addressing the housing complex's requirement for additional habitable floor area.

This dialectic between environmental optimization and architectural transformation substantiates the strategic value of a multi-criteria, comparative framework over isolated simulation exercises, and further specifies the answer to research question 2. A digital model supporting energy retrofitting must be capable of holding quantitative performance metrics and qualitative preservation constraints within the same evaluative structure. Passive, envelope-first strategies were observed to preserve the historic tectonic rhythm while imposing minimal disruption upon residents, whereas volumetric strategies expanded usable floor area at the expense of greater invasiveness, reduced reversibility, and less predictable interactions between glazing, solar gain and cooling demand. Neither category, taken in isolation, satisfies the full range of retrofitting objectives. Rather, it is their systematic comparison that renders the model useful for decision-making purposes.

With respect to how the usability and interoperability of EBIM models can be guaranteed for users with different skills and needs (research question 3), the experimentation indicates that the translation of underlying simulation datasets into synthetic, comparative dashboards constitutes the primary condition for their legibility to non-technical stakeholders, such

as municipal authorities and residents, who are not equipped to interpret raw energy or carbon outputs. It should be noted, however, that this degree of multi-criteria synthesis required a substantial simulation effort across eight distinct scenarios; for decision contexts limited to a preliminary screening of interventions, a reduced subset of criteria, such as EUI and reversibility alone, could plausibly support comparable decisions at a fraction of the modelling effort.

References chapter 4

Angileri, G., Bernardo, G., Currò, G., Fiandaca, O., Minutoli, F., Palmero Iglesias, L. M., & Russo, G. F. (2024). The Santa María Micaela Residential Complex in Valencia (Spain) Study of the Original Design to Assess Its Bioclimatic Potentials for Energy Upgrading. Buildings, 14(12), 3819.

ASHRAE. Available online: https://www.ashrae.org/ (accessed on 30 July 2026).

Azhar, S., Khalfan, M., Maqsood, T. (2012). Building information modeling (BIM): Now and beyond. Australas. J. Constr. Econ. Build., 12, 15–28. Available online: https://search.informit.org/doi/10.3316/informit.013120167780649 (accessed on 02 January 2026).

Berg, F., Flyen, A. C., Godbolt, Å. L., Broström, T., (2017). User-driven energy efficiency in historic buildings: A review. J. Cult. Herit. 2017, 28, 188–195. https://doi.org/10.1016/j.culher.2017.05.009.

CTE DB-SI, 2025. Código Técnico de la Edificación de España. Documento Básico SI Seguridad en caso de Incendio. Available online: https://www.codigotecnico.org/pdf/Documentos/SI/DBSI.pdf (accessed on 02 January 2026).

DB-HE1. Documento Básico Ahorro de Energía—Exigencia Básica HE 1: Condiciones Para el Control de la Demanda Energética, 2022. Available online: https://www.codigotecnico.org/pdf/Documentos/HE/DBHE.pdf (accessed on 13 October 2025).

Elnagar, E., Munde, S., Lemort, V. (2021). Energy efficiency measures applied to heritage retrofit buildings: A simulated student housing case study in Vienna. Heritage, 2021, 4, 3919–3937. https://doi.org/10.3390/heritage4040215.

Energy Use Intensity (EUI)—AIA. Available online: https://aiacalifornia.org/what-you-can-do-right-now/energy-use-intensity-eui/ (accessed on 30 July 2026).

European Comission. Ecodesign for Sustainable Products Regulation (ESPR). Available online: https://commission.europa.eu/energy-

climate-change-environment/standards-tools-and-labels/products-labelling-rules-and-requirements/ecodesign-sustainable-products-regulation_en (accessed on 18 July 2024).

European Green Deal for 2030. European Comission Priorities 2019–2024. Available online: https://commission.europa.eu/strategy-and-policy/priorities-2019-2024/european-green-deal_en (accessed on 30 July 2026).

European Commission. Political Guidelines 2024–2029. European Commission: Brussels, Belgium, 2024. Available online: https://commission.europa.eu (accessed on 30 July 2026).

European Comission. Energy Performance of Buildings Directive. Available online: https://energy.ec.europa.eu/topics/energy-efficiency/energy-performance-buildings/energy-performance-buildings-directive_en (accessed on 30 July 2026).

Grupo de Viviendas Antonio Rueda—DOCOMOMO Ibérico. Available online: https://docomomoiberico.com/edificios/grupo-de-viviendas-antonio-rueda/ (accessed on 13 October 2025).

Hu, M., Zhang, K., Nguyen, Q., Tasdizen, T. (2023). The effects of passive design on indoor thermal comfort and energy savings for residential buildings in hot climates: A systematic review. Urban Clim., 49, 101466.

ICOMOS. International Charter for the Conservation and Restoration of Monuments and Sites (the Venice Charter 1964). Available online: https://www.icomos.org/images/DOCUMENTS/Charters/venice_e.pdf (accessed on 30 July 2026).

INE. Instituto Nacional de Estadística. Household Projections, Years 2024–2039, 2024. Available online: https://www.ine.es/dyngs/Prensa/en/PROH20242039.htm (accessed on 30 July 2026).

ISO 14006:2020; Environmental Managment Systems—Guidelines for Incorporating Eco-Design. ISO: Vernier, Switzerland, 2020.

Jung, D.E., Kim, S., Han, S.; Yoo, S., Jeong, H., Lee, K.H., Kim, J. (2023). Appropriate level of development of in-situ building information modeling for existing building energy modeling

implementation. J. Build. Eng., 69, 106233. https://doi.org/10.1016/j.jobe.2023.106233.

Liang, W., Ahmad, Y., Mohidin, H.H.B. (2023). The development of the concept of architectural heritage conservation and its inspiration. Built Herit., 7, 21. https://doi.org/10.1186/s43238-023-00103-2.

Machado, N., Morioka, S.N. (2021). Contributions of modularity to the circular economy: A systematic review of literature. J. Build. Eng., 44, 103322.

Martínez-Molina, A., Tort-Ausina, I., Cho, S., Vivancos, J.L., (2016). Energy efficiency and thermal comfort in historic buildings: A review. Renew. Sustain. Energy Rev., 61, 70–85. https://doi.org/10.1016/j.rser.2016.03.018.

Mengual, J.F.P. (2016) Impulsores de la Modernidad en la Arquitectura Valenciana. La Arquitectura de Valls—García Sanz. Aportaciones a la Estandardización (1952-82). Ph.D. Thesis, Universidad Cardenal Herrera-CEU, Alfara del Patriarca, Spain, 2016.

Ministerio Para la Transición Ecológica y el Reto Demográfico, y el MINISTERIO de Transportes, Movilidad y Agenda Urbana. Condiciones Técnicas de los Procedimientos Para la Evaluación de la Eficiencia Energética. 2020.

Montiel-Santiago, F., Hermoso-Orzáez, M., Terrados-Cepeda, J. (2020). Sustainability and Energy Efficiency: BIM 6D. Study of the BIM Methodology Applied to Hospital Buildings. Value of Interior Lighting and Daylight in Energy Simulation. Sustainability, 12, 5731. https://doi.org/10.3390/su12145731.

Piselli, C., Romanelli, J., Di Grazia, M., Gavagni, A., Moretti, E., Nicolini, A., Cotana, F., Strangis, F., Witte, H. J. L., e Pisello, A. L. (2020). An Integrated HBIM Simulation Approach for Energy Retrofit of Historical Buildings Implemented in a Case Study of a Medieval Fortress in Italy. Energies 13(10):2601.

Reig Navarro, J. (2024). Mejoras de eficiencia energética en el grupo de viviendas Antonio Rueda de Valencia. Universitat Politècnica de València.

Sanhudo, L. P. N., & Martins, J. P. da S. P. (2018). Building information modelling for an automated building sustainability assessment. Civil Engineering and Environmental Systems, 35(1–4), 99–116.

Sanhudo L., Ramos, N. M.M., Poças Martins J., Almeida Ricardo M.S.F., Barreira E., Simões L. M., Cardoso, V. (2018). Building information modeling for energy retrofitting – A review

Tortosa Garcia, M. (2017). Estudio para la rehabilitación energética y de accesibilidad de vivienda social: el caso del grupo "Antonio Rueda" en Valencia. Universitat Politècnica de València.

USGBC (United States Green Building Council). USGBC LEED v5 for Building Design and Construction. Available online: https://www.usgbc.org/leed/v5 (accessed on 10 November 2025).

UN-EN 17037:2020/AC:2022; Daylight in Buildings. UNE Standards: Madrid, Spain, 2022.

Veerendra, G.T.N., Dey, S., Mantle, E.J., Manoj, A.V., Kumaravel, B., Babu, P.S.A., Rao, P.K.R (2024). Material estimation and energy analysis for a domestic building using Revit architecture and insight: A sustainable approach. Asian J. Civ. Eng. 2024, 25, 3431–3447. https://doi.org/10.1007/s42107-024-00988-z.

Zhang, T.; Yang, X.; Wu, Z.; Zhai, G.; Doan, D.T.; Sun, Q.; Gao, H. Application of Building Information Modeling for Energy Efficiency: A Systematic Review. Buildings 2025, 15, 3722. https://doi.org/10.3390/buildings15203722.

Disclaimer

This chapter is partially based on:

Bernardini, E., Dalprà, M., Maracchini, G., Massari, G. A., Albatici, R., *Digitalization of Existing Buildings to Support Renovation Processes: A Comparison of Procedures*. In *TEMA*, v. 2024, 10, n. 2 (2024), p. 140-153.

Zuanni, A., Bernardini, E., Cristofolini, A., Massari, G. A., Roman, O., *Integrated Modelling and Digital Representation for Design and Production*. In *Proceedings Graphic Thinking XVII International Conference on Graphic Expression Applied to Building– APEGA 2025*, Sangonera la Verde, Spain: Universidad Politécnica de Cartagena ediciones UPCT, 2025, p. 941-953.

5. Geometric and informative models to support renovation design workflow. A case study in Povo (TN)

The case study presented in this chapter, an example of contemporary residential heritage, addresses all three research questions jointly, focusing on how data acquisition strategies affect the construction of digital models, the characteristics such models must possess to support a prefabricated retrofit intervention, and how their usability and interoperability can be guaranteed across the heterogeneous chain of actors involved in an off-site manufacturing process.
The chapter is structured in two main parts. The first introduces the theoretical framework, discussing the role of Building Information Modelling within the ecological–digital transition of the construction sector and the potential of Off-site Manufacturing (OSM) to reduce the time, disruption, and quality uncertainty of traditional retrofits, with particular attention to the informative continuity that must be preserved across survey, modelling, and production interoperability.
The second part focuses on the *Condominio Pantè* case study, a residential building in Povo, Trento, developed within the European Horizon 2020 project "ARV", investigating how different survey strategies support both a preliminary energy assessment and the detailed design of a prefabricated timber-framed envelope, together with the development of a parametric object library bridging the architectural model and the physical production of retrofit components.
This case study tests the feasibility of specific acquisition and modelling strategies within an operative retrofit process, essential for scaling up modular interventions on the wider residential building stock.

5.1. Theoretical framework. From data acquisition to construction site

As already stated in the previous chapters, the renovation of the existing building stock is widely recognised as one of the most effective levers for reducing the environmental impact of the construction sector, given that a substantial share of the current housing stock predates the introduction of modern energy efficiency standards (Du et al., 2019). Traditional retrofit interventions, however, are often characterised by long execution times, significant disruption to occupants, and a level of quality that is difficult to control on site. Prefabrication has progressively gained relevance as a strategy capable of addressing these limitations, by transferring a substantial part of the construction process from the building site to a controlled manufacturing environment (Wang et al., 2020; Yin et al., 2019). This shift not only enables greater precision and quality assurance in the production of building components, but also allows on-site activities to be compressed into significantly shorter timeframes, thereby reducing the impact of the intervention on the everyday life of residents and on the surrounding urban context.

It is within this broader framework that the ecological–digital transition of the construction sector, and the role of Off-site Manufacturing (OSM) as one of its key strategies, can be properly situated. The digitization of OSM processes relies on a range of complementary technologies, among which Building Information Modelling stands out as a central driver, serving both as a tool and as a methodology spanning multiple phases of design and production (Habibi, 2017; Sanhudo et al., 2018; Yin et al., 2019; Tata, 2023). Several European demonstration projects (Du et al., 2019; Li & Chen, 2020; Pernetti et al., 2021) have tested prefabricated envelope and roof solutions integrating insulation, renewable energy systems, plug-and-play connections, and developed BIM-based platforms to support decision-making, design and life-

cycle assessment, confirming the potential of these approaches. This operative approach to research also results in the definition of a set of recurring financial, social and technical barriers, among which the fragmentation of the sector, the resistance to process innovation, and the lack of interoperability between proprietary software and data formats appear particularly critical.

From the analysis of these projects, several best practices emerge to address the technical challenges of modular retrofitting. One of the key requirements is the definition of clear digital workflows for data acquisition and management: since production methods vary across manufacturers and existing buildings rarely present standard features, large-scale standardisation of production processes is difficult to achieve, whereas optimising the digital workflow itself represents a more practical solution. This is particularly relevant during the pre-recognition phase, where digital survey techniques such as 3D scanning and photogrammetry can achieve high accuracy, but require specialised expertise and entail additional costs; balancing time, cost and accuracy at this stage is essential to support faster and more precise production (Massari et al., 2022). The adoption of standardised data acquisition and processing procedures, together with collaborative environments such as BIM, can support a more structured exchange of information among the multiple actors involved, architects, manufacturers, and other stakeholders (Vavallo et al., 2019; González, 2019). Nonetheless, BIM alone does not constitute a solution unless it is fully exploited in terms of data-sharing potential and carefully planned from the outset. A further and largely unresolved issue concerns the interoperability between design environments and manufacturing tools. Seamless integration between BIM and Computer-Aided Manufacturing (CAM) processes could significantly advance the automation of production, improving precision and efficiency while ensuring the accurate

translation of digital models into physical prefabricated components (Barbini, 2021).

These best practices, and in particular the emphasis placed on interoperability between design and production, point to a research problem that extends beyond the specific case of the OSM projects reviewed so far, that is ensuring the continuity of digital information across the entire chain leading from the survey of the existing building to the physical realisation of its prefabricated retrofit components (Massari et al., 2022). This continuity depends on choices made at each stage of the process, the accuracy pursued during data acquisition, the level of detail adopted in the information model, and the format through which that model is transferred to production tools, whose cumulative effect determines whether the digital workflow ultimately supports, or instead hinders, the goals of speed, precision and cost-effectiveness that motivate the adoption of prefabrication in the first place (Massari et al., 2022).

This issue is compounded by a further difficulty specific to the digitization of existing buildings, as opposed to new construction. While research and professional practice tend to converge for new buildings, thanks to established national and supranational standards (UNI EN ISO 19650; UNI 11337), the modelling of existing assets still encounters significant barriers, largely due to the difficulty of defining criteria for information restitution that are both applicable on a large scale and sufficiently flexible (Volk et al., 2014; Jordan-Palomar et al., 2018).

The literature on this topic can be broadly divided into two main strands. Studies oriented towards the knowledge and restoration of historically and artistically valuable buildings through HBIM methodologies (Lovell et al., 2023; Lo Turco et al., 2022), and contributions aimed at obtaining models suitable for performance analyses, particularly of an energy or structural nature (Sanhudo et al., 2018; Ursini et al., 2022;

Doukari et al., 2024). Specifically, the analytical focus shifts from assessing the existing building as a standalone structure to utilizing its features as the foundation for integrating prefabricated retrofitting components.

In this context, the intersection between the representation of existing buildings and the parametric modelling of prefabricated systems raises a specific problem, that is ensuring compatibility between information acquired on site, often affected by a degree of geometric uncertainty intrinsic to digital survey techniques, and the accuracy required by industrial production processes, typically in the order of a few millimetres (Larsen et al., 2011; Gilmour & Stroulia, 2022).

This problem can be articulated through three logically distinct moments, beginning with the initial acquisition and representation of the as-is state. At this stage, the selection of the digital survey technique, whether range-based, image-based, or a hybrid configuration dictates the density, accuracy, and homogeneity of the resulting geometric model. While a simplified volumetric representation may suffice for macro-level energy simulations, it lacks the geometric accuracy required for the millimetric positioning of prefabricated façade components.

This technical variance directly influences the subsequent construction of the information model and the definition of its Level of Development (LOD) (Abualdenien & Borrmann, 2022). Because modelling existing assets demands a highly selective approach, designers must prioritize geometric and semantic fidelity for elements interacting with the retrofit system, while leaving non-critical segments simplified (Massari et al., 2022). In the absence of standardized protocols, this selective synthesis introduces the unresolved challenge of determining exactly what informative content must be made explicit early on to safeguard data continuity.

Ultimately, the geometric and informative discrepancies culminate in the final transfer of design data to computer-

aided manufacturing (CAM) environments (Massari et al., 2022). At this intersection, the reliance on open-source exchange formats frequently triggers a loss of structural and parametric hierarchies native to the BIM platform, creating a technical bottleneck that demands manual data remediation before CNC timber machining can commence. These three moments, survey, modelling, and production interoperability, do not constitute isolated phases, but an informative continuum whose overall coherence, more than the quality of each individual phase, determines the effectiveness of the digital process as a whole (Table 5.1).

Consequently, managing this informative continuum requires a careful optimization problem that balances geometric accuracy against time and cost effectiveness. While maximizing data density and modelling resolution minimizes on-site assembly errors, it simultaneously escalates upfront computational costs, processing times, and specialized labour requirements. Conversely, over-simplifying early-stage workflows to reduce initial expenditures introduces geometric risks that compound down the line, leading to costly manual corrections during the CAM phase or structural misfits on the construction site. A viable digital workflow must therefore calibrate the accuracy of the survey and the depth of the BIM model to the specific tolerances of the industrial manufacturing process, establishing a baseline where digital investments directly translate into predictable, high-fidelity physical outputs.

Table 5.1 – Evaluation framework for the digital workflow phases, criteria, and measurement metrics.

Phase	Evaluation criteria	Measurement	
Acquisition	Survey technique coverage	Selectivity/ Completeness	
	Resulting data accuracy	Deviation/ Tolerances	
Modelling	LoD differentiation	Semantic completeness/ Information usefulness	time/cost
	Standardization	Flexibility/ Replicability	
Production	Information transferability	Informative loss/ Transmission	

5.2. Contextualisation. The "ARV" project and Povo residential building

The multi-family residential building selected as the demonstration case for this research is *Condominio Pantè,* located in the hillside district of Povo, in the municipality of Trento (Italy). The building represents a typical example of the Italian post-war residential heritage, constructed during the 1950s before the introduction of regulations concerning energy efficiency, thermal insulation, and environmental sustainability (Table 5.2 and Table 5.3). Due to its constructive characteristics, geometric regularity, and poor thermal performance, the building constitutes a representative case for investigating digital methodologies supporting deep energy renovation through industrialised construction systems.

The building consists of a three-storey T-shaped volume with a timber hip roof and an unheated attic (Figure 5.1). The structural system is composed of masonry walls built with brick blocks and irregular stone elements finished with external

plaster, while the envelope is entirely uninsulated. The residential units are distributed over staggered half-levels generated by the site's topography, with ancillary spaces located in the basement and attic. The façades are characterised by projecting balconies, irregular window arrangements, and locally protruding stone elements on the northern elevation, all of which contribute to the geometric complexity typically encountered in renovation projects of existing buildings.

From an energy perspective, the building exhibited all the critical characteristics of the Italian residential stock built before the first thermal regulations. Space heating was provided through autonomous gas boilers serving individual apartments, the external envelope presented a thermal transmittance significantly higher than current regulatory limits, and only two apartments had previously undergone partial window replacement. Consequently, the building offered an appropriate testing ground for investigating the integration of digital survey technologies, EBIM, and off-site manufacturing processes within a real renovation project.

The intervention was developed within the framework of the European Horizon 2020 project ARV – Climate Positive Circular Communities, whose objective is to demonstrate scalable renovation strategies capable of supporting the ecological and digital transition of the built environment through circular construction principles and industrialised renovation processes.

Within ARV, the Italian demonstrator investigates the application of prefabricated timber-based envelope systems to improve building energy performance while simultaneously reducing construction time, limiting disturbance to occupants, and increasing production quality through controlled manufacturing environments. Unlike conventional refurbishment projects, the intervention was conceived not only as an energy retrofit but also as an opportunity to

experimentally validate an integrated digital workflow capable of maintaining information continuity throughout the entire renovation process. Consequently, the case study became a living laboratory in which data acquisition, geometric modelling, design development, industrial production, and construction site activities could be analysed as interconnected phases of a single digital process rather than as independent operations.

Table 5.2 – Properties of the external perimeter walls layers before intervention.

External perimeter wall	Thickness [mm]	Conductivity [W/mK]	Conductance [W/m²K]	Resistance [m²K/W]
Limestone and gypsum plaster	20	0.70	35.0000	0.0286
Bricks and stones	440	1.35	3.0682	0.3259
Limestone and gypsum plaster	20	0.70	35.0000	0.0286

Table 5.3 – Properties of the attic slab layers before intervention.

Reinforced brick-concrete slab	Thickness [mm]	Conductivity [W/mK]	Conductance [W/m²K]	Resistance [m²K/W]
Ceramic tiles	15	1.3	86.6667	0.0115
Concrete screed	50	1.06	21.2000	0.0472
Brick-concrete slab	225	-	1.6667	0.6000
Internal plaster	10	0.70	70.0000	0.0143



Figure 5.1 – On the left, aerial photo of Condominio Pantè, on the right, the north façade with protruding stones. Aerial photo by Sovecar s.r.l.

Design strategy and selection of the retrofit solution

The development of the renovation strategy began with a comprehensive assessment of the existing building involving architectural surveys, thermographic inspections, structural evaluations, and energy analyses. These investigations were accompanied by continuous interaction among researchers, designers, manufacturers, and building owners, allowing technical requirements to be balanced with economic constraints and occupants' expectations throughout the decision-making process.

The intervention was designed in accordance with the Italian regulatory framework governing energy renovation, particularly Legislative Decree No. 192/2005 and the incentive scheme introduced by Law No. 34/2020 (Superbonus). Within this framework, two alternative retrofit scenarios were evaluated (Figure 5.2).

The first consisted of a traditional refurbishment strategy based on the application of an External Thermal Insulation Composite System (ETICS) combined with window replacement, boiler substitution, insulation of the first and last slabs, and installation of mechanical ventilation systems. Although representing the most widespread solution currently adopted in Italy, this approach requires extensive scaffolding, prolonged construction activities, and a significant presence of workers on site.

The second strategy considered a fully industrialised intervention based on prefabricated lightweight timber façade modules integrating thermal insulation and designed according to Off-Site Manufacturing (OSM) principles. Compared with traditional solutions, this approach offers considerable advantages in terms of construction speed, quality control, and reduction of on-site operations. However, its application within the Italian construction sector remains limited by the fragmentation of manufacturing processes, the relatively low diffusion of industrialised renovation systems,

and the need to customise each façade according to the geometric characteristics of the existing building.
Rather than adopting either solution independently, the design team selected a hybrid renovation strategy capable of combining the advantages of both approaches. The north and north-east façades, selected as experimental areas, were retrofitted using prefabricated timber modules, while the remaining elevations received a conventional ETICS solution. Additional interventions included roof insulation, replacement of windows not integrated within the prefabricated panels, and substitution of the existing heating systems with high-efficiency condensing boilers, including hybrid units where appropriate. This mixed approach enabled direct comparison between traditional and industrialised construction methods under identical environmental conditions while maintaining compliance with budgetary, technical, and regulatory constraints.

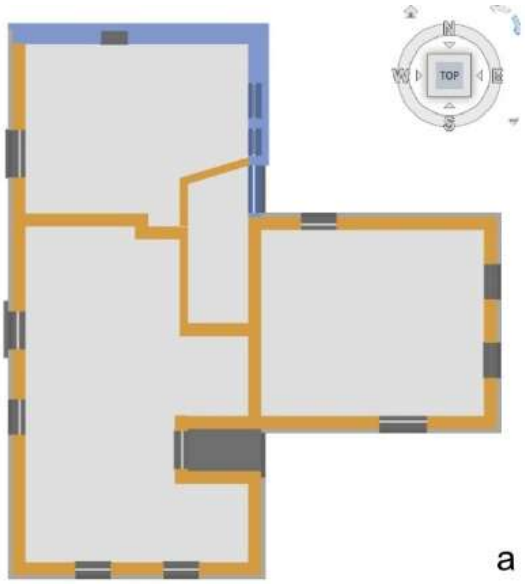

Figure 5.2 – The wall highlighted in blue are those on which the Renew-Wall system was applied, the north and north-east façades.

The Renew Wall prefabricated system

The industrialised solution adopted in the experimental façades is based on the Renew Wall system, developed by the local timber manufacturer Fanti Legnami S.r.l. as a prefabricated timber-framed modular façade specifically conceived for energy renovation of existing masonry buildings. Each panel consists of a fixed structural timber frame composed of horizontal beams and regularly spaced vertical studs, combined with a series of variable layers that can be adapted according to the specific requirements of each intervention. Mineral wool insulation is positioned within the structural frame, while an internal Oriented Strand Board (OSB) panel and an external vapour-permeable wood-fibre board provide structural bracing and optimise the hygrothermal behaviour of the façade package. Additional insulation layers and different external finishes can be incorporated depending on the desired architectural appearance and energy performance (Figure 5.3).

The system also integrates several customised technical components required to adapt industrial production to the irregular geometry of existing buildings. These include timber anchoring substructures fixed to the existing masonry, dedicated window subframes, sealing gaskets ensuring air and water tightness, metal joint covers protecting panel interfaces, and adjustable internal insulation layers capable of compensating for deviations from the theoretical façade plane. Such solutions allow the prefabricated components to accommodate construction tolerances while maintaining the dimensional precision required by industrial manufacturing.

The system was developed within four panel types (Figure 5.4): RW-F (full panel), RW-W (panel with a window opening), RW-D (panel with a door opening), and RW-C (corner panel).

Although originally conceived as a standardised industrial product, the application of Renew Wall within the Povo case study required significant geometric adaptation to the existing

building. This characteristic makes the demonstration particularly relevant from a digital perspective, as the success of the intervention depended largely on the ability to maintain accurate geometric information throughout the entire workflow, from the initial survey to panel production and installation.

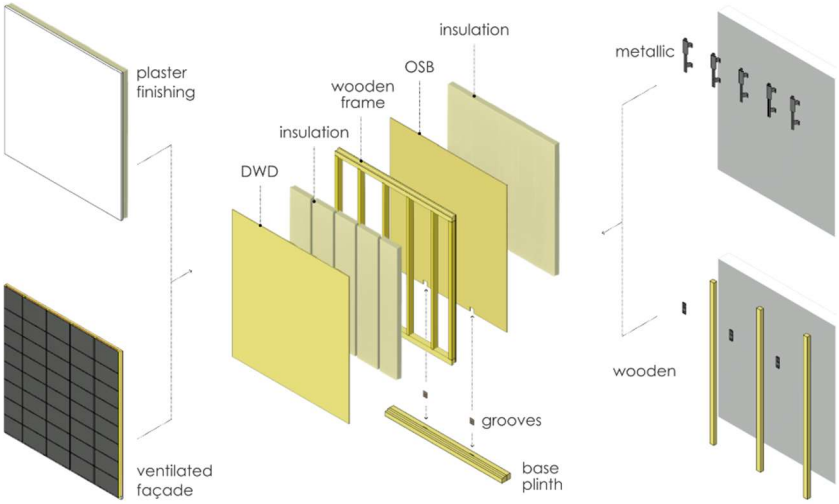

Figure 5.3 – Exploded view of the Renew-Wall panel highlighting the fixed and variable components.

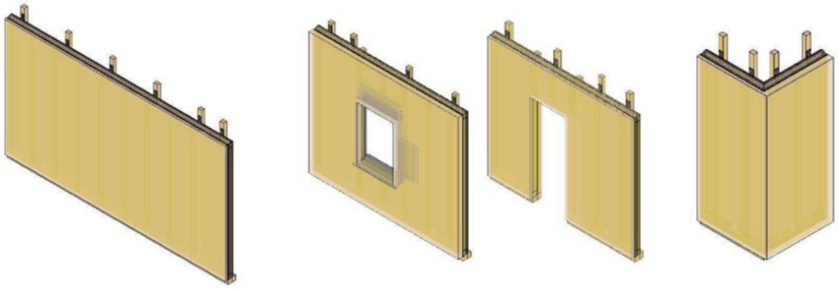

Figure 5.4 – The four panels configuration in BIM environment.[1]

[1] Image from Barbini et al. (2022). Renew-Wall: innovazione e comunicazione di un processo edilizio tra impresa, professione e ricerca. ARCHITETTURA, URBANISTICA, AMBIENTE, 1025-1036.

Digital project management as the backbone of the intervention

Beyond its technological characteristics, the Povo demonstration case provides an opportunity to investigate how digital information management can support the industrialisation of renovation processes. In this context, the digital model is not conceived merely as a three-dimensional representation of the existing building, but as a shared information environment progressively developed through the interaction of architects, engineers, manufacturers, and construction managers.

This approach addresses one of the central research questions of the study: how digital continuity can support industrialised renovation processes while responding to the geometric uncertainties of existing buildings. The Povo demonstrator thus represents not only an application of prefabricated façade technologies, but also a full-scale validation of an integrated workflow in which BIM functions as the connective infrastructure between data acquisition, design development, and production.

5.3. Workflow. Design modelling to support a renovation intervention through prefabricated components

Building on the theoretical framework outlined previously and on the specific technical constraints introduced by the *Condominio Pantè* case study, this section describes the digital workflow developed to support the design of the prefabricated envelope retrofit, from the acquisition of the as-is state to the definition of the information model used for production. The workflow is structured around the three moments identified as constitutive of the informative continuum, namely data acquisition, information modelling, and production interoperability, and is articulated here

through two complementary experimentations conducted on the case study.

The first experimentation addresses the acquisition phase, testing and comparing three digital survey techniques, low-cost LiDAR, close-range photogrammetry, and mobile SLAM scanning, against a traditional approach, with the aim of evaluating their relative feasibility and the usefulness of the resulting data. Consistently with the accuracy-cost/time trade-off discussed in the theoretical framework of this chapter, the comparison is conducted along the criteria of survey technique coverage and resulting data accuracy, in order to determine which acquisition strategy, or combination thereof, best supports the subsequent modelling phase.

The second experimentation concerns the construction of BIM model from the acquired and processed survey data, and is oriented towards two distinct, though interdependent, goals. The preliminary energy assessment of the existing building, and the detailed design of the intervention through prefabricated timber panels.

This dual purpose reflects the selective, use-oriented approach to Level of Development discussed above, whereby the depth and semantic richness of the model are calibrated to the specific requirements of each downstream application, from macro-level performance simulation to the millimetric interfacing required by the Renew Wall system.

Taken together, the two experimentations reconstruct the full workflow of a renovation project based on prefabricated components, and provide the empirical ground on which research question 3 is addressed in the remainder of this chapter.

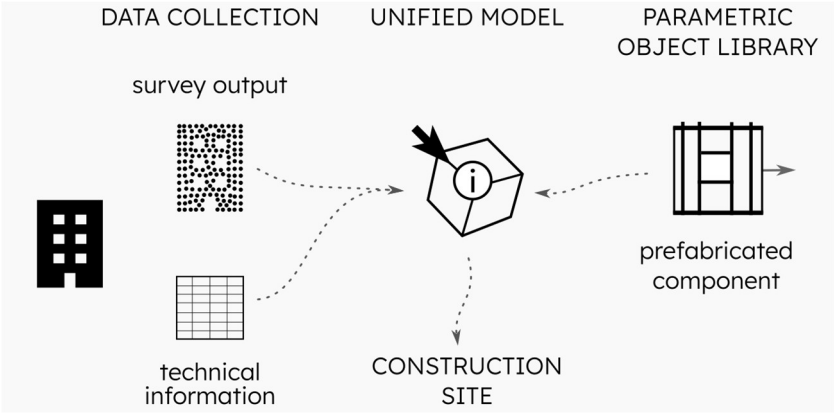

Figure 5.5 – Graphic synthesis of the data integration workflow for construction management. The diagram illustrates how data collection and a parametric object feed into a unified model to guide the construction site operations.

5.3.1. Comparison of data acquisition and processing strategies

As in the Calliano case study, a topographic total station survey[2] provided the common metric benchmark for the comparison, complemented here by a TLS and UAV-photogrammetry cloud supplied by the contractor. The outputs of the three strategies were aligned to these references and evaluated for density and deviation, following the same criteria introduced in Chapter 3[3] (Table 3.1).

The first strategy relied on the LiDAR sensor integrated in a mobile device[4]. Given the short range of the sensor, 5 meters, and the height of the building, the upper floors were reached through a lifting platform, while the ground level could be surveyed directly (Figure 5.6). Of thirty scans acquired, nine were retained, aligned to the topographic references, cleaned, and merged. Density and accuracy were consistent at close

[2] The total station used for this study is a Topcon GPT-1001, part of the equipment supplied by the LAMARC laboratory.

[3] Cloud Compare FOSS was used for the analysis.

[4] The used device was an iPad Pro, operated through the free Scaniverse application and supplied by the LAMARC laboratory.

range but degraded beyond five metres, under strong or backlit illumination, and on large uniform or reflective surfaces, while three-dimensional features such as the north façade's protruding stones were captured reliably. Ground-level acquisition took under an hour, the upper floors about two and a half, for a total processing time of roughly four and a half hours, at negligible instrument and software cost.

The second strategy used photogrammetric reconstruction from two complementary photo sets, the 3DEye telescopic-pole system[5] and a camera[6], yielding 960 detailed and 142 context photographs, of which 802 and all context images respectively were processed in photomodelling software[7], using the topographic points as reference points per image (Figure 5.6). The resulting cloud matched the topographic boundaries but was sparse and unevenly distributed, particularly where lighting or reference points were insufficient. Comparison with the TLS cloud nonetheless confirmed that the reconstructed façade planes were close to straight, indicating good geometric accuracy despite lower density. Acquisition took about one hour at ground level and two for the upper floors, but processing exceeded one working day owing to the manual identification of reference points, with costs concentrated in camera equipment and software licences.

The third strategy employed a mobile scanner[8] (Figure 5.6). A single thirty-minute scan, acquired from ground level and the lifting platform, was aligned to the topographic references and cleaned. Unlike the first two strategies, SLAM performed

[5] The 3DEye system is the same used in chapter 3, composed of a digital camera (Sony Alpha 2000) supported by a gimball and fixed on a telescopic pole, supplied by the LAMARC laboratory.

[6] A Canon EOS600D was used, supplied by the LAMARC laboratory.

[7] 3DF Zephyr was used for photomodelling.

[8] The MLS acquisition was carried out using the GeoSLAM Zeb Horizon mobile mapping system, supplied by SemprebonLux S.r.l.; data acquisition was performed by Ing. Rudy Faitini (SemprebonLux).

consistently on large, homogeneous surfaces and was largely unaffected by lighting, though accuracy decreased with distance from the trajectory. Its principal limitation was instrument cost, offset by markedly faster acquisition and processing. Across the three strategies, acquisition distance, reference-point availability, and lighting emerged as the main factors affecting density and accuracy, confirming at the scale of a residential retrofit case the same accuracy–feasibility trade-off already observed for the mobile and static techniques compared in Calliano. The comparative indicators are summarised in Table 5.4.

The suitability of the resulting clouds for the two modelling goals was then assessed within the BIM environment. For energy simulation, all three strategies produced clouds accurate enough to support a simplified volumetric reconstruction, useful to energy modelling goals. The roof geometry, however, could not be reliably reconstructed from any of the three clouds. For the design of the prefabricated intervention, none of the three strategies met the four-to-seven-millimetre (1σ) tolerance required by off-site production.

Table 5.4 – Comparison of clouds obtained through the tested strategies.

Strategy	Raw data	N. of points	Density [pts/m³]	Deviation (min–max) [mm]
LiDAR cloud	30 scans	5,707,700	20,465	3.0– 27.4
Photogrammetry cloud	944 photos	1,835,233	15,216	5.8 – 98.3
SLAM cloud	1 scan	45,492,604	270,147	2.1 – 30.0



Figure 5.6 – Pictures of the acquisition campaign. From top, left: topographic survey; 3Deye system; Ipad Pro; MLS GeoSLAM Zeb Horizon. Pictures by LAMARC.

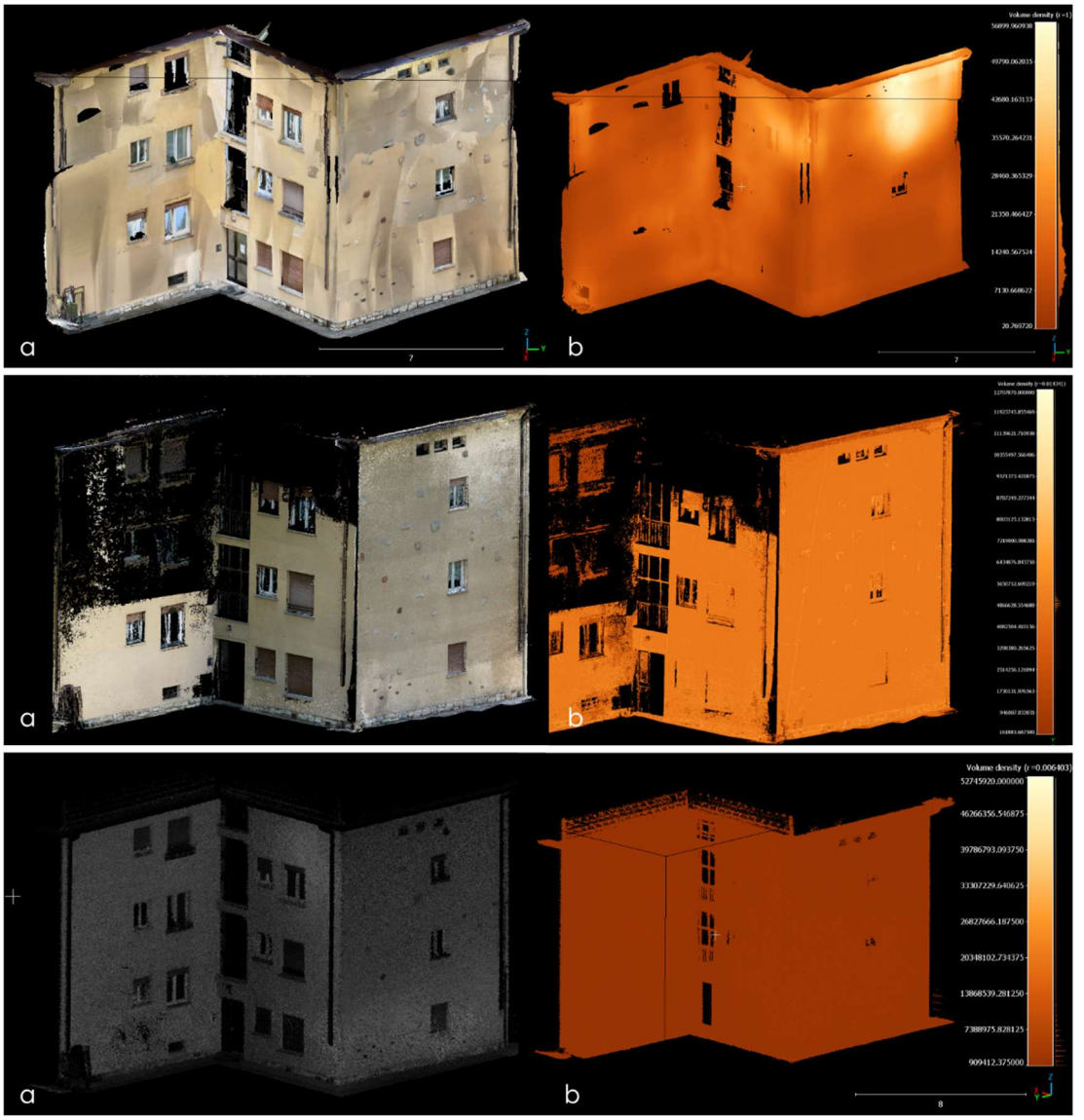

Figure 5.7 – Point clouds obtained through the three tested acquisition strategies, each shown as a colourised/textured view (a) and a point-density map (b): LiDAR cloud (top), photogrammetry cloud (middle), SLAM cloud (bottom).

Table 5.5 – Comparison of costs, acquisition and processing time and modelling suitability related to the tested strategies.

Strategy	Cost* [€]	Acquisition time [hours]	Processing time [hours]	Modelling suitability	
				(a) energy	(b) prefab. design
LiDAR cloud	1,000 / 1,500	1 ground level 2.5 lifting platform	0.25/cloud alignment	Yes (no roof)	No (yes, ground attachments only)
Photogrammetry cloud	4,000 + software	1 ground level, 2 lifting platform	> 16 reference points identification	Yes (no roof)	No
SLAM cloud	15,000 / 60,000	0.5 ground level + lifting platform	0.25/cloud alignment	Yes (no roof)	Yes (no roof)

5.3.2. Modelling for energy assessment and prefabricated component design

Once the acquired point clouds had been evaluated for their geometric reliability, the second experimentation moved from data acquisition to the construction of the BIM model itself. Point clouds were progressively integrated into the BIM environment to generate the digital representation of the existing building: during the early design stages the model supported feasibility assessments and stakeholder communication by visualising the proposed transformation, and as the project advanced it was enriched with geometric and semantic information, becoming the reference framework for the definition of prefabricated panels, construction details, quantities, and production requirements.

This progressive enrichment extended the workflow beyond the design phase proper. Once the architectural model was validated, the information required for fabrication was transferred to the manufacturing company's technical

department, where façade segmentation, panel optimisation, anchoring systems, and construction details were developed further through CAD and CAD/CAM environments. Rather than producing a separate dataset for each phase, the process relied on the same underlying model, refined and adapted at each stage to the needs of the actor receiving it, an information continuity whose actual robustness across the design–production interface is examined in detail later in this section.

The same point cloud data were used as the starting point for both modelling paths, following a shared initial sequence of modelling steps in Revit, consistent with established protocols for existing buildings (Sanhudo et al., 2020; Abualdenien & Borrmann, 2022): the insertion and localisation of the topographic and point cloud data, the definition of building levels, the tracing of perimeter walls and roof, and the positioning of openings and balconies on the façades, all using the cloud as reference. From this common starting point, the two modelling paths diverge sharply in the level of geometric detail pursued and in the additional information required, as described separately below.

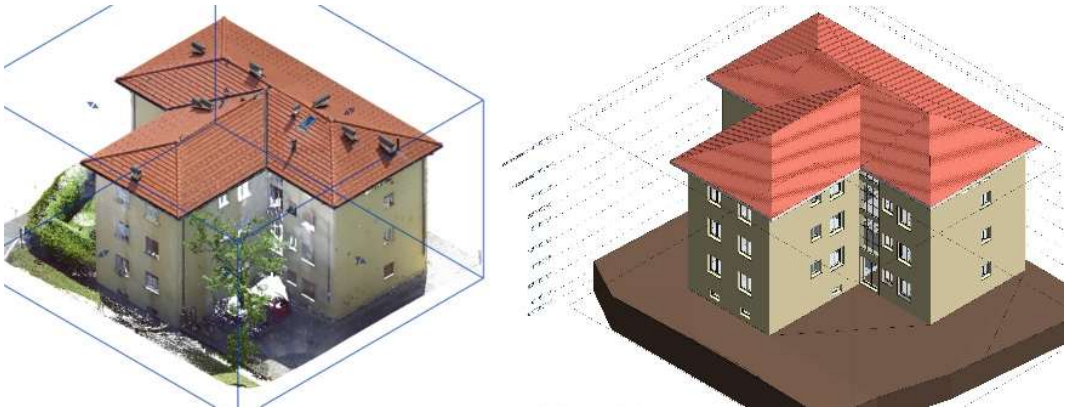

Figure 5.8 – On the left, the point cloud of the existing building imported in the BIM environment. On the right, the corresponding Revit model, with building levels, perimeter walls, and roof traced using the cloud as reference.

Modelling for energy assessment

For the energy assessment, an excessively faithful reconstruction of the building's surfaces and volumes proved counterproductive: too much geometric detail tends to generate errors when the model is transferred to energy analysis software. A simplified volumetric model was therefore adopted, obtained by tracing an orthogonal grid from the point cloud, which made the cloud's millimetric accuracy largely irrelevant to this goal. Beyond geometry, the energy model also required information not derivable from the survey. Spatial data were added first: internal subdivisions, slabs, and walls separating the individual units, together with room entities defining the volume and use of each space (
Figure 5.9). Envelope and construction data followed, defining the stratigraphy, layer thicknesses, and thermal properties of walls, floors, and roof, together with the characteristics of the windows. Building service data specified each unit's heating and cooling installations.

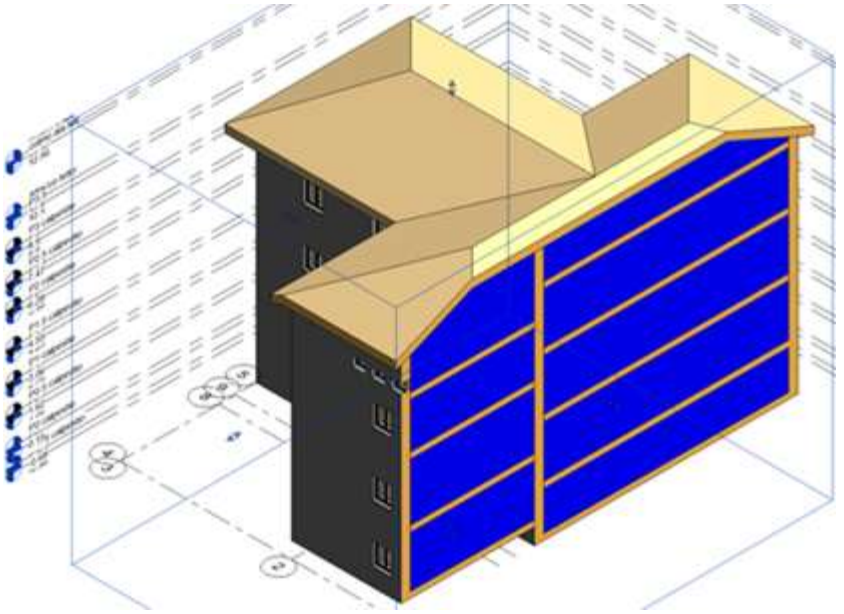

Figure 5.9 – Simplified volumetric model of the building, with room entities (highlighted in blue) defining the volume and use of each space for the energy assessment.

Finally, climatic data describing the context completed the model, providing the boundary conditions for the energy simulation. All the non-geometric information was compiled from a technical report on the building.
Constructing this model surfaced a further layer of practical difficulty beyond the initial choice of LOD. The model was exported in hbjson and idf format through the Revit Pollination plug-in, to allow direct management of surfaces and volumes from Revit and their transfer to the Design Builder energy analysis engine (Figure 5.10). However, the irregular geometries, non-orthogonal angles, and excessively fragmented spaces inherited from the as-is survey initially prevented a usable model for analysis. Resolving this required rectifying near-orthogonal corners and non-perfectly-straight walls, and simplifying the internal layout by treating each residential unit as a single homogeneous thermal zone.
A further complication concerned the placement of room entities, which cannot be managed directly from the plug-in interface and had to be positioned manually on the correct level and with the correct height settings.
A three-dimensional check of the rooms was used to verify their placement before export (
Figure 5.11).

Modelling for the design of the prefabricated intervention

For the design of the prefabricated envelope, the model needed to preserve the building's actual geometric irregularities, such as bulging surfaces and non-orthogonal corners, rather than simplify them away.
The positioning of openings, balconies, and other elements protruding from the façade had to be accurate to within a few millimetres to ensure a correct fit between the existing substrate and the Renew Wall panels, a tolerance an order of magnitude stricter than that required for the energy model. As established in the previous section, however, none of the three tested acquisition strategies produced point clouds meeting

this requirement: their accuracy was sufficient to support a simplified volumetric reconstruction, but not the millimetric positioning of façade components. To address this gap the point cloud from TLS was used.

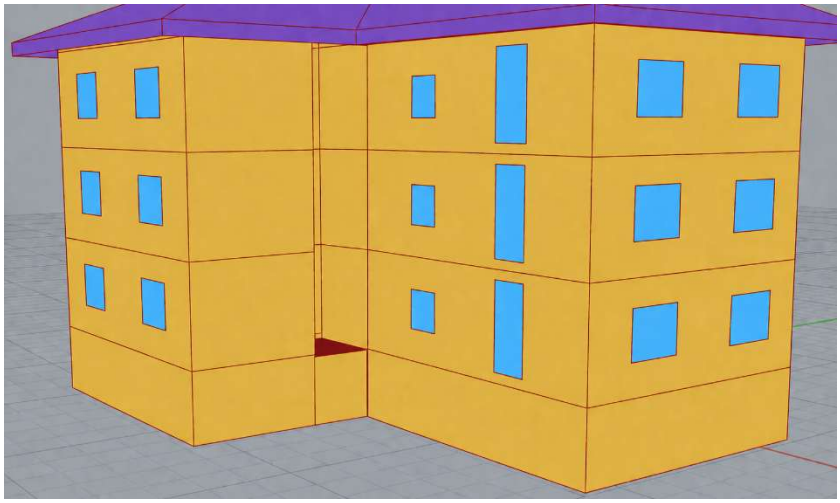

Figure 5.10 – Simplified model exported through the Revit Pollination plug-in and transferred to the Design Builder energy analysis engine.

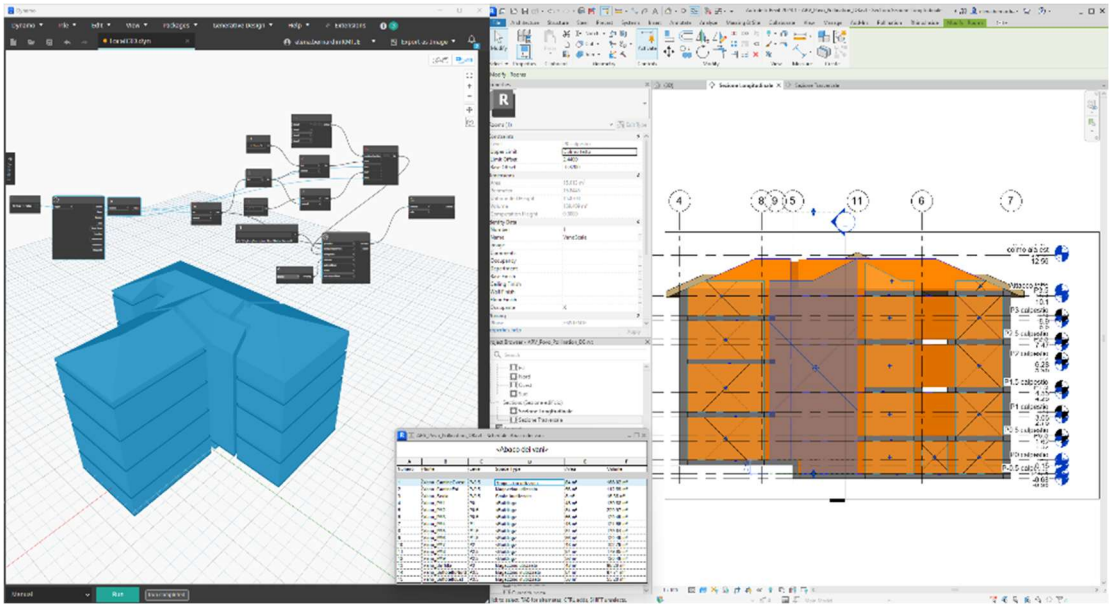

Figure 5.11 – Three-dimensional check of the room entities' placement, performed through Dynamo prior to export for energy simulation.

A parallel line of work concentrated on the design side of the workflow, developing a library of parametric objects for the Renew Wall panels, conceived as a bridge between the architectural model of the existing building and the production of the panels themselves (Zuanni et al., 2026).
The panel family was modelled in Revit as a line-based generic model, structured as a host family acting as the geometric and logical container for a set of nested families corresponding to the panel's constituent components, vertical studs, top and bottom rails, OSB and DWD boards, base plates, insulation layers, anchoring plates, and connections, each assigned dimensional, material, and visibility parameters and classified according to its function.
The host family is governed by a constrained parametric grid of reference planes and lines, driven by conditional formulas that automatically generate and distribute components according to panel length, the presence of openings, and corner configurations, allowing the model to respond adaptively to changes in input while maintaining typological consistency. Consistently with the selective approach to information content already applied to the as-is model, its level of development was calibrated to the minimum content necessary for quantity takeoff and production specifications, rather than to an exhaustive reconstruction of every physical component. The system was first validated on a basic full-panel type (RW-Full) and then extended to window, door, and corner variants (RW-Window, RW-Door, RW-Corner), together offering a range of configurations through the combination of panel typology, connection system (linear timber or point metal anchoring), exterior finish, and mounting condition.
The library was applied to the case study model by introducing a design-state phase in which the panel layout was adapted to the building's actual geometry, with constraints such as maximum panel length and minimum and maximum stud spacing keeping the design aligned with the requirements of

production, transport, and installation, while automatically generated schedules allowed each panel to be quantified directly from the model. The interoperability between design and production environments was then tested by exporting the model from Revit in IFC format and importing it into Dietrich's, the software used by the manufacturer to generate CNC machining files.

In the exchange tested in this case study, semantic and alphanumeric information was preserved, whereas the hierarchical relations and parametrisation native to the Revit model were not: spatial position and geometry transferred correctly, while dimensions, component counts, and anchoring type became unmanageable or unmodifiable once imported.

This finding substantiates, on a specific software pairing, the BIM–CAM interoperability bottleneck anticipated in the theoretical framework of section 5.1, confirming that open exchange formats can preserve geometric and informative content without preserving the structural logic needed to modify a model during pre-production.

Unlike the energy model, then, this modelling path could not be completed on the basis of the acquired survey data alone: the parametric library made it possible to design and quantify a prefabricated intervention consistent with the existing building's constraints, but its transfer into a production-ready format remained subject to the same loss of parametric structure that literature identifies as a still-unresolved link in the informative continuum from survey to fabrication.

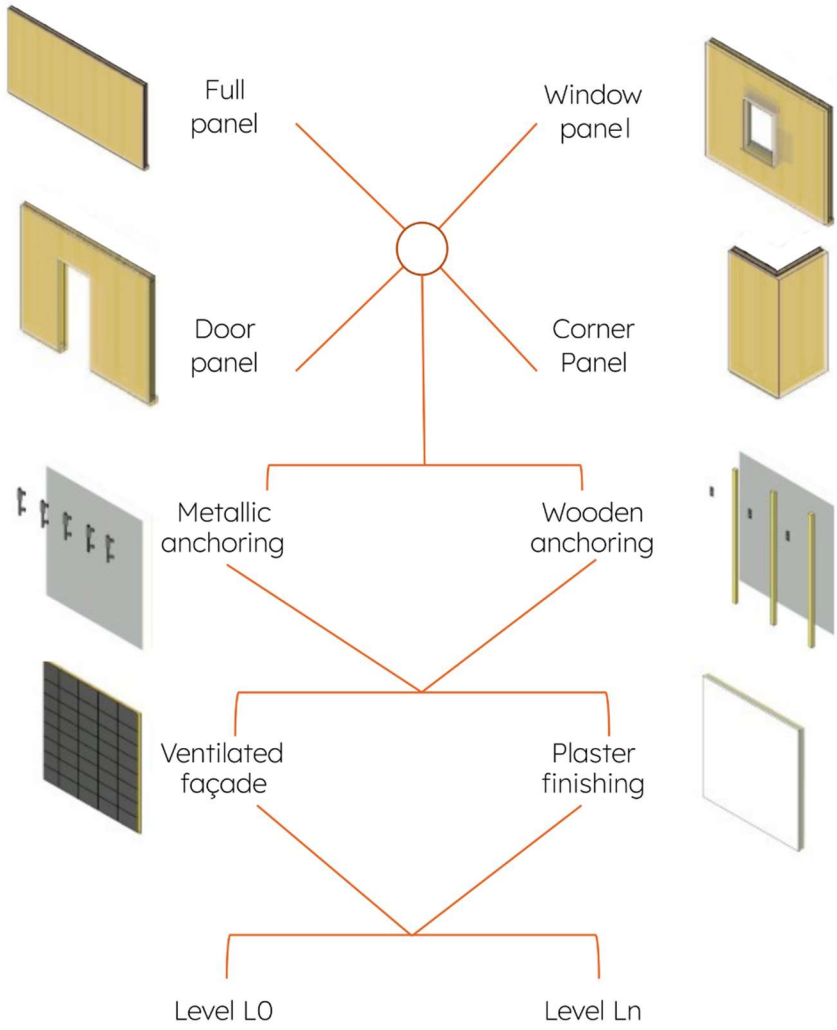

Figure 5.12 – Configuration taxonomy of the Renew Wall parametric panel family, combining panel typology (Full, Window, Door, Corner), anchoring system (metallic or wooden), exterior finish (ventilated façade or plaster), and mounting level[9].

[9] Image from Zuanni et al. (2026), Integrated Modelling and Digital Representation for Design and Production. In Proceedings Graphic Thinking XVII International Conference on Graphic Expression Applied to Building– APEGA 2025, p. 941-953.

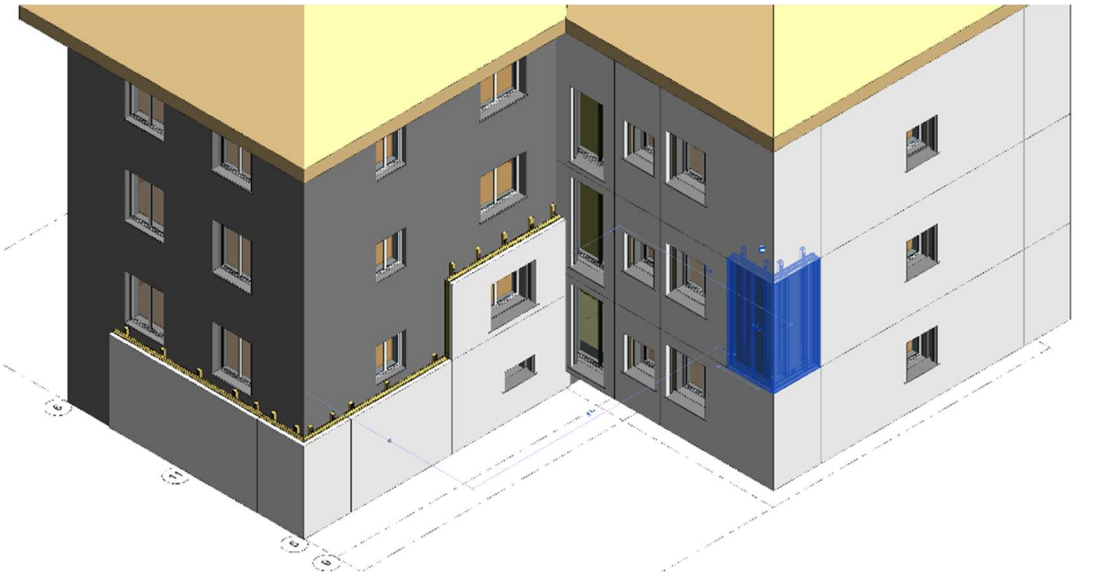

Figure 5.13 – View of the Renew Wall panel object library applied to the building's north and north-east façades.[10]

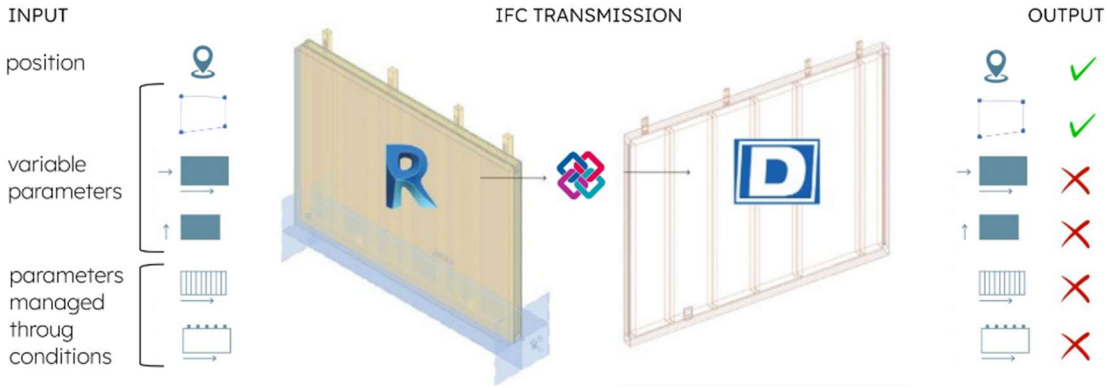

Figure 5.14 – Schematic of the Revit–Dietrich's IFC data exchange test, showing which information, position, variable parameters, and condition-managed parameters, was correctly preserved or lost in the transfer.[11]

[10] Ibidem.
[11] Ibidem.

5.4. Answer to the RQ. Considerations on the case Povo study

In the Povo case study, the results address how the methodology adopted for data acquisition affects the construction of digital models useful for supporting renovation processes (research question 1), and how the usability and interoperability of these models can be guaranteed across users with different skills and needs (research question 3).

None of the three acquisition strategies tested proved capable, on its own, of satisfying the full range of accuracy requirements posed by a prefabricated retrofit intervention. All three supported a simplified volumetric reconstruction sufficient for energy simulation, yet none approached the millimetric tolerance required for the positioning of prefabricated components. This outcome confirms, in the context of a residential retrofit rather than a heritage asset, that the choice of acquisition technique cannot be optimised in the abstract, but must be calibrated against the specific downstream use of the resulting model. Unlike in *Casa Demartin* case, the gap here could not be closed by allocating additional processing time or by combining techniques, since it is fixed by the tolerance of the industrial manufacturing process itself rather than by the survey technology.

This same logic determined the divergence between the two modelling paths developed from the same acquired data: the energy model was deliberately simplified and enriched with non-derivable semantic information, while the prefabrication model preserved the building's actual irregularities and relied on the highest-accuracy dataset available. Taken together, these divergent LOD strategies substantiate, for an energy retrofitting process, the specific characteristic already anticipated in the theoretical framework (research question 2): the depth and geometric fidelity of a digital model must be selectively differentiated according to the phase and purpose

of the analysis, rather than pursued uniformly across the whole informative continuum from survey to production.

With respect to the usability and interoperability of the resulting models across a heterogeneous chain of users (research question 3), the parametric Renew-Wall panel library demonstrates that production-relevant information can be encoded directly within the BIM environment through a structured host-and-nested-family approach. Its transfer into the manufacturer's CAM environment, however, exposed a persistent interoperability bottleneck, preserving geometry and semantic content but not the hierarchical and parametric logic needed to modify the model downstream. This finding indicates that open exchange formats alone are not sufficient to guarantee interoperability for actors beyond the design phase: legibility for surveyors and BIM specialists does not automatically extend to legibility for production actors, and a genuinely interoperable EBIM model must be understood as one whose structural logic, not merely its geometric and alphanumeric content, survives the transition between design and manufacturing environments.

Overall, the Povo case study indicates that ensuring the continuity of digital information from survey to fabrication is less a matter of maximising accuracy or semantic richness at any single stage than of calibrating each stage, acquisition technique, level of development, exchange format, to the tolerance and the users of the specific downstream application. Some questions, however, remain open: chiefly, how to reconcile the divergent LOD requirements of the energy and production models within a single, non-redundant BIM environment, and how to resolve the loss of parametric structure at the BIM–CAM interface, which, at present, still demands manual remediation before industrial production can proceed.

References chapter 5

Abualdenien, J., & Borrmann, A. (2022). Levels of detail, development, definition, and information need: A critical literature review. Journal of Information Technology in Construction, 27, 363–392. doi.org/10.36680/j.itcon.2022.018

Barbini, A. (2021). Automatic and parametric integration of BIM objects in an urban context. (3DModeling&BIM: Data Modeling & Management for AECO Industry online (Roma) 14 aprile 2021, pp. 128-142.

Barbini, A., Bernardini, E., Massari, G., & Roman, O. (2022). Renew-Wall: innovazione e comunicazione di un processo edilizio tra impresa, professione e ricerca. ARCHITETTURA, URBANISTICA, AMBIENTE, 1025-1036.

D'Oca, S., Ferrante, A., Ferrer, C., Pernetti, R., Gralka, A., Rizal, S., Op 't Veld, P. (2018). Technical, Financial, and Social Barriers and Challenges in Deep Building Renovation: Integration of Lessons Learned from the H2020 Cluster Projects" in Buildings 8 (12): 174. doi.org/10.3390/buildings8120174

Daniotti, B., Masera, G., Bolognesi, C., Lupica Spagnolo, S., Pavan, A., Iannaccone, G., Signorini, M., Ciuffreda, S., Mirarchi, C., Lucky, M. and Cucuzza, M. (2022), "The Development of a BIM-Based Interoperable Toolkit for Efficient Renovation in Buildings – From BIM to Digital Twin", in Buildings, vol. 12, issue 2, article 231, pp. 1-15. doi.org/10.3390/buildings12020231

Doukari, O., Kassem, M., Scoditti, E., Aguejdad, R., & Greenwood, D. (2024). A BIM based tool for evaluating building renovation strategies: The case of three demonstration sites in different European countries. Construction Innovation, 24 (1), 365–383. doi: 10.1108/CI-12-2022-0314

Du, H., Huang, P., Jones, P. (2019). Modular facade retrofit with renewable energy technologies: The definition and current status in Europe. Energy and Buildings 205: 109543. doi.org/10.1016/j.enbuild.2019.109543

Faltýnová, M., Matoušková, E., Šedina, J., Pavelka, K. (2016). Building Facade Documentation Using Laser Scanning and Photogrammetry and Data Implementation Into Bim. The International Archives of the Photogrammetry, Remote Sensing and Spatial Information Sciences XLI-B3: 215-220. doi:10.5194/isprsarchives-XLI-B3-215-2016

Gilmour, L., Stroulia, E. (2022). Ortho-photogrammetry for prefabricated energy-efficiency retrofits. Automation in Construction 134:104082. doi.org/10.1016/j.autcon.2021.104082

Habibi, S. (2017) The promise of BIM for improving building performance. Energy and Buildings 153: 525-548. doi.org/10.1016/j.enbuild.2017.08.009

Jordan-Palomar, I., Tzortzopoulos, P., Garc, J., & Pellicer, E. (2018). Protocol to Manage Heritage-Building Interventions Using Heritage Building Information Modelling (HBIM). Sustainability, 10 (4), 908. doi: 10.3390/su10040908

Larsen KE, Lattke F, Ott S, Winter S (2011) Surveying and digital workflow in energy performance retrofit projects using prefabricated elements. Automation in Construction 20, 20:8 999–1011 https://doi.org/10.1016/j.autcon.2011.04.001

Li, X., Shen, G. Q., Wu, P., & Yue, T. (2019). Integrating Building Information Modeling and Prefabrication Housing Production. Automation in Construction, 100, 46–60. doi: 10.1016/j.autcon.2018.12.024

Lo Turco, M., Giovannini, E. C., & Tomalini, A. (2022). Parametric and Visual Programming BIM Applied to Museums, Linking Container and Content. ISPRS International Journal of Geo-Information, 11 (7), 7. doi: 10.3390/ijgi11070411

Lovell, L. J., Davies, R. J., & Hunt, D. V. L. (2023). The Application of Historic Building Information Modelling (HBIM) to Cultural Heritage: A Review. Heritage, 6 (10), 6691–6717. doi: 10.3390/heritage6100350

Malacarne, G., Monizza, G. P., Ratajczak, J., Krause, D., Benedetti, C. and Matt, D. T. (2016). Prefabricated timber façade for the energy refurbishment of the Italian building stock – The Ri.Fa.Re. Project, in Energy Procedia, vol. 96, Elsevier, pp. 788-799. doi.org/10.1016/j.egypro.2016.09.141

Masera, G., Iannaccone, G. and Salvalai, G. (2014), "Retrofitting the existing envelope of residential buildings – Innovative technologies, performance assessment and design methods", in Advanced Building Skins Conference Proceedings of the 9th Energy Forum, Bressanone, Italy, October 28-29, 2014, Economic Forum, Munich, pp. 987-994. doi.org/10.13140/RG.2.1.2543.0887.

Massari GA, Barbini A, Bernardini E, Roman O (2022) Energy retrofitting of existing buildings. Geometric-informative modelling and management. AGATHÓN International Journal of Architecture, Art and Design 12: 146-157. doi.org/10.19229/2464-9309/12132022

Pernetti, R., Pinotti, R., & Lollini, R. (2021). Repository of Deep Renovation Packages Based on Industrialized Solutions: Definition and Application. Sustainability, 13 (11), 6412. doi: 10.3390/su13116412

Rovers, R., Lupíšek, A., Borodinecs, A., Almeida, M. G. (2018). A Guide. into Renovation Package Concepts for Mass Retrofit of different types of Buildings with Prefabricated Elements for (n)ZEB Performance.

Sanhudo, L., Ramos, N.M.M., Poças Martins, J. (2018). Building information modeling for energy retrofitting – A review. Renewable and Sustainable Energy Reviews 89: 249-260. doi.org/10.1016/j.rser.2018.03.064

Yin X, Liu H, Chen Y, Al-Hussein M (2019). Building information modelling for off-site construction: Review and future directions. Automation in Construction 101: 72-91. doi.org/10.1016/j.autcon.2019.01.010

Tata, A. (2023). Procedure per la modellazione HBIM del patrimonio architettonico. PUBLICA. /https://www.publicapress.it/wp-content/uploads/2023/10/Procedure_per_la_modellazione_HBIM_del_patrimonio_architettonico_.pdf

Torres, J., Garay-Martinez, R., Oregi, X., Torrens-Galdiz, I. J., Uriarte-Arrien, A., Pracucci, A., Casadei, O., Magnani, S., Arroyo, N., Cea, A.M., (2021). Plug and Play Modular Façade Construction System for Renovation for Residential Buildings" in Buildings 11 (9): 419.

Volk, R., Stengel, J., & Schultmann, F. (2014). Building Information Modeling (BIM) for existing buildings—Literature review and future needs. Automation in Construction, 38, 109–127. doi: 10.1016/j.autcon.2013.10.023

Wang, M., Wang, C.C., Sepasgozar, S., Zlatanova, S. (2020). A Systematic Review of Digital Technology Adoption in Off-Site Construction: Current Status and Future Direction towards Industry 4.0. Buildings10(11): 204. doi.org/10.3390/buildings10110204

Ursini, A., Grazzini, A., Matrone, F., & Zerbinatti, M. (2022). From scan-to-BIM to a structural finite elements model of built heritage for dynamic simulation. Automation in Construction, 142, 104518. doi: 10.1016/j.autcon.2022.104518

6. Conclusions

This thesis set out from the premise that the heterogeneity of the existing building stock makes a single decarbonization pathway insufficient, and that digitization has been proposed, at policy level, as the connective infrastructure capable of absorbing this heterogeneity by providing the differentiated information base a renovation strategy requires. The literature reviewed to contextualise the problem indicates that whether digitization can deliver on this promise in practice remains an open question, limited less by any shortage of technical capability than by two specific gaps: the absence of a standardized specification for existing-building models, and the difficulty of validating proposed frameworks against the different actors who must use them across a project's life cycle. The three research questions that followed asked, in turn, how data acquisition shapes the resulting digital model (RQ1), what characteristics such a model needs to support energy retrofitting (RQ2), and how its usability and interoperability can be guaranteed across users with different skills and needs (RQ3), and were tested through three case studies spanning progressively different conditions of the existing stock. This conclusive chapter discusses what the case studies jointly revealed in response to the research questions, considers the limitations of this work, and outlines possible future developments of this research.

6.1. Discussion: the case studies in relation to the research questions

The three case studies were designed to test the fundamental processes of acquisition, processing, and modelling phases against progressively different conditions of the existing stock, and their combined results allow the three research questions

to be answered not in the abstract, but as a function of the specific purpose and users each model was built to serve.

With respect to RQ1, how acquisition methodology affects the resulting digital model, the first and third case studies point to the same underlying principle from two different directions.

In Calliano, integrating static and dynamic acquisition techniques produced a highly reliable geometric model, but at a processing cost that was only justified because the case pursued advanced architectural documentation; for an exploratory performance analysis, a lower level of accuracy, comparable to the initial MLS output, would have sufficed.

In Povo, the experimentation was designed around a different objective: rather than pursuing the highest achievable accuracy, as in Calliano, it tested low-cost, fast acquisition techniques specifically because these are what a disruptive, large-scale diffusion of deep renovation would require if it is to reach ordinary, unconstrained buildings, the largest portion of the existing stock, and the one least likely to justify a costly, bespoke survey campaign for each intervention. Tested against this more demanding goal, the technique-purpose relationship revealed a hard constraint rather than a matter of diminishing returns: none of the three low-cost strategies tested met the millimetric tolerance required for prefabricated component design. Together, the two cases show that the acquisition-to-model relationship is not governed by a single accuracy standard to be maximised, but by the specific downstream use the model must support; and that, where that use is a scalable, industrialized retrofit process rather than a single, well-resourced documentation effort, even combined low-cost techniques may not be sufficient on their own to close the gap.

With respect to RQ2, what characteristics a model needs to support energy retrofitting across its phases, the second and third case studies converge on the same conclusion from complementary evidence. In Valencia, the systematic

comparison of passive and active retrofit strategies, evaluated jointly rather than in isolation, was what rendered the informative model useful for decision-making: neither strategy alone captured the full trade-off between energy performance and heritage preservation.

In Povo, the same principle emerged across purposes: the same survey data gave rise to two deliberately divergent models, one simplified and semantically enriched for energy simulation, the other geometrically faithful for prefabrication. In both cases, a single, uniformly detailed model would have been not more useful, but less: the depth and fidelity a model needs are not properties of the model in isolation but of the phase and purpose it is currently serving.

With respect to RQ3, how usability and interoperability can be guaranteed across users with different skills and needs, the second and third cases again identify the same structural limitation.

In Valencia, the tested modelling process demonstrated its capacity to reach different professional profiles without requiring them to acquire specialised technical skills: translating simulation outputs into synthetic, comparative dashboards was sufficient to make multi-criteria results directly readable and interpretable. This level of translation, however, was acceptable just because the case addressed a preliminary design phase, where a synthetic comparison across scenarios is the intended output; a later, detailed design phase would likely demand a different degree of technical engagement from these same actors.

In Povo, this kind of translation could not fully close the gap between different professional users: technical legibility for surveyors and BIM specialists did not extend automatically to the manufacturing company's technical department, since the IFC exchange with the fabricator's CAM environment preserved geometry and semantic content but lost the

hierarchical and parametric logic needed to modify the model downstream.

Read together, these findings indicate that interoperability cannot be treated as a single, format-level property of a model. It is a per-actor condition, and open exchange formats, while necessary, are not on their own sufficient to guarantee it. Across all three questions, the case studies converge on a single argument that runs through this thesis: the informative continuum from survey to use is coherent not when any one stage is maximised, but when acquisition, modelling, and exchange are each calibrated to the specific downstream requirement they must serve, a condition that recurred, in different forms, whether the requirement was a target level of documentation, a decision to be supported, or an actor who had to act on the result.

6.2. Limitations and future developments

This conclusion rests on three case studies, each addressing a different, specific condition of the existing stock, a pre-modern heritage building, a mid-twentieth-century heritage complex, and an ordinary, unconstrained residential building. This breadth was a deliberate design choice, allowing the same questions to be tested against different conditions, but it also means that each individual finding was validated once, in one context, rather than across a broader sample. The extent to which, for instance, the Povo prefabrication tolerance finding would generalise to other manufacturing systems, or the Valencia dashboard approach to other categories of non-technical stakeholders, remains to be tested.

Each case study also left a specific technical question open. In Povo, the divergence between the energy and production models raises the unresolved question of how to reconcile both sets of requirements within a single, non-redundant BIM environment, and the loss of parametric structure at the BIM-CAM interface currently still demands manual remediation. In

Valencia, the multi-criteria synthesis that made the model legible to non-technical stakeholders required a substantial simulation effort across eight scenarios, whose scalability to a reduced-resource decision context has not been tested. More broadly, as argued in the introduction, no standardized specification yet exists for calibrating the level of information need of existing-building models against a shared benchmark; this thesis addressed that gap case by case, but did not resolve it at a general level.

These limitations point directly to future developments: testing the acquisition-model-use relationship identified here across a larger and more diverse sample of buildings and manufacturing systems; developing exchange strategies, or dedicated schemas, capable of preserving parametric logic across the BIM-CAM interface; and empirically validating, with actual non-technical users, whether the dashboard-based translation strategy identified in Valencia generalises beyond the specific stakeholder group tested there. The integration of BIM with complementary technologies, digital twins, AI-assisted processing, already emerging in the broader literature reviewed in Chapter 1, offers a further avenue through which the calibration this thesis argues for could eventually be automated rather than performed case by case.

6.3. Conclusion

This thesis set out from a specific concern: that digitization, proposed at policy level as the connective infrastructure capable of supporting a differentiated decarbonization strategy across a heterogeneous building stock, might not yet deliver on that promise in practice. The three case studies developed here indicates that the technical means to do so are available, but that they do not function automatically. What determines whether a digital model actually supports a renovation process is not the accuracy, richness, or interoperability it achieves in the abstract, but whether each of

these properties is deliberately calibrated to the specific acquisition purpose, retrofit phase, and user it is meant to serve. This is the central methodological contribution of this work: not a single, general-purpose model for existing-building decarbonization, but an empirically grounded framework for calibrating the informative continuum from survey to use, tested across three different conditions of the existing stock, and capable of informing how future digitization efforts are structured across the equally heterogeneous stock, still awaiting renovation.

Acknowledgments

Behind this thesis there is a long and non-linear path, and many people who helped me get through it. My sincere thanks go to every one of them.

I am deeply grateful to Prof. Giovanna A. Massari, whose guidance and trust have been fundamental to this research and to my growth, on both a professional and a human level.

My sincere thanks go equally to Profs. Rossano Albatici and Michela Dalprà, whose support and availability have been precious throughout this journey.

To my colleagues, in strictly alphabetical order, Ambra Barbini, Anna Maragno, Chiara Chioni, Federico Casagrande and Gaia Eccli, for sharing spaces and ideas, bur mostly moments of joy and support. To Prof. Starlight Vattano, whose presence, advice and friendship have meant far more to me than any academic role could suggest.

To the entire LPE group, and especially to Profs. Simone Torresin and Gianluca Maracchini, for their valuable feedback during the annual reviews, and to Paolo Bottura, for his irreplaceable presence.

To Prof. Luis Palmero Iglesia, who warmly welcomed me and actively involved me in his group at the Escuela Técnica Superior de Ingeniería de Edificación (ETSIE) of the Universitat Politècnica de València.

To all my colleagues of the 38th doctoral cycle, but also to many from earlier and later cycles and other young researchers, with whom I cultivated a spirit of brotherhood and sharing in the colourful corridors of Mesiano and beyond.

To the entire Department staff, for their availability and support, technical and otherwise.

Finally, and above all, my special thanks go to my family, for their constant support and encouragement.